University of Windsor

Scholarship at UWindsor

2010

Application of electrical methods to assess the quality of concrete

William Clements
University of Windsor

Follow this and additional works at: https://scholar.uwindsor.ca/etd

---

APPLICATION OF ELECTRICAL METHODS

TO ASSESS THE QUALITY OF CONCRETE

by

William Clements

A Thesis

Submitted to the Faculty of Graduate Studies

Through the Department of Civil and Environmental Engineering

in Partial Fulfillment of the Requirements for

the Degree of Master of Applied Science at the

University of Windsor

Windsor, Ontario, Canada

2010

Canada

Author's Declaration of Originality

I hereby certify that I am the sole author of this thesis and that no part of this thesis has been published or submitted for publication.

I certify that, to the best of my knowledge, my thesis does not infringe upon anyone's copyright nor violate any proprietary rights and that any ideas, techniques, quotations, or any other material from the work of other people included in my thesis, published or otherwise, are fully acknowledged in accordance with the standard referencing practices. Furthermore, to the extent that I have included copyrighted material that surpasses the bounds of fair dealing within the meaning of the Canada Copyright Act, I certify that I have obtained a written permission from the copyright owner(s) to include such material(s) in my thesis and have included copies of such copyright clearances to my appendix.

I declare that this is a true copy of my thesis, including any final revisions, as approved by my thesis committee and the Graduate Studies office, and that this thesis has not been submitted for a higher degree to any other University or Institution.

ABSTRACT

The desire for a non-destructive testing method for concrete strength has always been present in civil engineering. An emphasis on testing the electrical properties of concrete has existed for many years without the connection drawn between the electrical properties and strength of concrete. This study was designed to determine if a relationship between the electrical properties and strength of concrete exists. It was found that a linear relationship exists between the capacitive reactance and strength of concrete, as concrete cures and sets. It was also found that increasing the electrode distance increases the reactance, increasing the electrode contact area decreases the reactance and decreasing the cement content decreases the reactance.

DEDICATION

I would like to dedicate this thesis to Diana, because without her help, understanding and love this would have never been possible.

ACKNOWLEDGEMENTS

TABLE OF CONTENTS

List of Tables

List of Figures

1   INTRODUCTION

1.1   *General*

Concrete is currently one of the most widely used construction materials in the world, making concrete one of the most widely researched materials in civil engineering. The most important parameter of any concrete is the final strength achieved after the hydration process has been completed. Currently, the only way of testing the strength of a concrete is through semi-destructive testing, which causes some damage when performed on the concrete that has been cast in place. There is an urgent need for development of a method that can determine the concrete strength as it cures and sets.

1.2   *Problem Statement*

The process of creating a non-destructive test method which is able to determine concrete strength has been taking place for many years. Many methods have been used, however, there has always been an emphasis put on the electrical properties of concrete and whether these methods can help in predicting the strength of concrete. In order to use the electrical properties of concrete to determine the strength, a clear relationship must be made between these two parameters. Hence, this study was designed and carried out to investigate the relationship between the strength and electrical properties of concrete.

1.3   *Objectives*

The following were the objectives:

- Determine if a relationship exists between the electrical properties and strength of concrete.
- Investigate the effect of electrode distance, electrode contact area, and cement content on the electrical properties of concrete.

1

1.4   *Scope of Work*

The following were the major activities under the scope of work for this project.

- Undertake a detailed literature review to provide insight into how the problem statement should be addressed, in terms of research methodology.
- Carry out the testing to determine both the electrical properties and strength of concrete.
- Analyze the test data to determine if a relationship exists between the strength of concrete and electrical properties of concrete as concrete cures and sets.
- Analyze the test data to determine if the electrode distance, electrode contact area, and cement content of the concrete specimens affect the electrical properties of concrete.

1.5   *Methodology*

The methodology of the study included casting concrete in different sizes of moulds with different concrete mixes to measure the electrical properties, in conjunction with simultaneously casting concrete cylinders to measure the strength of the specified concrete mix. The experimental program was completed in three phases using various mould types and concrete mixes.

1.6   *Organization*

The contents of this thesis are organized as follows: Chapter 2 consists of a detailed literature review conducted before the experimental program began, Chapter 3 outlines the and testing procedures and steps followed in the experimental program, Chapter 4 discusses a representative electrical circuit that can be applied to concrete, Chapter 5 presents and discusses the results found in the experimental program and Chapter 6 includes a summary of the thesis, conclusions drawn from the work and any recommendations for the future.

2   LITERATURE REVIEW

2.1   *General*

The intent of this literature review is to gain knowledge into the previous research completed on the electrical properties of concrete and how they can be related to the mechanical properties of concrete. In order to establish how the quality of concrete can be related to its electrical properties, research began with cement paste which consists only of water and cement (the elements responsible for the binding of concrete). This research was integral in establishing that cement paste is the primary medium that electrical current will pass through in concrete. It was found by many researchers that concrete will not resist current as well as the aggregate it is made from because the current will pass through the path of least resistance which is in turn the cement paste. Testing the electrical properties of concrete and mortar was the next step, where the main objective would be to change the physical properties of the specimens and observe the effect on the electrical properties that would result.

After completing this literature review it was apparent that the relationship between the electrical properties and the strength of concrete should be explored further. Different concrete mixes and different specimen sizes were investigated in order to find a relationship between the strength of a given concrete and its corresponding electrical properties.

2.2   *Cement Paste*

2.21   Relationships between Electrical and Physical Properties of Cement Pastes

Taylor and Arulanandan (1974) performed a study to determine whether it would be possible to predict important mechanical properties of cement pastes from measurements of the electrical properties at early ages of setting. Taylor and Arulanandan completed important research by explaining some of the physical properties of concrete and how they can be affected by different parameters like the amount of absorbed water present in the concrete, the geometry and distribution of the capillary pores, the number of solid-solid contacts and the ratio of the amount of cement paste to space available in the

concrete. After this it was considered what paths that the current would take while passing through the cement paste including: through the solution and conducting particles in series, through the particles in contact with each other, and through the solution was considered. A model was proposed to show the fractional cross-sectional path of the current through the cement paste as shown in Figure 2.1, where d is the length of the current path through the conducting solid, c represents the length of the current path through the solution, b represents the length of the current path through the "solid" particles and a represents the cross-sectional area of the solution and conductive solids in series.

Liquid

$(1-d)$

1

d

Solid

a   b   c

1
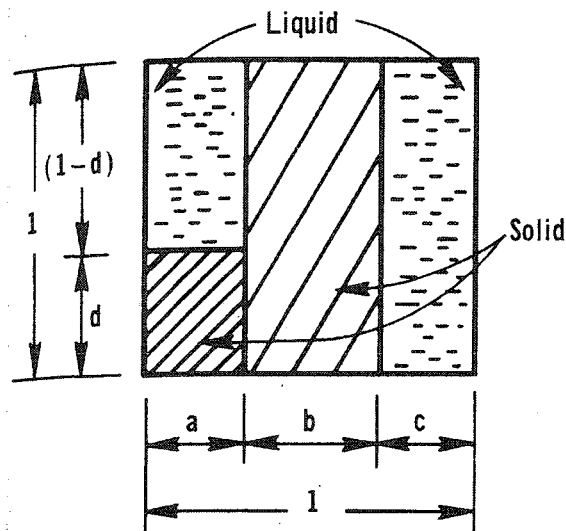
**Figure 2.1: Schematic for the conduction of electricity through cement paste
(Taylor and Arulanandan, 1974)**

The relationship was made between the parameter b and the strength and elasticity of the cement paste making b the most important parameter in this study.

The cement paste specimens were 12.7 mm by 38.1 mm and they were tested for their dielectric constant and conductivity over a frequency range of 1MHz to 100MHz. The water/cement (W/C) ratios used were 0.3, 0.35 and 0.4 where the electrical properties were tested after about 24 hours of curing. Along with these specimens 50.8 mm x 101.6 mm cement paste cylinders were cast in order to test the compressive strength of the pastes at the ages of 3, 7 and 10 days.

It was found that for every W/C ratio the solid-solid contacts increased with time, where they increased rapidly over the first day and then more gradually during the first week. Also, it should be noted that only a W/C ratio of 0.3 or 0.35 is needed in order for the complete chemical conversion of cement to occur, and the parameter b became very sensitive to the W/C ratio of 0.4 meaning that b is very sensitive to an excess of water present in a cement paste.

The importance of the parameter b can be seen in Figure 2.2 where it is shown how b can used to predict the strength of a cement paste at day 7 if it is measured at day 1.
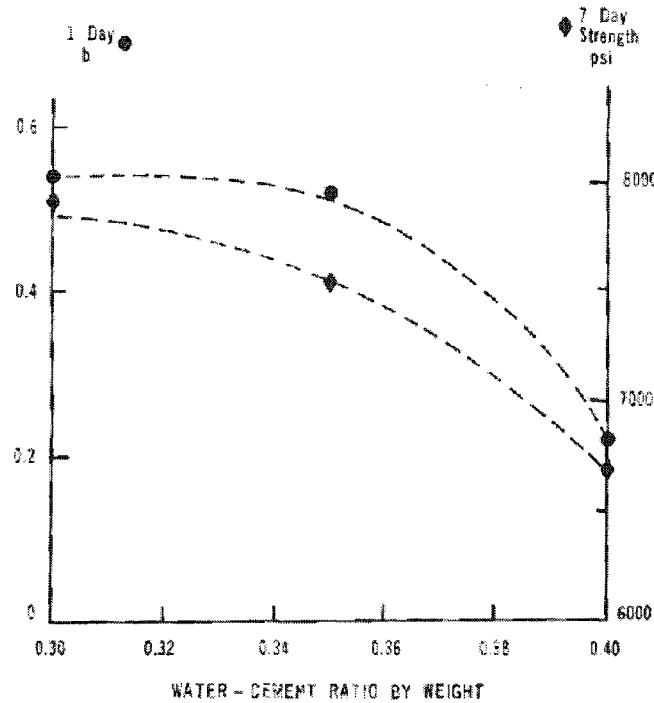
Figure 2.2: Strength of cement paste measured and calculated using b parameter
(Taylor and Arulanandan, 1974)

The model using b is conservative when compared to the measured 7 day strength which is advantageous because it would be safer, as the actual strength would be higher than the predicted value. Taylor and Arulanandan suggest that it would be possible to create a field measuring device able to predict the strength of early age concretes from the determination of the parameter b. The use of this technique would be very useful but it

has not been studied further beyond the application of the purely academic material of cement paste and not concrete.

2.2.2 Effect of Water Content in Cement Pastes

Tashiro et al. (1987) investigated the dependence of the electrical resistivity on the evaporable water content and pore-size distribution of hardened cement pastes. The three different cements used in this study were ordinary Portland cement (OPC), alumina cement (AC) and ultra-rapid hardening cement (URHC).

The water/cement ratio used in the cement pastes was 0.4 and the moulds used were 15 mm x 40 mm x 15 mm with two 6 mm x 25 mm steel electrodes spaced at 5 mm. The specimens were cured at 20°C for one day and then removed from the moulds and dried in an oven at 60°C to evaporate any water present in the paste. The specimens were cooled at 20°C and the electrical resistance was measured along with the weight. The evaporable water content was measured by the difference in this weight and the weight of the specimens after drying in an oven at 100°C for 12 hours.

Figure 2.3 shows the relationship between the log of the resistivity and the reciprocal of the water content for each curing time of 3, 7, and 28 days.
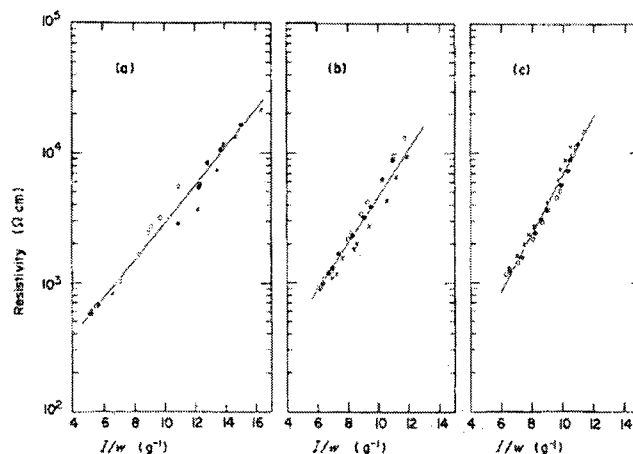
Figure 1 Variation of electrical resistivity with the reciprocal of the evaporable water content, *w*, for hardened OPC, the curing times are (a) 3 days, (b) 7 days and (c) 28 days.

Figure 2.3: Variation of resistivity of cement pastes with the reciprocal of water content

(Tashiro et al., 1987)

6

The magnitude of the resistivity remained relatively the same but the slope of the line in Figure 2.3 (C) increases with time. Figure 2.4 shows the change in the slope C with time which shows that the slope levelled off by the time the concrete was fully cured at 28 days.
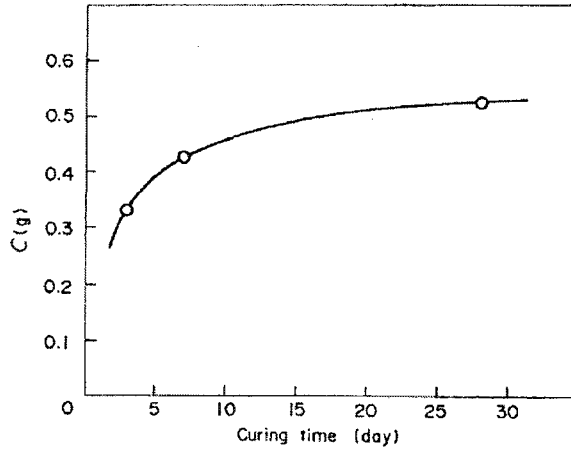
Figure 2.4: Variation of slopes from Figure 2.3 with time

(Tashiro et al., 1987)

Figure 2.5 shows the variation of the resistivity with which cement type is used. The C value and resistivity of the AC and URHC cements is considerably higher than that for OPC.
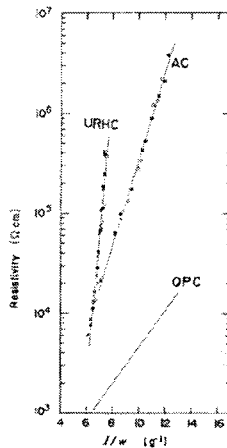
Figure 2.5: Variation of resistivity with the reciprocal of water content of different cements (Tashiro et al., 1987)

7

This result shows that the slope C reflects the difference between the curing time and the type of cement used. A test of the pore volume was also performed using a mercury penetration porosimeter, with the results displayed in Figure 2.6.
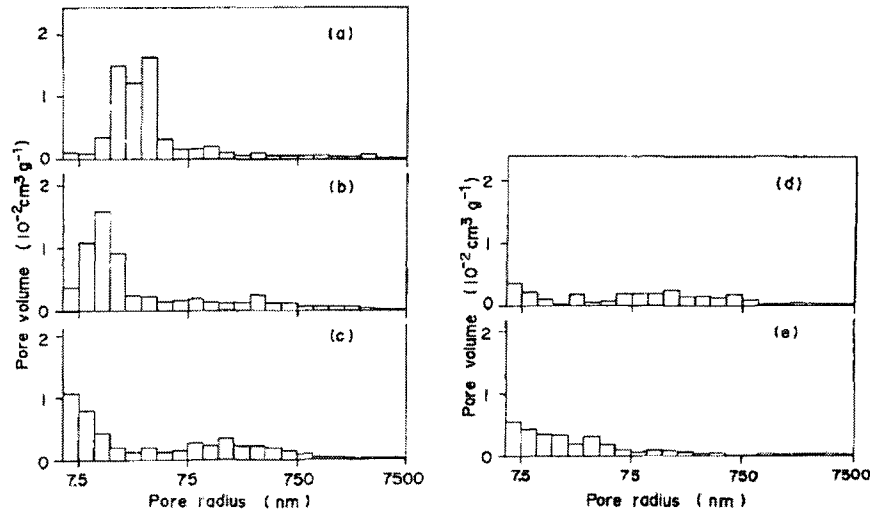
Figure 4 Pore-size distributions of various hardened cement pastes; (a) OPC (curing time 3 days), (b) OPC (7 days), (c) OPC (28 days), (d) AC (7 days), and (e) URHC (7 days).

Figure 2.6: Pore size distribution of different cement pastes

(Tashiro et al., 1987)

From the figure it was concluded that OPC creates a cement paste with more pores of smaller size than that of AC and URHC while also containing larger pores on average than AC and URHC. In conclusion of this study, it was found that the C value can characterize hardened cement pastes with different curing times and types of cements.

This study presents a clear difference in the electrical properties of cement paste, when there is a change in water content or the type of cement used. The only suggestion for this study would be that the electrical measurements were taken every day in order to create a full data set for the proposed C value and how it varies with time.

2.2.3   Impedance of Cement Pastes

McCarter et al. (1988) completed research with the intent of finding the impedance response of cement paste over a large frequency range at different times during the hardening process. The frequency range used in this study was 20 to 110 MHz, and the specimens were tested on days 1, 14, and 25. While it is given that the cement paste had a

water to cement ratio of 0.3, the size of the specimens was not given in the report. This is a vital piece of information that is needed when considering cement paste as a dielectric, as the impedance is dependent on the size of the specimen. The author should have provided this information in the article in order for others to compare their work or so research could be duplicated. Regardless of this, the impedance plots produced show a familiar shape of a straight line at low frequencies then a semicircular arc after intercepting with the Real Impedance Axis. The bulk resistance is given by the intercept and was found to increase with time as the values given were: 190 Ω at 1 day, 404 Ω at 14 days, and 528 Ω at 25 days. The frequency at which the cement paste relaxes (Imaginary impedance lowers) decreased with time, indicating that as the cement paste aged the capillary pores constricted and slowed the current passing through the paste.

The conclusion made was that it could be possible to give a quantitative measure of the degree of hydration of a cement paste. While a more interesting conclusion to be made is that the impedance plot formed for cement paste bears the same shape as that of mortar and concrete found in other studies. This would give further evidence into the fact that in concrete or mortar the current passes primarily through the cement paste. Even though the author did not make this conclusion this study was informative and remains important when attempting to classify the electrical mechanics of cement based materials.

2.2.4 Effect of Water Type on Cement Paste

The objective of the research performed by Wahed and Hekal (1989) was to study the effect of the water type of a cement paste on its conductivity.

They used three different cement types: Portland cement, slag cement, and blended cement. The slag cement consisted of 60% Portland cement, 35% blast furnace slag, and 5% gypsum, while the blended cement consisted of 65% Portland cement, 15% blast furnace slag, 15% cement kiln dust, and 5% gypsum. The different cement types were mixed with either regular drinking tap water or chloride solution or sea water or sulphate solution or ground water in order to attain a liquid to cement ratio of 0.3. The specimens used for the conductivity measurements were cast in cylinders with an internal diameter of 16 mm and length of 12 mm. There were stainless steel endplates attached to the

cement pastes cylinders, and a conductometer was used to measure the conductivity at 20°C for the first 5 hours after mixing. Conductivity-time curves were established for all of the different specimens where each curve shared the common characteristic having a single maximum conductivity achieved during the early stages of hydration.

Figure 2.7 shows the conductogram for Portland cement. The figure illustrates tap water causes the lowest conductivity and the ground water and MgSO4 solution provide similar conductivity.
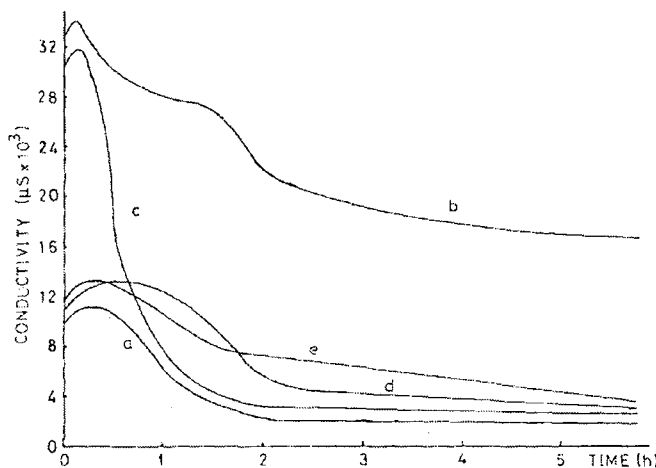
Figure 1 Conductograms of Portland cement paste: (a) tap water, (b) NaCl solution, (c) sea water, (d) MgSO₄ solution and (e) ground water.

Figure 2.7: Conductivity with time using Portland cement paste
(Wahed and Hekal, 1989)

The media containing chloride ions (NaCl and sea water) had a much higher conductivity, which was likely due to the fact that chloride ions accelerate the effects of hydrolysis in cement. It was also interesting to note there was a sharp decrease in the conductivity of the sea water specimen after the maximum, which was likely due to the sharp decrease of chloride ions as the sea water creates large amounts of ettringite in the cement paste. The conductogram for the slag cement is shown in Figure 2.8, which shows the conductivity is initially lower for these specimens.
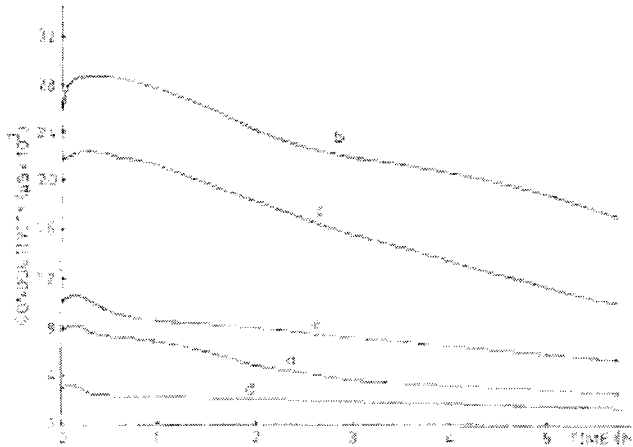
Figure 2 Conductograms of slag cement paste (a) tap water, (b) NaCl solution, (c) sea water, (d) MgSO$_4$ solution and (e) ground water.

Figure 2.8: Conductivity with time using slag cement paste

(Wahed and Hekal, 1989)

This likely occurred because the free calcium hydroxide produced during the Portland cement hydration was consumed by the slag hydration reducing the conductivity. The specimen cast with the SO$_4$ solution was lower than the tap water and the ground water specimen was slightly higher. As expected the NaCl solution had the highest conductivity followed by the ground water due to the phenomenon explained earlier. Figure 2.9 illustrates the conductogram for the blended cement paste, which resulted in markedly low conductivity values for the tap water specimen as the kiln dust was introduced.
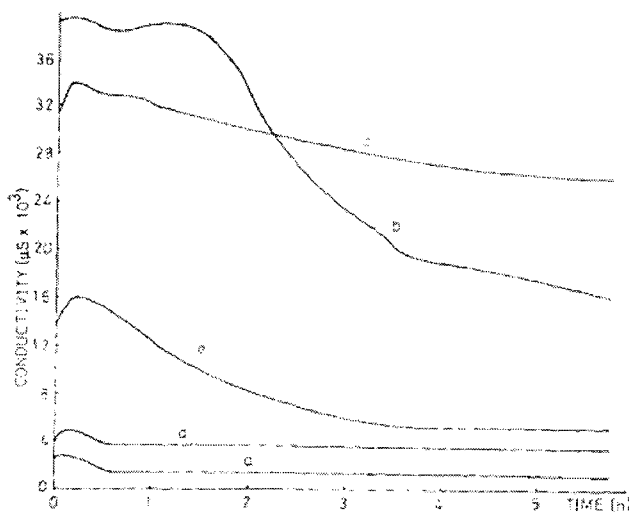
Figure 3 Conductograms of blended cement paste: (a) tap water, (b) NaCl solution, (c) sea water, (d) MgSO$_4$ solution and (e) ground water.

Figure 2.9: Conductivity with time using blended cement paste

(Wahed and Hekal, 1989)

11

The MgSO$_4$ solution and ground water caused slightly lower conductivities during early hydration. The sea water specimen had the second highest conductivity initially and it became the highest after 2 hours when the NaCl specimen lowered significantly. The NaCl specimen had the highest initial conductivity and two maximums before decreasing sharply after 2 hours.

Wahed and Hekal (1989) made several conclusions including the fact that different water types and cement substitutions can change the electrical response of cement pastes. This has application into the fact that it could be possible for popular cement additives to change the electrical response of concretes. If this was possible then the presence of these additives could be studied in a certain concrete mix, or their presence could be accounted for when taking electrical measurements on a concrete specimen.

2.3   *Mortar*

2.3.1   Effect of Water Content on the Electrical Impedance of Mortar

Berg et al. (1992) performed one study found on mortar. The objective was to determine how the dielectric response of cement mortar depends on the water content in a wide frequency range. The aim was to make use of dielectric measurements as an indicator of water content in cements, mortars, and concretes although only mortars were studied.

The specimens used were 80 mm x 80 mm cubes of mortar with the water/cement (W/C) ratios of 0.5, 0.62 and 0.78. Three polished 40 mm x 40 mm nickel plates were embedded at a distance of 10 mm and 20 mm apart to ensure electrode polarization was easily distinguishable from bulk conduction effects. The specimens were allowed to harden for 24 hours with most of the specimens sealed in plastic to ensure evaporation occurred orthogonal to the electrodes. One specimen of each W/C ratio was completely sealed in plastic. The specimens were stored in air for 3 months with several stages of oven treatment to see the effects of continuing hydration. The final heat treatment was performed for 24 hours at 378K (106°C) to remove any weakly bound water referred to as evaporable water. It was shown that the higher the W/C ratio the higher the percentage of evaporable water.

The complex impedance ($Z = Z_1 + Z_2j$) was found by applying a small sine voltage to a pair of electrodes and measuring the current moving through the concrete, in the frequency range of 10^{-3} to 10^7 Hz. The first electrical properties tested were the real and imaginary capacitance, which were tested at 3 days with no heat treatment, 74 days with no heat treatment, 74 days with a heat treatment for 24h at 333K, 74 days with a heat treatment for 24h at 363K, and 74 days with a heat treatment for 24h at 378K.

The results for the real capacitance are shown in Figure 2.10 (a), where it can be seen that the real part of capacitance decreases with frequency, curing time, and increasing heat treatment. It should be noted that the values of the real part of capacitance seemed to converge at higher frequencies regardless of curing time or heat treatment. The results for the imaginary part of capacitance are shown in Figure 2.10 (b), where it can be seen that the imaginary capacitance also decreased with frequency, curing time, and increasing heat treatment.
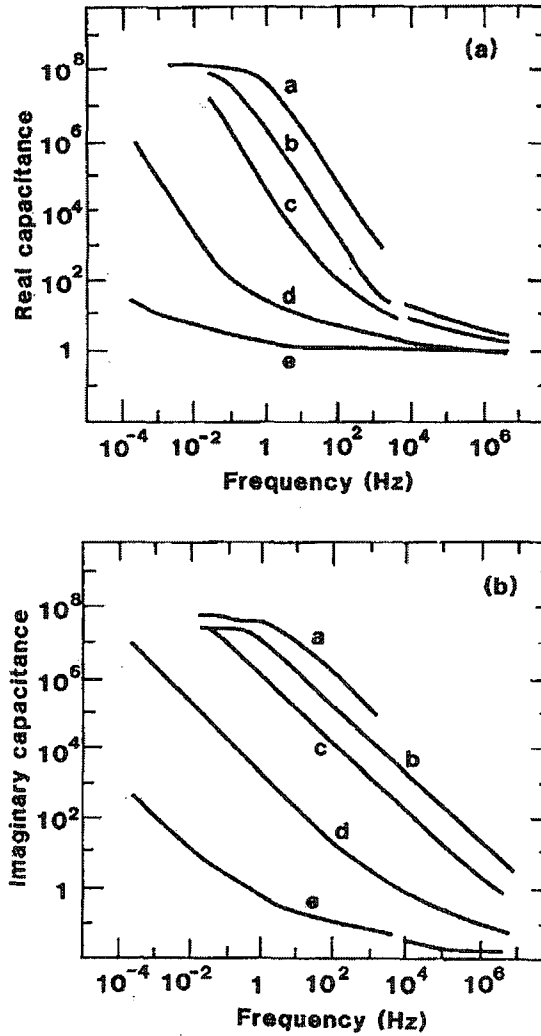
FIG. 1. (a) Real and (b) imaginary parts of the complex capacitance of cement mortar with water/cement ratio 0.78 are depicted as a function of frequency. The capacitance is given in units of the permittivity of space. The measurements were taken after storage of the sample for (a) 3 days, (b) 74 days in air and after heat treatments for (c) 24 h at 333 K, (d) 24 h at 363 K and (e) 24 h at 378 K.

Figure 2.10 (a) & (b): Variation of real and imaginary capacitance with frequency (Berg et al., 1992)

The imaginary impedance maintained more variation at higher frequencies than the real capacitance and it did not seem to converge. The real and imaginary impedances were also measured and shown for the specimen with a water/cement ratio of 0.78 in Figure 2.11.
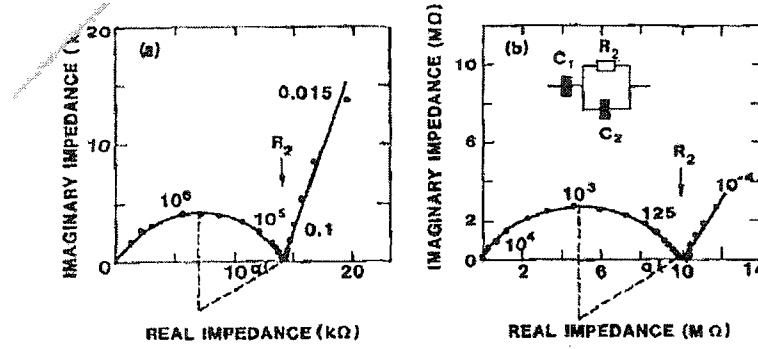
FIG. 2. The imaginary part of the impedance is shown as a function of the real part for mortar with a W/C ratio of 0.78. A constant high frequency capacitance has been subtracted. Points denote experimental values while lines are drawn as a guide for the eye. Frequency values for some experimental points are given in the figures. The measurements were carried out after heat treatment during (a) 24 h at 333 K and (b) 24 h at 363 K. An equivalent circuit that describes our results is given as an inset in (b). Here C_1 and C_2 are constant phase elements, while R_2 denotes the bulk dc resistance and α is the phase angle.

Figure 2.11: Complex impedance plot for mortar
(Berg et al., 1992)

The features of the plot included a straight line at low frequencies and a semi-circular arc with the centre below the axis at high frequencies. The straight line is indicative of a constant phase element (CPE) C_1 and the semi-circle signifies a resistance (R_2) and another CPE (C_2) in parallel, which was in turn the proposed circuit model of mortar. The dielectric response of the element C_1 was proven to be due to electrode polarization, and therefore the other elements of the circuit described the bulk dielectric response of the mortar. The element R_2 was indicated by the intersection with the real impedance axis in the complex impedance plot, while the element C_2 can be calculated by the equation:

$$C_2 = C_{02} \left(\frac{if}{f_0}\right)^{n_2 - 1} \tag{2.1}$$

Where C_{02} is the amplitude and f_0 is the characteristic frequency. The exponent n_2 can be obtained from the angle α by the equation:

$$n_2 = 1 - \left(\frac{2\alpha}{\pi}\right) \tag{2.2}$$

The amplitude C_{02} was obtained numerically from the maximum point of the semi-circular arc in the impedance plot. The conductance of the specimens was also measured over a period of 100 days; the conductance was seen to decrease with time in Figure 2.12, where initially the conductance was higher with increased water content.
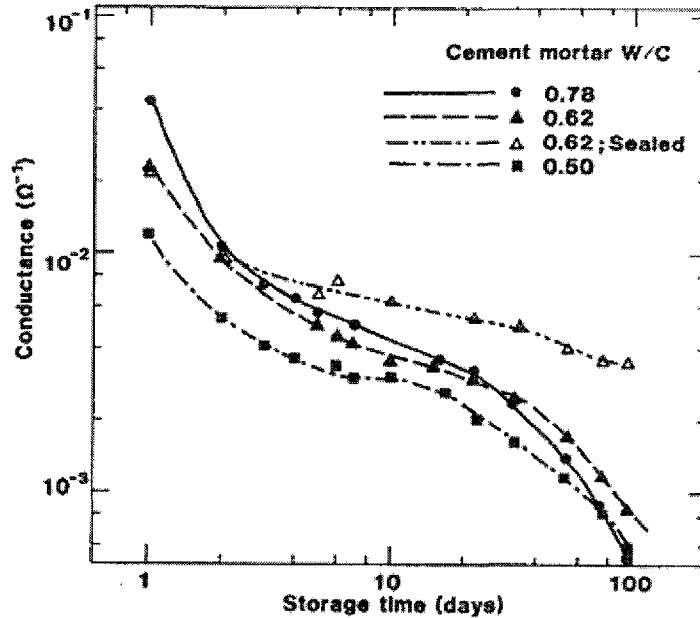
FIG. 3. Conductance as a function of storage time after preparation for cement mortars with different W/C ratios as given in the figure. Results for three samples open to air and a sealed sample with W/C ratio 0.62 are given.

Figure 2.12: Variation of conductance with storage time

(Berg et al., 1992)

While at the end of the storage period the specimen with the highest water content had the lowest conductance, which is due to the fact that this specimen had a higher rate of evaporation than the other specimens and it had lost almost all of the evaporable water by the end of the storage period.

The amplitude of C_{02} was found to be a function of the water content and was independent of the W/C ratio for specimens with a water content greater than 0.4. The exponent n_2 was found to be around 0.7 in this experiment, which agreed with the work of other researchers in this area. Using these parameters it was suggested that that the

16

value of C_2 could be modeled for any cement mortar at any frequency if the amplitude of the said mortar was known. In conclusion it was noted that the higher the W/C ratio of a mortar the higher the initial conductance would be, while also the higher the W/C ratio of a mortar the lower the final conductance would be. Therefore it was proposed that the dielectric response of mortar could be used to estimate the degree of curing as well as the original water content of an unknown mix. An equivalent electric circuit was proposed to be a CPE (C_2) in parallel with a resistance, where the values of the necessary parameters were discovered making the use of this equivalent circuit very plausible to model the dielectric response of a given mortar if the amplitude is known.

This research was helpful in the sense that it helps develop the theory behind the conduction of electricity through a cement material like mortar, and has applications to the masonry industry where it might be possible to estimate the quality or W/C ratio of a given mortar using electrical methods.

2.4   *Concrete*

2.4.1   Electrical Resistivity of Concrete

Whittington et al. (1981) tried to find a relationship among the resistivity of concrete, the ratios of the concrete mix, and the electrical properties of the components of concrete. Another goal of the research was to determine a relationship between the conduction of electricity through concrete and a proposed electrical model.

The importance of this research seems to be that it was the first study on the resistivity of concrete giving the expected result of the electrical resistivity increasing with time. It was proposed that the electrical current applied to concrete would have three possible paths through the concrete including: through the aggregate and cement paste in series, through aggregate particles in direct contact with each other, and through the cement paste only. A schematic is shown in Figure 2.13 which shows the approximate resistivity of the concrete if it took the path indicated in the figure, it should be noted that these values were assumed due to previous research and should not be taken as actual measured values.

17
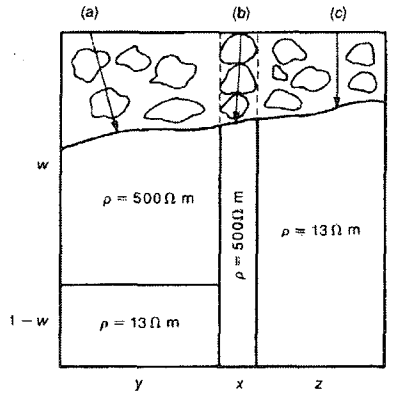
Figure 2.13: Conduction model for concrete

(Whittington et al., 1981)

The figure was helpful in quickly showing that the resistivity of concrete will be much lower if the current only passes through the cement paste and not through the aggregate, as the resistivity of the aggregate is several orders higher than that of the cement paste. Such it is that electrical current will take the path of least resistance through the concrete and will thus pass mostly through cement paste explaining why the resistivity of the concrete is much closer to that of cement paste than the aggregate (Concrete resistivity = 25 to 45 Ω·m, Cement Paste resistivity = 10 to 13 Ω·m and Aggregate resistivity = 5×10^3 to 1×10^6 Ω·m).

After concluding that the current would mostly pass through the cement paste Whittington et al. considered whether the cement paste could be broken down into two components being the free evaporable water and the cement-water paste, and whether the resistivity could be quantified for each component. It was brought to the reader's attention that the amount of evaporable water present in concrete was almost impossible to quantify, as it was difficult to determine the electrical resistivity of the evaporable water and it would also be difficult to determine the electrical resistivity of the compounds of hydration. And it was concluded that taking the paste as a whole which would control the overall resistivity of the concrete, was a more than reasonable assumption. The formation factor (F) was a concept introduced as the ratio of the resistivity of the composite to the resistivity of the matrix, which in the case of concrete would be the resistivity of the concrete to the resistivity of the cement paste. The concrete

18

specimens used were 100 mm cubes with brass plate electrodes on either side of the concrete which also acted as part of the mould during the first 24 hours of specimen life. Along with the 100 mm cubes of concrete, 70 mm mortar cubes were tested for the formation factor because of the high fractional volume of cement paste. There were many different mixes used in the tests as outlined in the paper using normal Portland cement, oven-dried fine aggregate with a specific gravity of 2.65 and coarse aggregate with a grain size no larger than 13 mm and a specific gravity of 2.61. Six specimens were cast for each concrete mix at each W/C ratio. The specimens were removed from the moulds after 24 hours and cured in a water bath at 23°C. The weight of the cubes was measured in order to calculate the density before they were submerged in the water bath. The electrodes were attached to the specimens using a low-resistance cement paste, so the measured resistance values would not be changed. There were also some specimens stored outdoors beneath 200 mm of sand after 13 days of curing inside; this was tested in order to simulate concrete with an outdoor lifespan. Due to the polarization effects discussed earlier, the resistance was measured directly from the specimens using a non-disclosed ohmmeter using a low-frequency alternating current. All of the specimens were tested over a 3 to 4 month period, while the concrete stored outdoors was considered to have experienced a reasonable amount of climate change to simulate the life of an outdoor concrete.

The results for the early life of the concrete and cement paste was found to show a gradual increase of resistivity in concrete until the concrete sets and then the resistivity increases more rapidly, while the cement paste had decreasing resistivity in the first 5 hours before increasing. This decrease in resistivity was thought to be the cause of the hardening of the cement paste being an exothermic reaction which would increase the temperature and therefore, lower the resistivity or due to an increase in the number of ions going into solution. The decrease in resistivity was not present in concrete likely because the concrete has a lower amount of fractional volume of cement paste, or possibly due to the coarse aggregate accepting the heat transfer from the chemical reaction and negating a decrease in resistivity. It was important to note the relationship between the water/ cement ratio and resistivity was inversely proportional, with an increase in the W/C ratio resulting in a lower resistivity overall. The specimens stored in

the water bath were found to reach an almost constant resistivity by about 20 days regardless of the W/C ratio, where the increase in resistivity during the first 20 days was likely due to the loss of evaporable water. The concrete specimens that were cured outdoors were found to have a more variable resistivity over time than the other specimens, and the change in resistivity was assumed to be due to the temperature change over time, which was outlined earlier in the paper to vary with temperature. It was also interesting to note that the temperature coefficient (α) of the cement paste was found to be 0.022/°C and the temperature coefficient of most electrolytes is 0.025/°C. The last thing tested in this study was the formation factor (F) which was found to follow the equation $F=1.04\varphi^{-1.20}$ where φ represents the fractional volume of cement paste present in the concrete tested. This negative linear relationship shows that as φ increases the F decreases which validates the theory shown earlier in the paper, F for a certain mix and W/C ratio is reasonably constant and that the resistivity could be found for mixes with different fractional volumes than the ones used in the study.

The final conclusions of this study were that as the W/C ratio of concrete increased the resistivity decreased showing that the strength decreased as the resistivity decreased. Since the resistivity of the aggregate is almost infinite when compared to that of the cement paste, showing that the resistivity of the concrete is almost completely dependent on the resistivity of the cement paste in the concrete. The electrical resistivity of concrete was directly related to the rate of hydration of the cement paste, suggesting that the strength of the concrete could be linked to the resistivity. This study was very important in setting up the framework for concrete to be studied in an electrical sense by using many different mixes and W/C ratios making the link between many of these variables in concrete and how they affect the resistivity of concrete. The realization that current travels almost entirely through the cement paste in concrete is an important discovery, because it creates a solid foundation for understanding how concrete acts as an electrical material. The use of specimens that were stored outdoors was an interesting idea but the data does not seem as relevant because it was not used in the calculation of the formation factor and the resistivity data was exceedingly variable.

2.4.2   Dielectric Properties of Concrete

The intent of a study by Wilson et al. (1984) was to find if high-frequency impedance measurements could detect entrapped air inside of cast concrete. The other objective was to find the effect of increasing the amount of coarse aggregate on the high-frequency impedance measurements.

The specimens used were 150 mm cube with electrodes on opposite faces with a coaxial connection to the impedance analyzer. The basic concrete mix used had water/cement ratio of 0.5 and cement:sand:coarse aggregate ratio of 1:1.5:3. The variations on this mix were one specimen with 5% more coarse aggregate, one specimen with 5% more air volume, and one specimen with 10% more air volume. All impedance measurements were carried out on the concrete specimens after 6.02 days of setting over the frequency ranges of 1 to 100 MHz and 500 to 700 MHz.

The results of the lower frequency band were collected in Figure 2.14, which shows that the impedance steadily declined with frequency up until 30 MHz where it began to fluctuate.

The fluctuation was accounted to the coaxial to parallel plate transition where minor resonances occurred. It can be noted that between 1MHz and 10MHz all of the mixes had a higher impedance as compared to the normal mix, with the high air mix having the highest impedance and the low air mix having the lowest impedance. At a frequency of 1 MHz the normal mix showed an impedance of around 250 Ω while the other mixes were all near the 300 Ω mark. The results for the higher frequency range are shown in Figure 2.15 which shows an increase in aggregate caused a decrease in resonant frequency, while a large increase in air caused an increase in resonant frequency.
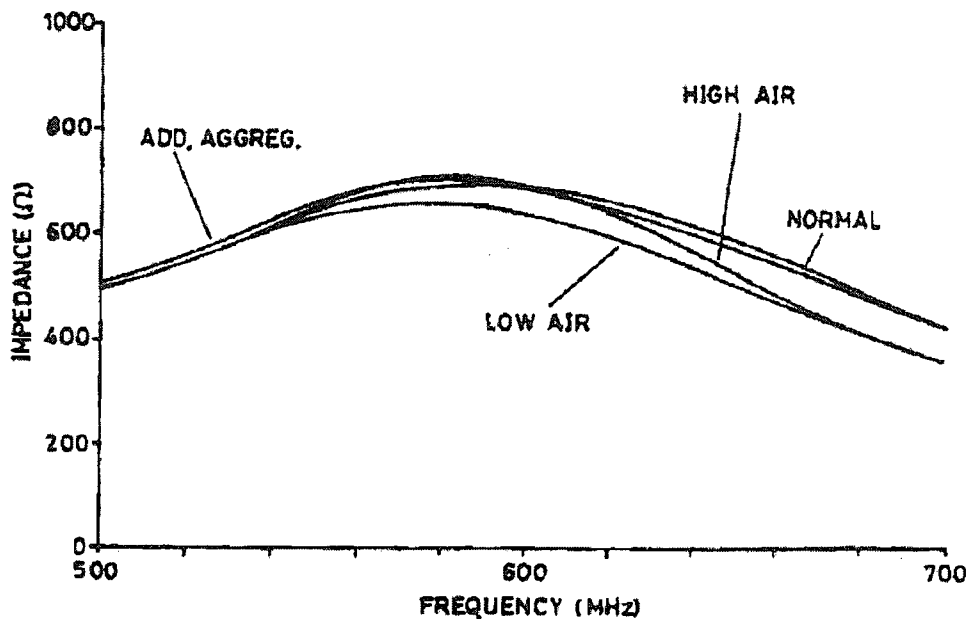
Figure 2.15: High frequency impedance plot of concrete

(Wilson et al., 1984)

The impedance was also measured at specific days over one month where the specimens were stored in a water bath until measurements were taken. Over the low frequency range the impedance at 30 MHz divided by the impedance at 1 MHz appeared helpful as it showed variation between the specimens. As can be seen in Figure 2.16 the specimens with added air had an impedance ratio closer to that of the normal specimen than the specimen with added aggregate.
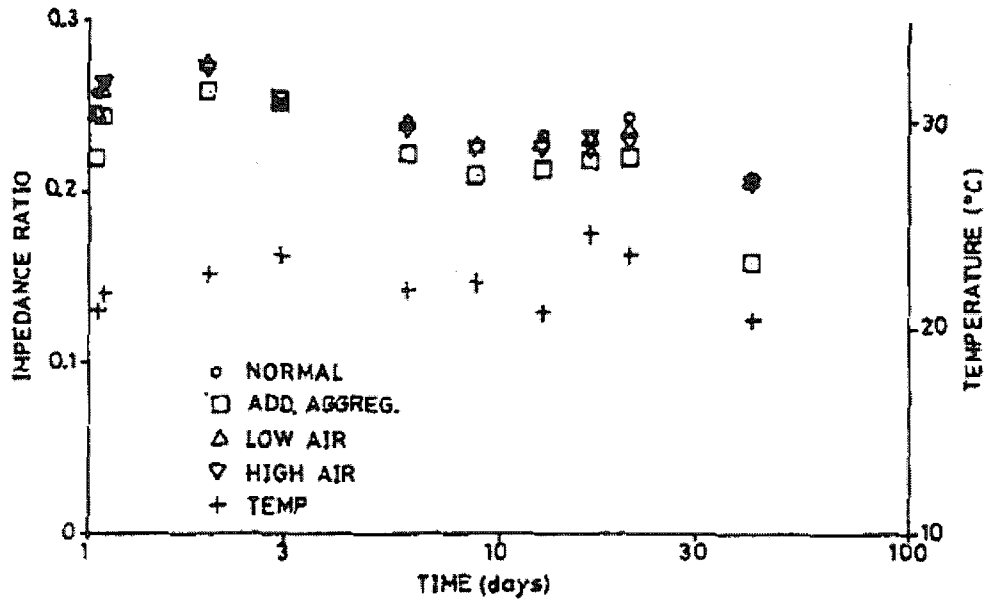
Figure 2.16: Variation of impedance and temperature with time

(Wilson et al., 1984)

This study indicates that it is possible to detect the difference between a specimen with additional air voids and a specimen with excess aggregate. Excess air voids could possibly result in lower strength.

The resistivity and relative permittivity were also calculated using the impedance data collected at 6.02 days. The results for the lower frequency range are given in Figure 2.17 showing a steady decrease in both resistivity and relative permittivity as frequency increased, while the resistivity and relative permittivity had values of 40 Ω and 125 Ω respectively at 1MHz.
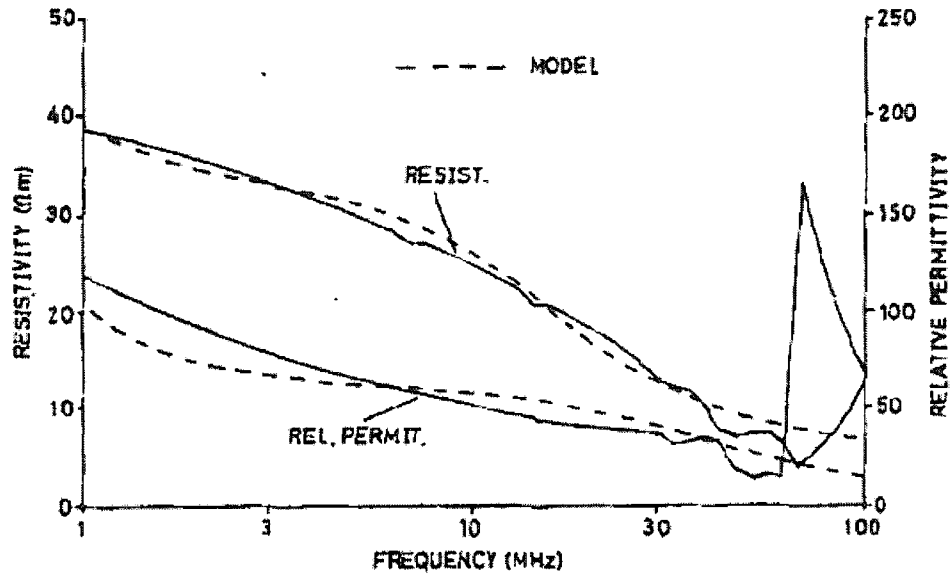
Figure 2.17: Low frequency plot of resistivity and relative permittivity

(Wilson et al., 1984)

The higher frequency range had the results in Figure 2.18 yielding a resistivity over 70 Ω and relative permittivity of 3 at 500 MHz. It should be noted that the results at both frequency ranges should be questioned again due to the coaxial line transition, which were found at about 70 MHz. The very high values of the relative permittivity at low frequencies were estimated to be due to Maxwell-Wagner effects, which assume the current passes through the water which would have a relatively high conductivity. A proposed model for this effect is also shown in Figure 2.17 which accounts for randomly oriented conducting needles and a continuous water channel with a very thin insulating layer of gas generated by electrolytic effects.

24
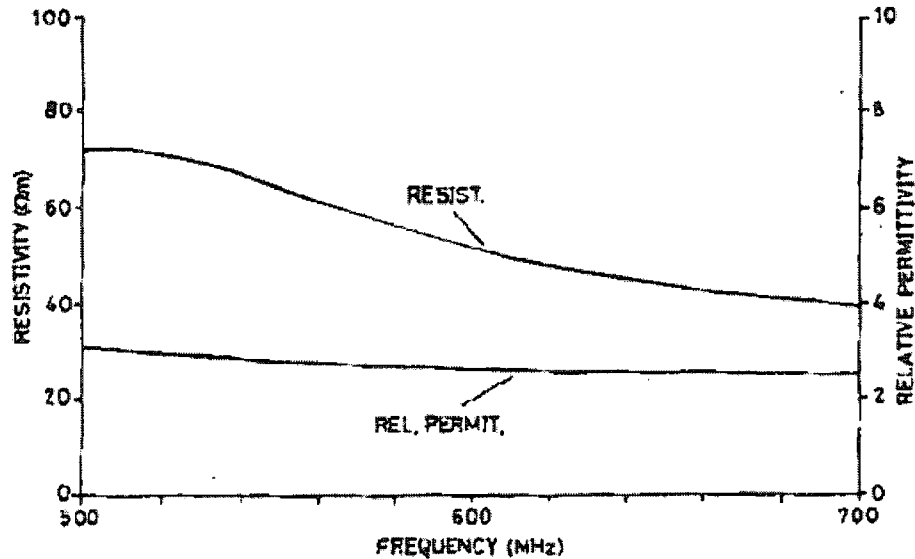
Figure 2.18: High frequency plot of resistivity and relative permittivity (Wilson et al., 1984)

The model gives the general shape of resistivity and relative permittivity but there are discrepancies between the model and measured values. The variation in the values was likely due to the fact that the model assumes the conducting needles throughout the cement paste matrix are the same length, even though concrete can have a great variation in pore sizes.

In conclusion it was found in this study that it was possible to detect small variations in the constituents of concrete. The researchers could have described the impedance measurements at different days and if there was as much variation between mixes as there was at 6.02 days. If the variation was noticeable at 1 day or earlier, there could be more application for this research in terms of detecting the quality of a certain concrete after it is cast in place. Also, it would have been beneficial to see the variation between the mixes beyond 6.02 days and whether the variation increases with time. It is possible the impedance measurements could have been used on concrete that is already in service and whether it has experienced deterioration by comparing it to a test specimen of the same mix.

2.4.3   Relationship between Resistivity and Strength of Concrete

The work of Whittington and Wilson (1986) had the intention of creating a non-destructive test method for concrete using the measurement of electrical properties, with the final result being a quality control test for structural concrete. The purpose of the study was to make an alternative test of concrete strength in comparison to the current tests used to measure the mechanical properties of concrete, as the electrical properties are comparable to the mechanical properties because they both depend on the same chemical reactions that take place in concrete during the hydration process.

An in-depth analysis of the chemistry involved in the hydration on cement was performed in order to appreciate the significance of the electrical parameters used. The main purpose of this analysis was to explain that the water and cement reacted to produce a matrix of compounds making the cement paste, which locks the fine and coarse aggregate together to create concrete. The mechanical and electrical properties of concrete depend on the amount of hydration that the components of concrete have achieved, the way the water is distributed and the condition of the concrete matrix. When it comes to the electrical properties of concrete it can be considered to be a large amount of insulating material (coarse aggregate) imbedded into a conducting matrix of cement paste. The concrete was modeled as two resistances in parallel, one of them representing the aggregate and the other representing the cement paste. Even though the cement paste had a lower volume ratio than the aggregate, it had a lower resistivity and is therefore expected to control the resistivity of the concrete overall.

The specimens used were 150 mm cubes of concrete were used in the experiment along with two 14 SWG stainless-steel electrodes placed on opposite faces to obtain the electrical data. One electrode was also fitted with a temperature sensor in order to take temperature measurements as well. The moulds were made from PVC to accommodate both the 150 mm concrete cube and the electrodes, and when the mould was removed a good bond was found between the concrete and the stainless-steel electrodes. The only concrete mix used in this study incorporated a cement: sand: aggregate ratio of 1:1.5:3 and a water/cement ratio of 0.5. As in previous studies using BS 1881 (1983) as a guideline the concrete was cured for 24 hours and then placed in a water bath at 20°C,

until resistivity measurements were made and the specimens were removed from the bath and allowed to dry for 5 minutes before making the measurements then placed directly back into the bath. The resistivity data was collected using an automatic measurement system making it possible to record the data of 15 different specimens at once, for a complete time cycle of 100 days being the maximum. The specimens were removed from the water bath using an automatic hoist before each resistivity measurement was taken, at a frequency of 2.0 kHz using a square wave AC signal. In order to take the temperature measurements the signal was amplified to 7.2 kHz. The percentage of error in the resistivity measurements was found to be less than 2% if the resistivity measured was greater than 1 $\Omega \cdot m$, which included most of the measurements taken in the study.

The results of the experiment are greatly concluded in both Figures 2.19 and 2.20. Figure 2.19 shows the change in resistivity over time while Figure 2.20 shows the correlation between the strength of concrete and the resistivity. The results in Figure 2.19 are as expected with the resistivity increasing gradually with time until it sets and then increasing more rapidly when it sets.
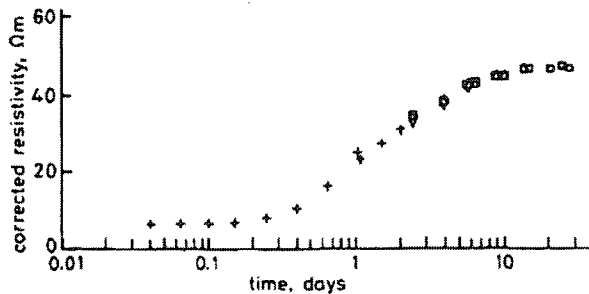
Figure 2.19: Variation of resistivity with time

(Whittington and Wilson, 1986)

The conclusion made by Whittington and Wilson was that the curve in Figure 2.19 could be used in the quality control of concrete, as any concrete with a resistivity measured outside of this calibration curve would be considered suspect.
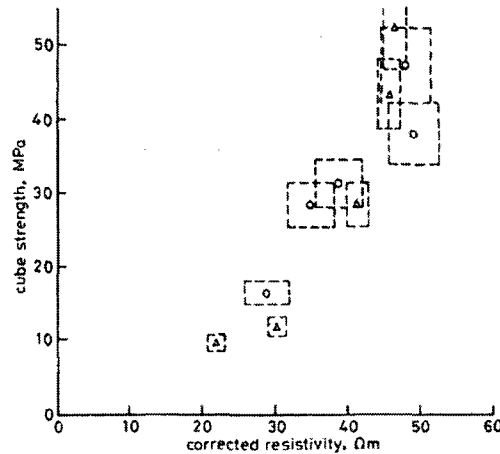
Figure 2.20: Correlation of resistivity and strength

(Whittington and Wilson, 1986)

Figure 2.20 is very ambiguous as the day at which the strength and resistivity were measured is not indicated, and was only said to be between 2 to 28 days. The figure also contains dashed boxes around the data points which indicate the amount of error to be expected from the values obtained. However, conclusion was made by the author that the correlation between resistivity and strength is linear and the resistivity of concrete increases as the strength increases. It should, however, be noted that the increase in resistivity is very small.

2.4.4 Variation of Electrical Properties of Concrete with Frequency

Whittington and Wilson (1990) attempted to propose certain mechanisms which control the conductivity and dielectric constant of concrete in order to develop an electrical model. This electrical model would then be compared with the electrical measurements, with the validity of the model being discussed.

The concrete specimens were cast in a PVC mould with two stainless-steel electrodes on opposite faces. The mould was a 150 mm cube with a coaxial line attached to the electrodes to create a direct link to an impedance analyzer. The specimens remained in the moulds during all measurements. The measurements were carried out on four identical specimens at a frequency range of 1 to 100 MHz, using a HP4191A RF impedance analyzer. The concrete mix used in this study had a water/cement ration of 0.5

and a cement:sand:aggregate ratio of 1:1.5:3. The impedance measurements were taken at a time of 1 hour after the concrete was mixed and 1 day after the concrete was mixed.

The conductivity at 1 hour was found to be constant at 0.2 S/m until about 20 MHz and dropped virtually to zero at 100 MHz. While the conductivity at 1 day was found to be about 0.03 S/m and stayed constant until about 10 MHz and increased to 0.2 S/m at 50 MHz and then back down to zero. The dielectric constant was found to be positive but declining until 2 MHz when it dropped below zero and remained negative up to 100 MHz. While the dielectric constant remained positive but declining until 50 MHz. The results of the electrical experiments could be best explained by electrode polarization, the change in behaviour from homogeneous conduction best described as the Maxwell-Wagner effect and viscous conduction effects.

Electrode polarization occurs when ions reach the electrodes and gas is produced, since concrete is so viscous the gas cannot escape creating another capacitance in parallel to the resistive bulk and causing a low conductivity in concrete. This polarization model is represented by a capacitor in series with a capacitor and resistor in parallel having the impedance:

$$Z = \frac{1}{j\omega C_1} + \frac{R}{1 + j\omega C_2 R} \qquad (2.3)$$

Although the circuit can be made into an equivalent circuit of a resistance in parallel with a capacitor having the admittance:

$$Y = \frac{1}{R_p} + j\omega C_p \qquad (2.4)$$

While the conductivity (σ) and dielectric constant (ε) can be postulated by the equations derived in the text, and were best used to model the conductivity after 1 hour. The result of this model is seen in Figure 2.21 and shows that the polarization model is not accurate at lower frequencies when considering the dielectric constant.
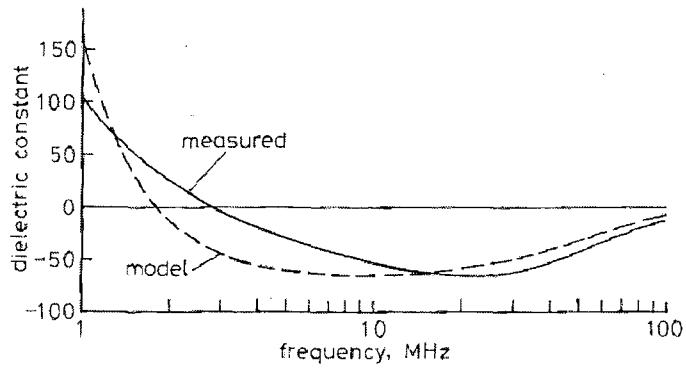
Figure 2.21: Comparison of dielectric constant at one hour

(Whittington and Wilson, 1990)

The model is close from 1 to 10 MHz and it was possible that the polarization mechanism is more complex than the model or the polarization was not complete across the electrode. The Maxwell-Wagner effect occurs when the frequency of a field is greater than the critical frequency and the charge carriers cannot redistribute fully. The cause of the effect is a reduced dielectric constant, an increase in electrical loss and an increase in conductivity. The model produced by the Maxwell-Wagner equations best fits the conductivity and dielectric constant after 1 day which can be seen in Figure 2.22 and Figure 2.23, respectively.
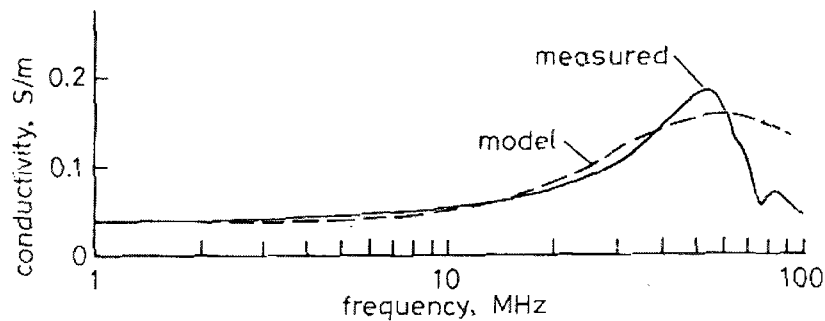
Figure 2.22: Comparison of conductivity at one day

(Whittington and Wilson, 1990)
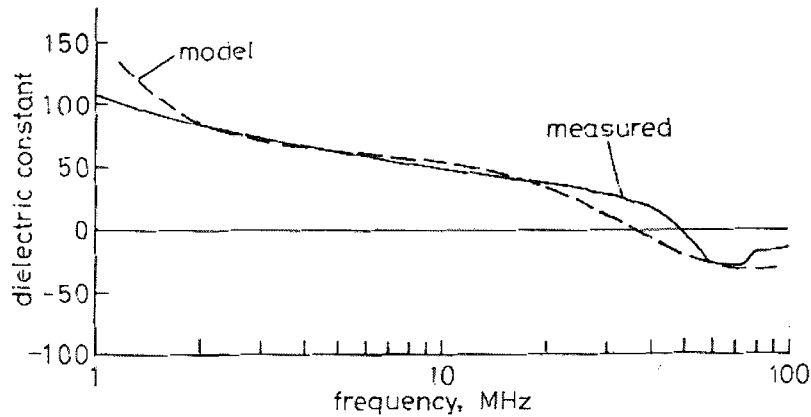
Figure 2.23: Comparison of dielectric constant at one day

(Whittington and Wilson, 1990)

The Maxwell-Wagner model was close to the measured conductivity in Figure 2.22 at low frequencies, but the variance increased as the frequency increased. The model in Figure 2.23 followed the dielectric constant at low and high frequencies. The discrepancy in the Maxwell-Wagner model was most likely due to the assumption of the volume and geometry being fixed, when in reality there can be statistical distribution in these variables. The viscous conduction effect occurs when the ability of an ion to respond to an alternating electric field is restricted because the frequency has reached a cut-off point. This electrical model best represented the conductivity after 1 hour as seen in Figure 2.24. The model closely followed the measured conductivity with variance occurring above 20 MHz.
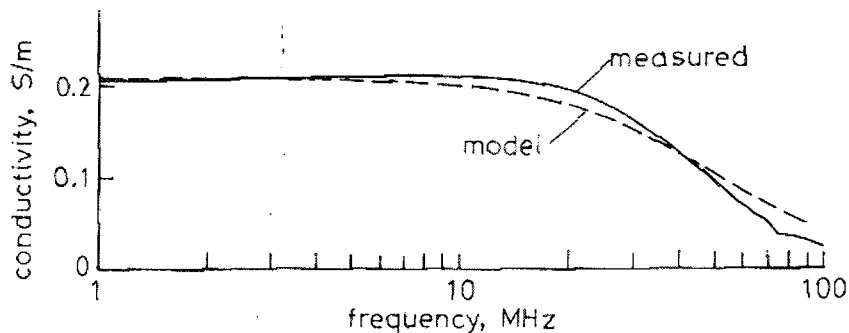
Figure 2.24: Comparison of conductivity at one hour

(Whittington and Wilson, 1990)

31

This research has brought forth three great electrical models of concrete which can each explain the behaviour of concrete as an electrical material in different ways. Although it would be interesting to see if the models could resemble the measured data (conductivity and the dielectric constant), beyond one day possibly including 7, 21, and 28 days which are important days pertaining to concrete strength. If the models made would be verified for these milestones dates in concrete life a decisive connection could be made between the electrical and mechanical properties of concrete.

2.4.5 Effect of Cement Type on the Impedance of Concrete

McCarter (1996) attempted to find the AC impedance response of fresh concrete over a frequency range of 100 Hz to 10 MHz. While the paper also searched for how the use of replacement cementitious materials like pulverized fuel ash (PFA) and granulated blast-furnace slag (GGBS), would affect the electrical properties of concrete. The coarse aggregate used in this study ranged from 5 to 20 mm, and the fine aggregate ranged in size from 150 μm to 5 mm. There were many different mixes used in the study, where the water/cement ratio ranged from 0.38 to 0.56. Ordinary Portland Cement (OPC) and Sulphate-Resisting Portland Cement (SRPC) were used as the main cements in this study, while PFA and GGBS were used at 30% and 50% replacement respectively.

As in studies completed previously by this author the concrete specimens used were 150 mm cubes with two 150 mm stainless-steel electrodes attached to opposite faces in order to take electrical measurements. For each mix used in the study three specimens were tested for their electrical properties over a frequency range of 100Hz-10MHz using a Solartron 1260 impedance analyzer. The electrical measurements were taken 30 minutes after each concrete specimen was mixed. The results of the measurements taken on the mixes containing only OPC can be seen in Figure 2.25.
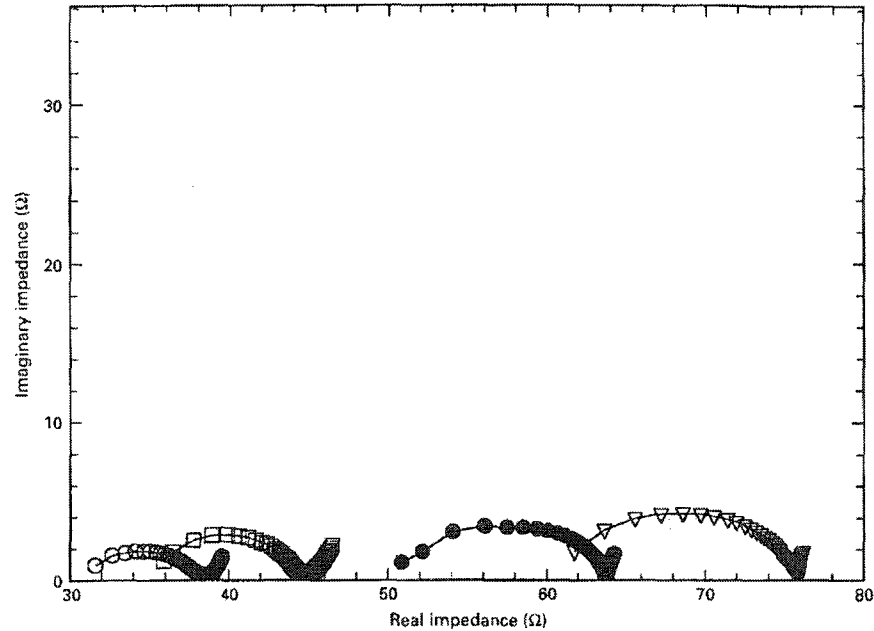
Figure 1 Complex impedance spectra for OPC concretes: (∇) Mix 1, water content 135 kg m⁻³; (□) Mix 3, water content 180 kg m⁻³; (●) Mix 7, water content 150 kg m⁻³; (○) Mix 10, water content 215 kg m⁻³.

Figure 2.25: Complex impedance plot for Portland cement
(McCarter, 1996)

From the figure it is seen that with the increasing water content there was a decrease in real impedance (resistance) and only a slight decrease in the overall imaginary impedance (reactance). The impedances were found overall to be less than 80 Ω at any frequency or using any mix, with the shape taking on a decreasing line into an arc as the frequency increases. The bulk resistance of the concrete (R_{bulk}) was found to be the intercept of the impedance arc with the Real impedance axis. R_{bulk} was found to decrease as the water content in the OPC concrete increased. When the cementitious replacement GGBS and SRPC were used the results are displayed in Figure 2.26, it was found that the specimens using GGBS had a higher R_{bulk} than the specimens only using OPC.
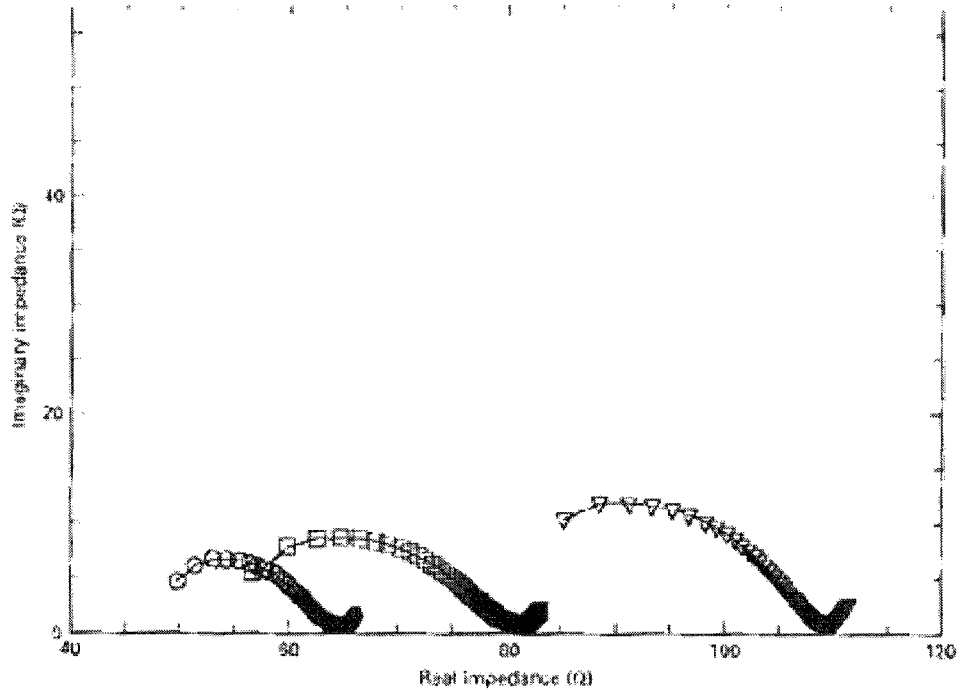
Figure 2.26: Influence of cement product used on impedance plot

(McCarter, 1996)

This increase in R_{bulk} was likely due to the reduction of cement paste which is inherently the path through the concrete, making it more difficult for the electricity to pass through the concrete and increasing R_{bulk}. The use of SRPC also increased R_{bulk} over OPC, which was due to rapid hydrolysis and the smaller amount of free water for the electricity to pass through. The results of the concrete using PFA replacement are found in Figure 2.27, agreeing with the OPC specimens that with increasing water content R_{bulk} decreased.
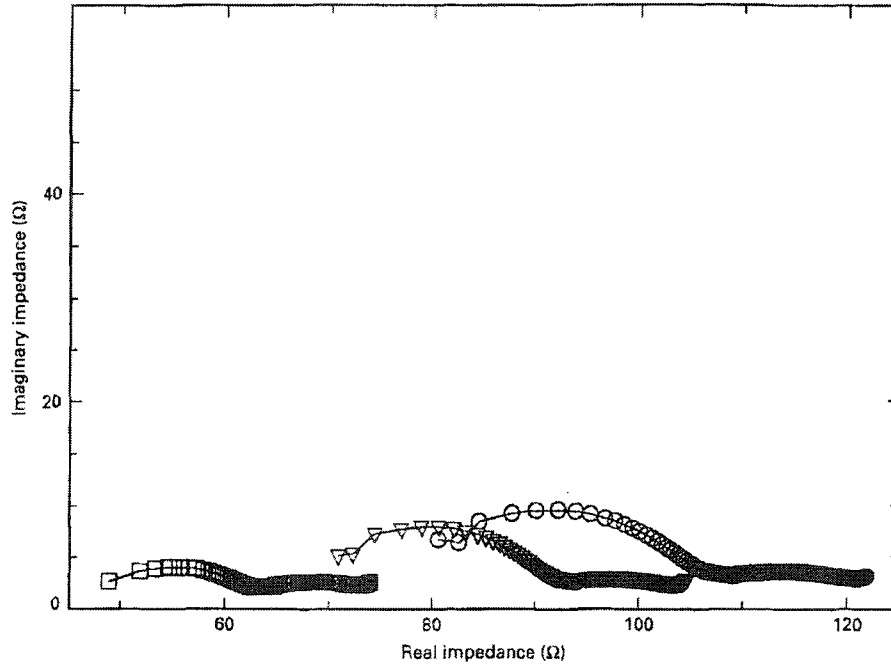
Figure 3 Complex impedance spectra for PFA concretes. (□) Mix 2, (○) Mix 8, (▽) Mix 9.

Figure 2.27: Influence of using PFA on impedance plot
(McCarter, 1996)

The variance in R_{bulk} seemed to be larger than that of OPC while the difference in water content was considerably lower, therefore a change in water content had a larger effect on the R_{bulk} of PFA concretes than OPC only concretes. The figure also presents a flatter and distinctively different curve than the OPC concretes, making it apparent that the impedance measurements are a practical procedure to determine the presence of PFA in concrete. This was the most practical discovery of this study, but the fact that PFA is present in concrete does not have that much relevance from a civil engineering perspective. The only relevance occurs if the amount of PFA used in the concrete can be determined before setting and whether it complies with specifications. The paper also introduced the fact that impedance measurements can be inconsistent at high frequencies, which is important for future researchers to consider.

2.4.6 Electrical Properties of Concrete and Concrete Constituents

Wilson and Khalaf (1999) considered the use of electrical measurements to determine the movement and special distribution of water within freshly mixed concrete. Using this technique to determine the moisture content, rates of water absorption and absorption of the individual components of concrete could be used to create a model for how concrete resists electrical current. In order to create greater differentiation between all of the specimens, two types of sand were used along with three types of coarse aggregate and one type of ordinary Portland cement.

The moulds used in this study were plastic 150 mm cubes with two stainless-steel plates on either side of the cube which were used as electrodes. The first specimens cast were a cement paste with a water/cement ratio of 0.3, which had a temperature sensor placed inside of the paste which recorded the temperature during all of the electrical measurements. Next there were four different concrete mixes tested that had a W/C ratio of 0.55 and roughly the same cement:sand:aggregate ratio of 1:2.20:3.30, while all of the specimens used a different coarse aggregate including whin, quartz, granite and oven-dried whin. Before the cement products were tested the coarse and fine aggregates were saturated and tested for the resistance using an impedance analyzer at a frequency of 10 kHz, then the cement paste and concretes were tested in the same manner.

The resistance plot for the aggregates was high initially but then dropped rapidly until about 200 minutes where the final resistance was found to be higher for the coarse aggregate (1000-2000 Ω) than the fine aggregate (600-800 Ω). It was also found that the resistance changed with the type of aggregate used, where quartz had the highest resistance among the coarse aggregate and concrete sand had a higher resistance than the builder's sand. The final resistance of the cement paste (16 Ω) was found to be much lower than the aggregate with the resistance increasing over time instead of decreasing, while the temperature also increased with the time and resistance of the cement paste. It was concluded that changing the type of aggregate would change the resistance of the concrete, the aggregates can be ordered by final resistance from highest to lowest as: whin (75 Ω), oven-dried whin (70 Ω), quartz (65 Ω) and granite (50 Ω).

The fact that the resistance of the concrete is considerably lower than that of either type of aggregate is further proof that the cement paste is the primary factor governing the electrical resistance of concrete. From this research it would seem that the type of coarse aggregate used should be another factor to consider when trying to employ the electrical properties of concrete to conclude the mechanical properties of concrete. But the variation is so small between the resistance values found that it seems almost trivial to consider this as well, because the mix proportions and W/C ratio will have the biggest impact on the electrical properties of concrete.

2.4.7 Determination of Concrete Setting Time

Manchiryal and Neithalth (2008) observed the effect that changing the water/cement ratio, fly ash content, aggregate/cement ratio and aggregate size had on the dielectric response of cement paste and concrete. The cement paste was cast in acrylic moulds sized 50 mm x 50 mm x 150 mm, where stainless steel plates (0.75 mm thick) were placed on either side of the mould after the cement paste was added. An impedance analyzer was connected to the moulds via alligator clips and impedance measurements were taken over a frequency range of 1 Hz to 1 MHz, where the bulk resistance was taken as the intercept with the real axis in the complex impedance plot. Measurements for the cement pastes were taken every 15 minutes for the first 6 hours then every 30 minutes for the next 3 hours and after the conductivity became more gradual every 6 hours.

The concrete mixes were cast in acrylic moulds with the dimensions 75 mm x 75 mm x 250 mm with stainless steel plates of the same thickness placed at 50 mm from the edges of the mould. The impedance measurements were carried out in the same manner as the procedure described for the cement pastes. After 24 hours the concrete specimens were removed from the moulds and either placed in a saturated limewater bath (saturated specimens) or covered in a non-conducting water resistant tape and stored at 70% RH and 23°C ± 2°C (sealed specimens).

The conductivity-time plots created were divided into 5 distinct phases including: Phase 1 implicating the zone where the conductivity is maximum and constant, Phase 2 representing the zone where the conductivity began to slowly drop, Phase 3 (3 to 12

hours) showing a faster rate of decrease in conductivity, Phase 4 the decrease in conductivity became more gradual and finally Phase 5 where the slow and steady reduction of the conductivity occurred until it became almost constant. In Figure 2.31 it can be seen that the cement paste with no fly ash had a higher conductivity during Phase 1 than the specimens with fly ash and the specimen with the lowest W/C ratio (0.32) and highest fly ash replacement (20%) had the lowest overall conductivity.
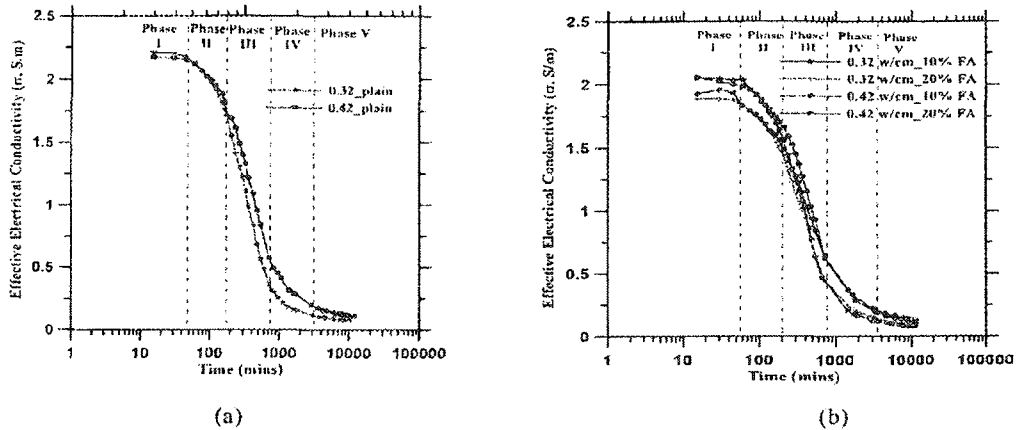
Figure 1--Effective conductivity variation with time for: (a) plain cement pastes, and (b) for pastes with fly ash replacements

Figure 2.28: Effective conductivity of cement pastes

(Manchiryal and Neithalth, 2008)

An equation for the effective conductivity for cement pastes and concretes was suggested by the author to be:

$$\sigma_{eff} = \sigma_f + \frac{\sigma_0 - \sigma_f}{1 + \left(\frac{t}{t_s}\right)^b}$$

(2.5)

Where σ_f is the conductivity in Phase 5, σ_0 is the conductivity in Phase 1, t_s is the final setting time, and b is a constant determined by experimental procedure. This model seemed to be quite accurate for both cement pastes and concretes as the model gave an R^2 value of 0.99 when the model was compared to the experimental data collected. From all of the concrete specimens tested the following observations were made: the use of fly ash substitution decreased the conductivity in Phase 1 and 5, the higher the aggregate to cement ratio was the lower the conductivity was and the curing condition had no effect on

the specimens during the first 24 hours while the conductivity for the saturated specimens was higher than the sealed specimens beyond 24 hours.

The reduced conductivity in the specimens containing fly ash was explained by the reduction of cement content and therefore a reduction in the amount of ions available to carry charge. The fly ash content and the W/C ratio were found to be the parameters that effected the setting time the most. The fact that the setting time was found to be related to the effective conductivity in the model showed it could be possible to determine the setting time by taking conductivity measurements on a certain concrete. This would be an important discovery indeed as it would be possible to know when a concrete in the field has become fully set by taking conductivity measurements and whether construction could continue over the concrete already cast.

2.5   *Summary*

There were many studies completed within the scope of electrical properties of cement materials and the beginning of classifying concrete as an electrical material. While some main conclusions can be made from all of the studies previously completed stating with the fact that the ability of concrete to resist electric current is reduced as the amount of water in concrete increases. The ability of concrete to resist electric current increases as the concrete ages and free water evaporates from the surface.

Possibly the most relevant finding is the fact that the electrical properties of concrete rely heavily on the cement paste created inside of the concrete matrix during the hydration process. While all of these findings have been made, work needs to continue in this area in order to create a definite relationship between the strength of concrete and its electrical properties.

3   EXPERIMENTAL PROGRAM

3.1   *Concrete Materials*

The concrete and cement paste used in this study consisted of the following components: cement, sand, coarse aggregate and water. The Type 10 Portland cement (CSA A23.1/A23.2, 2009) was used for both the concretes and cement pastes used in the experimental program.

Fine sand that conformed to Canadian Standard specification (CSA A23.1/A23.2, 2009) was used as the fine aggregate in the concrete mixes. To ensure the sand met the standard three separate sieve analyses were performed using a mechanical sieve shaker on a 750 g sample in each test. The results of the sieve analysis were found to be between the upper and lower limits recommended in CSA A23.1/A23.2, and the average of the three sieve analysis tests can be seen in Figure 3.1.
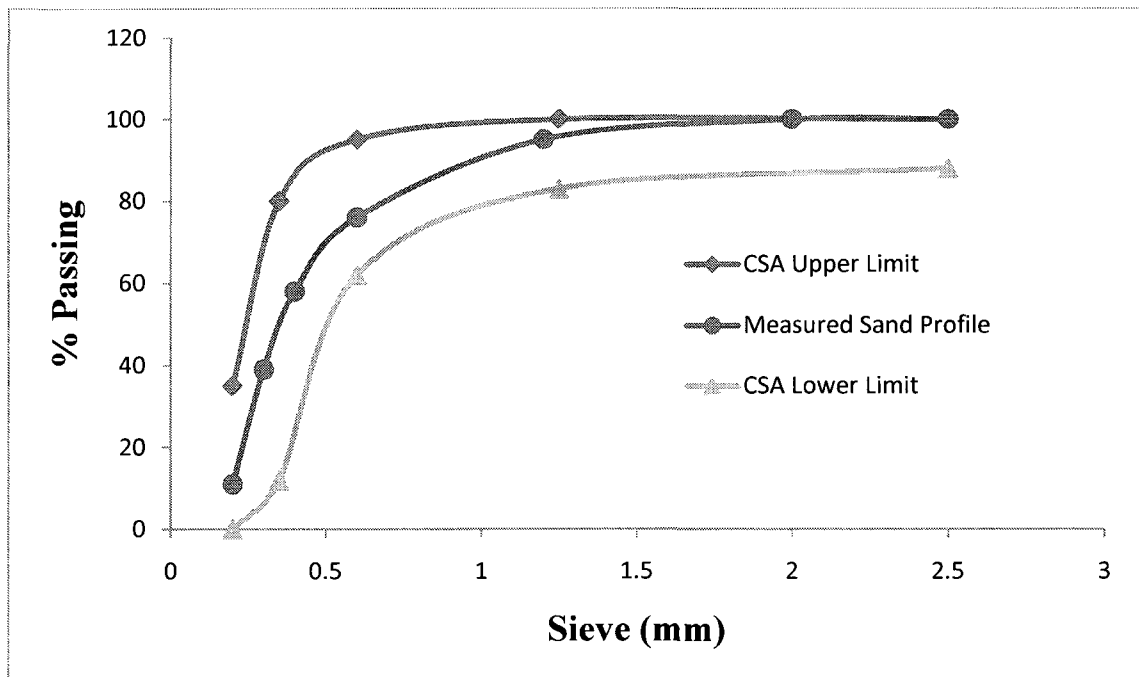
Figure 3.1: Sand gradation results

The coarse aggregate used in the concrete mixes was Forwell crushed stone (Figure 3.2) that contained stones as large as 10 mm in diameter while also consisting of very fine particles. Therefore, a grain size analysis was required in order to find the variation in

size of the coarse aggregate used in the concrete for the experimental program. A list of the sieve numbers and the corresponding grain sizes can be found in Table 3.1. Three sieve analyses using a mechanical sieve shaker were performed using a 750 g sample for each test. The average percent passing and average percentage by weight were found from the three separate tests and the results can be seen in Table 3.2.
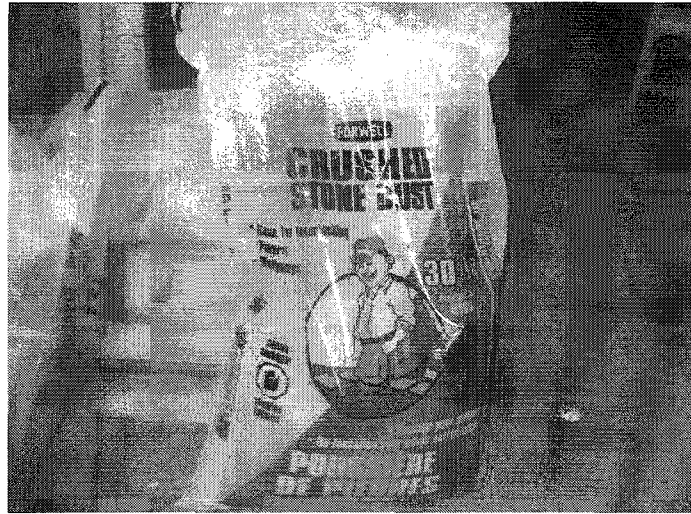
Figure 3.2: Crushed stone dust used in experimental program

Table 3.1: Standard sieve sizes

Mesh	Standard Opening Size (mm)
No. 16	1.18
No. 10	2.00
No. 7	2.80
No. 6	3.35
No. 4	4.75
$\frac{3}{8}$ in	9.50

Note: Larger sieve openings (1 in to $\frac{1}{4}$ in) are designated by a sieve mesh size that corresponds to the size of the opening in inches, while smaller sieve mesh sizes of $3\frac{1}{2}$ to 400 are designated by the number of openings per linear inch in the sieve.

Table 3.2: Grain size analysis results

Mesh	Average % Weight	Average % Passing
Tray	45.16	N/A
No. 16	14.76	45.17
No. 10	10.33	59.93
No. 7	5.62	70.26
No. 6	12.65	75.88
No. 4	10.36	88.53
$\frac{3}{8}$ in	1.11	98.89

It is apparent from Table 3.2 that over 45% of the crushed stone was very fine dust, smaller than 1.18 mm (Sieve No. 16). If these fine particles were considered to be part of the coarse aggregate the concrete mix would become very inaccurate. The crushed stone was then processed through a larger sieve to separate the desired size of stone from the dust particulate. The desired stone size was in the range of 5 mm, due to the relatively small size of the concrete moulds used to acquire electrical data in the experimental program. A larger sieve machine was used to collect the aggregate between Sieve $\frac{3}{8}$ in (9.50 mm) and Sieve No. 8 (2.36 mm), it should be noted that Sieve No. 8 (2.36) was used in place of Sieve No. 7, as Sieve No. 7 was not available for the larger mechanical sieve machine. Therefore, the concrete mixes used in this study incorporated a coarse aggregate with the minimum grain size of 2.36 mm (Sieve No. 8) and a maximum grain size of 9.5 mm (Sieve. No. $\frac{3}{8}$ in). The results of the three sieve analyses along with the average values can be found in Figure 3.3.
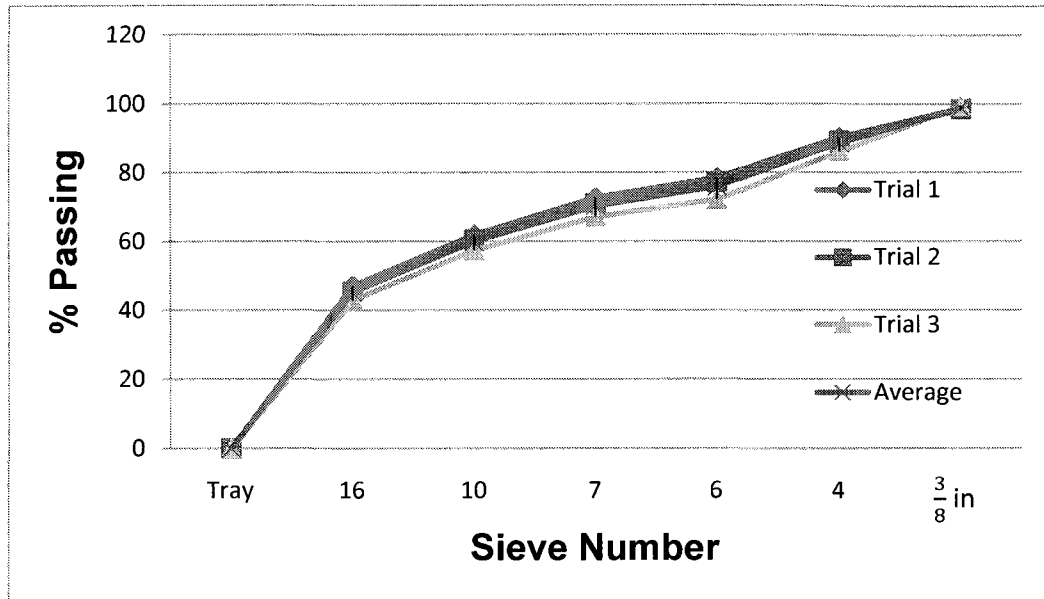
Figure 3.3: Results of sieve analysis on coarse aggregate

The water used for all of the concrete and cement paste mixes was regular drinking water from the tap collected on site in the University of Windsor concrete casting lab located in 19B Essex Hall.

3.2 *Concrete and Cement Paste Mixes*

Three different concrete mix trials were mixed in order to find the optimum concrete mix for each phase of the study. Each component of the concrete mix was measured accurately using a scale (accurate to 0.1 g). The trial mixes were then poured into a mould and removed after 24 hours to determine the qualities of each mix. All of the n mixes were cast in 50 mm steel cube moulds which can be seen in Figure 3.4. A base mix (A1) was established using a cement:sand:coarse aggregate (C:S:A) ratio of 1:2:3 and a water/cement (W/C) ratio by weight of 0.5. In most civil engineering construction, a W/C ratio of 0.4 to 0.6 is chosen when no admixtures are used. Hence, in this study, a W/C ratio of 0.5 was chosen as the reference value. It was found that a W/C of 0.5 provided a mix with good workability. Along with this base mix several other mixes (A2 to A5) were cast with the same C:S:A ratio but with different W/C ratios in order to determine the best possible mix. The mixes of Trial I can be seen in Table 3.3.

Table 3.3: Concrete mixes of Trial I

Material	A1 Base Mix		A2		A3		A4		A5	
	Weight (g)	% Weight	Weight (g)	% Weight	Weight (g)	% Weight	Weight (g)	% Weight	Weight (g)	% Weight
Cement	48	15.38	48	15.38	48	15.38	48	15.38	48	15.38
Sand	96	30.77	96	30.77	96	30.77	96	30.77	96	30.77
Coarse Aggregate	144	46.15	144	46.15	144	46.15	144	46.15	144	46.15
Water	24	7.69	36	11.54	42	13.46	48	15.38	54	17.31
W/C Ratio	0.5		0.75		0.875		1		1.125	
C:S:A Ratio	1:2:3		1:2:3		1:2:3		1:2:3		1:2:3	
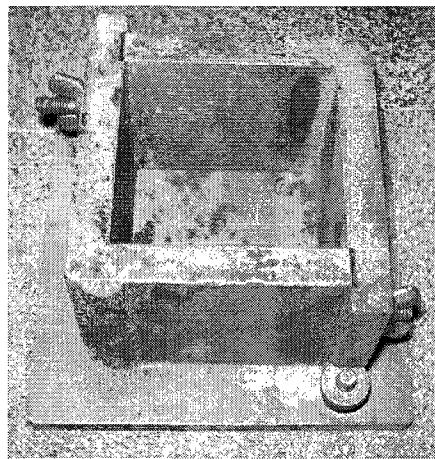
Figure 3.4: Steel cube mould

The concrete samples of Trial I were removed from the moulds after one day to investigate the quality of each concrete mix. After inspecting each specimen it was found that each mix produced an excess of voids around the surface of the mould. This indicated that the amount of coarse aggregate in the mix required reduction in the next trial of concrete composition. Therefore, none of the mixes in Trial I were chosen for this study.

Trial II of the concrete composition consisted of a lesser amount of coarse aggregate (crushed stone) in the base mix (B1) and larger amounts of sand and cement. Mixes B1, B2, and B3 all followed this general trend while mix B4 was created to give a particular

W/C ratio of 0.5 with increased workability. The different mixes of Trial II are outlined in Table 3.4

Table 3.4: Concrete mixes of Trial II

Material	B1 *Base Mix*		B2		B3		B4	
	Weight (g)	% Weight	Weight (g)	% Weight	Weight (g)	% Weight	Weight (g)	% Weight
Cement	60	19.61	72	23.53	84	27.45	79.8	26.08
Sand	102	33.33	114	37.25	126	41.18	126	41.18
Coarse Aggregate	108	35.29	84	27.45	60	19.61	60	19.61
Water	36	11.76	36	11.76	36	11.76	40.2	13.14
W/C Ratio	0.6		0.5		0.43		0.5	
C:S:A Ratio	1:1.7:1.8		1:1.6:1.16		1:1.5:0.7		1:1.6:0.75	

As with the previous trial, the samples of Trial II were removed from their moulds after one day of curing time and inspected for quality. It was determined that mix B4 was the best possible mix in Trial II because it contained very few voids and possessed a desired W/C ratio of 0.5. Therefore, mix B4 was chosen as the best possible concrete mix for the small moulds used in this study, and mix B4 was considered as **Concrete Mix I** in the experimental program. The cement paste mixes did not require composition trials because the only materials used in cement paste are cement and water, the cement paste mixes used in the experimental program are in Table 3.5.

Table 3.5: Cement paste mixes

Material	Cement Paste Mix I (C)		Cement Paste Mix II (D)	
	% Weight	Weight (g)	% Weight	Weight (g)
Cement	62.0	248	72.0	600
Water	38.0	152	28.0	235.96
W/C Ratio	0.62		0.39	

After Concrete Mix I was established another concrete mix was desired that contained the smallest amount of cement possible. Trial III of the concrete composition consisted of a reduced amount of cement and water as compared to Concrete Mix I (Mix B4 in Table

3.4). Hence, the amount of coarse aggregate (crushed stone) increased by weight. The mixes tested in Trial III can be seen in Table 3.6.

Table 3.6: Concrete Mixes of Trial III

Material	C1		C2		C3	
	Weight (g)	% Weight	Weight (g)	% Weight	Weight (g)	% Weight
Cement	55.8	18.2	45	14.7	43.8	14.3
Coarse Aggregate	138	45.1	129.4	42.3	144	47.1
Stone	72	23.5	98.5	32.2	78	25.5
Water	40.2	13.1	36.1	11.8	40.2	13.1
W/C Ratio	0.72		0.8		0.92	
C:S:A Ratio	1:2.5:1.3		1:2.9:2.2		1:3.3:1.78	

During casting it was apparent that mix C3 could not be used simply because the cement required to complete hydration was not present in the mix. For this reason only mix C1 and C2 were considered for use in the experimental program. After removing the specimens from the moulds one day after casting, there was little difference in the quality of the two specimens. Therefore, mix C2 was found to be the mix with the lowest amount of cement possible in a concrete mix and mix C2 was referred to as **Concrete Mix 2** during the remainder of the experimental program. Hence, the four mixes which were finally chosen in this study were Cement Paste Mix I, Cement Paste Mix II, Concrete Mix I, and Concrete Mix II. It can be noted that Cement Paste Mix II had the highest proportion of cement content where as Concrete Mix II had the lowest proportion of cement content.

3.3   Development of Concrete Moulds

The determination of the electrical properties of concrete was one of the main focuses of the experimental program. Therefore, the best possible technique for acquiring the electrical data was considered a very important aspect of the experimental program. The initial attempt at acquiring the electrical properties of concrete involved attaching steel electrodes to two opposite parallel surfaces of the concrete cubes using aluminum tape (Figure 3.5 a), and recording the electrical values using an APPA-95 multimeter (Figure

3.5 b). This process resulted in unusual electrical values. For example the resistance (R) of concrete after one day was found to be around 25 MΩ and the capacitance (C) was found to be around 50 nF, which seemed unusual when compared to the data reported by other researchers in this area of this study. Hence, this method of electrode assembly was abandoned and in subsequent trials, aluminum electrodes were embedded into the concrete instead.
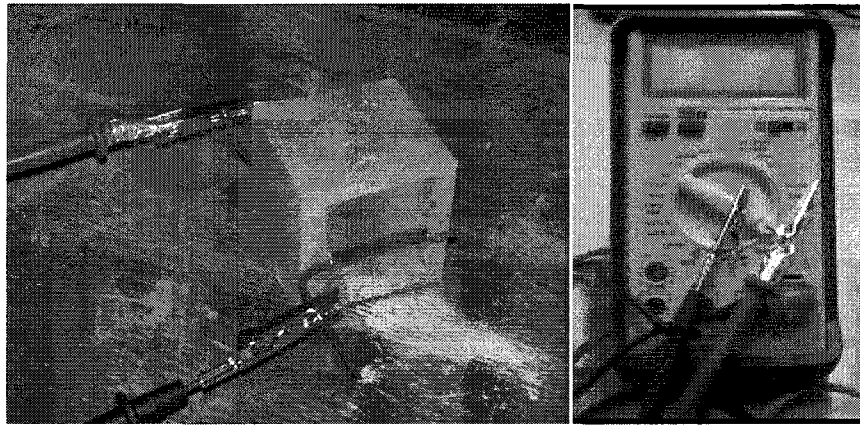
Figure 3.5 (a) and (b): (a) Concrete cube with face electrodes and (b) APPA multimeter

The use of embedded electrodes began with altering the 50 mm steel cube moulds to accommodate three aluminum plates spaced at 10 mm and 20 mm respectively (Figure 3.6).
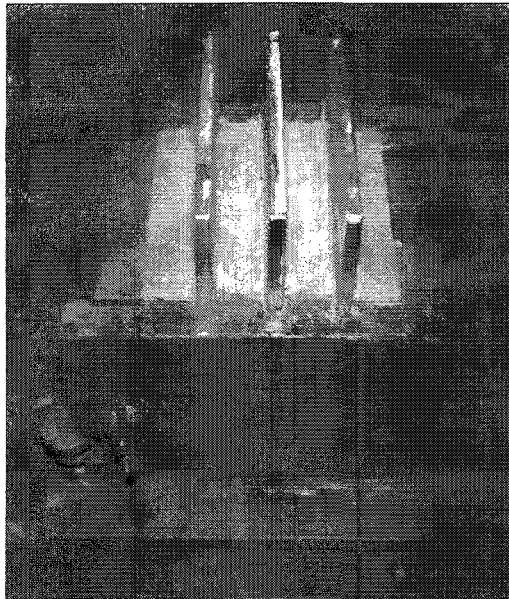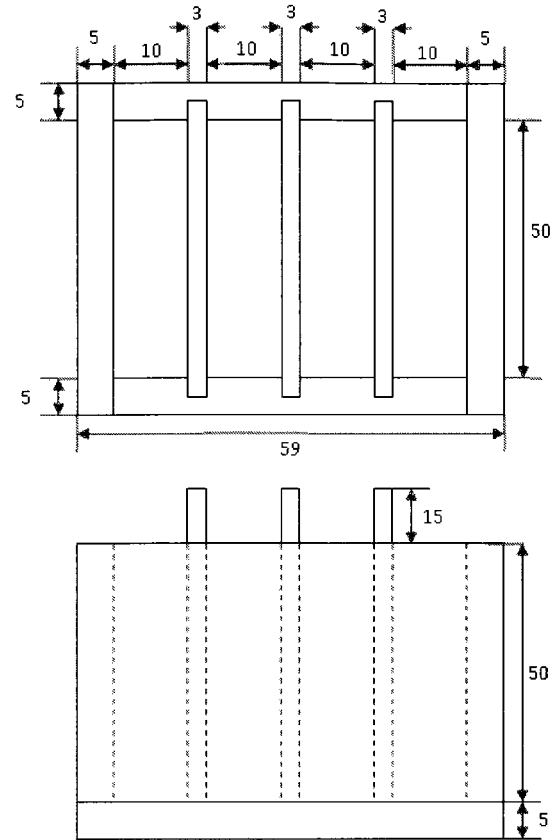
(a) Photo   (b) Sketch

Figure 3.6: Concrete cube with embedded aluminum electrodes

Prior to testing, the concrete samples were required to be removed from the steel mould. This was due to the fact that the contact between the aluminum electrodes and steel mould was assumed to create a short circuit resulting in erroneous electrical data. Although it was observed that as the set concrete was removed from the moulds a weak bond existed between the concrete and aluminum electrodes which caused the electrode to segregate from the concrete. Hence, the use of this type of mould was then disregarded as the concrete sample could not be removed from the mould. Therefore, the use of an electrically non-conductive material was chosen in order to proceed with the experimental program.

New moulds were built using acrylic which is a non-conductive material. Aluminum plates of 4 mm thickness were used as electrodes. Three different moulds were designed in order to study the effect that the electrode contact area and distance between the electrodes had on the electrical properties of the concrete. The details of each mould can be seen in Table 3.7, and the moulds themselves can be seen in Figure 3.7, Figure 3.8 and Figure 3.9.

Table 3.7: Dimensional properties of concrete moulds

	Concrete Mould I	Concrete Mould II	Concrete Mould III
Specimen Cross-Section	50 mm x 50 mm	100 mm x 100 mm	200 mm x 200 mm
Number of Electrodes	2	3	3
Electrode Spacing(s)	20 mm	20 mm and 40 mm	40 mm and 80 mm

*Specimen cross-section refers to the area of contact between concrete and one face of each electrode.
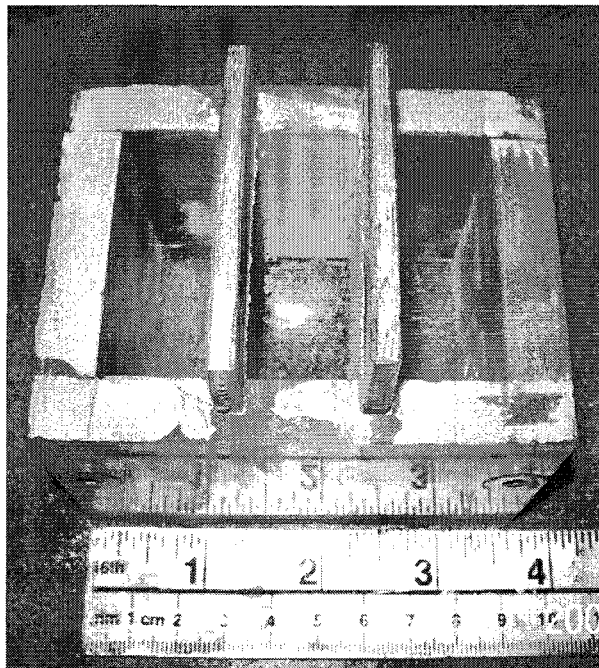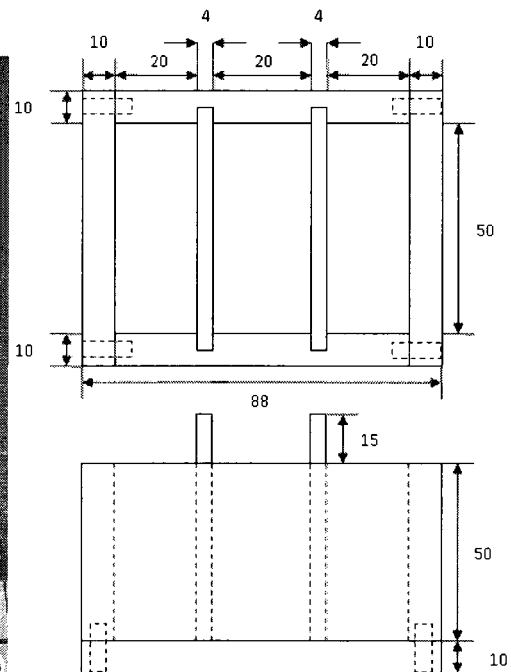
(a) Photo   (b) Sketch

Figure 3.7: Concrete Mould I

49
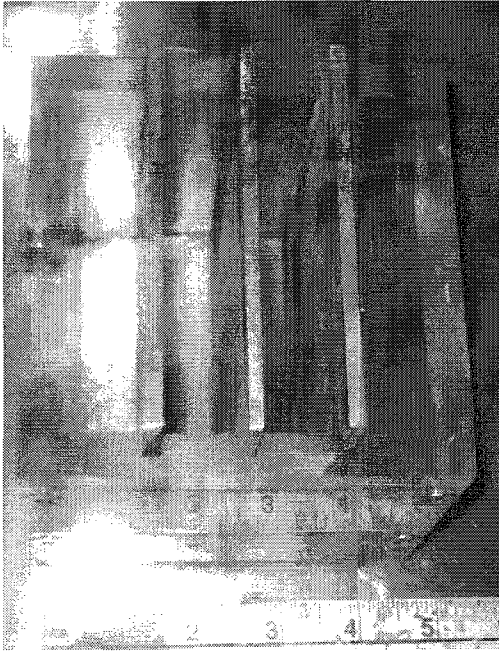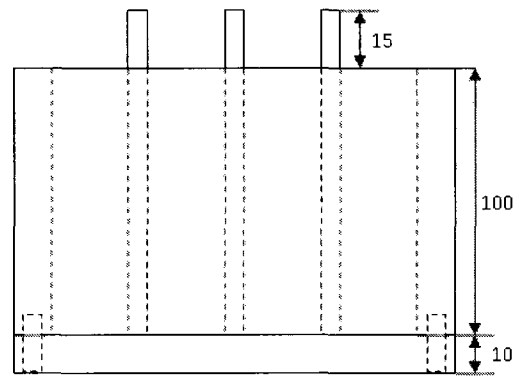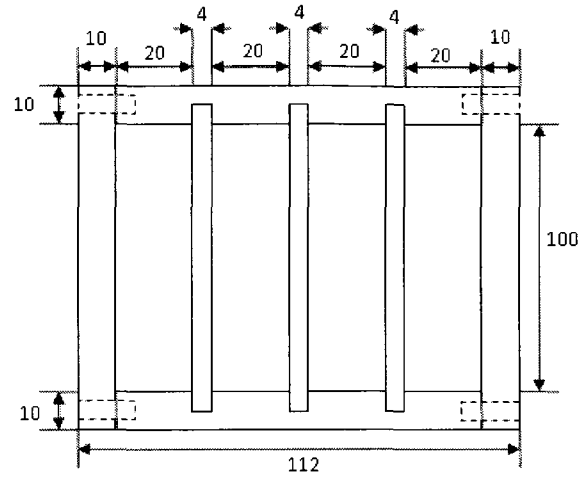
(a) Photo   (b) Sketch

Figure 3.8: Concrete Mould II
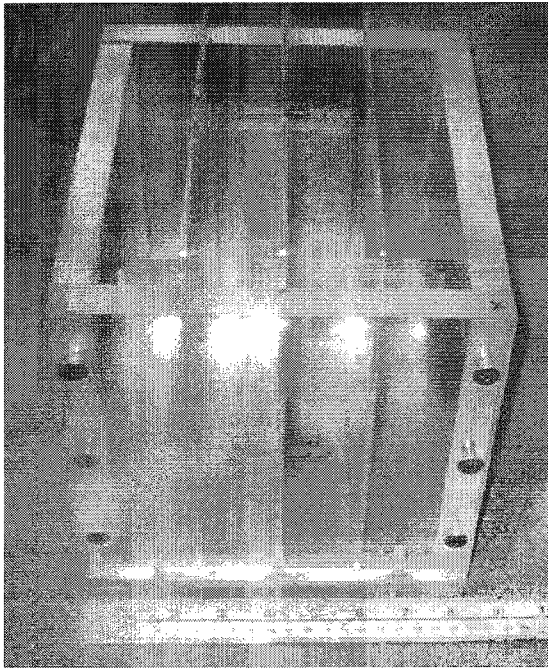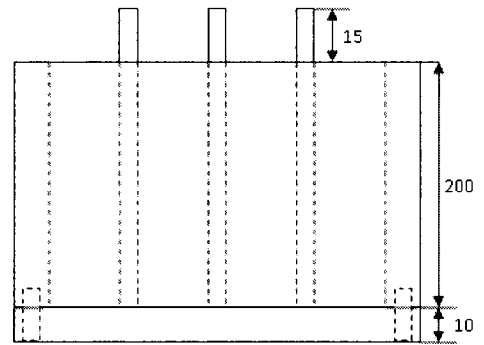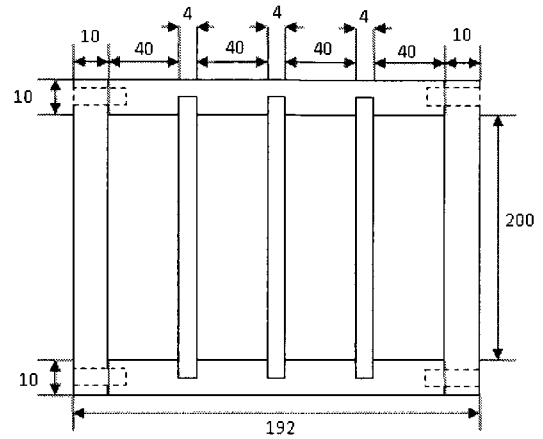
(a) Photo   (b) Sketch

Figure 3.9: Concrete Mould III

3.4   *Test Matrix*

The test matrix chosen in this study can be seen in Table 3.8.

Table 3.8: Test matrix

Phase	Electrical Specimens			Concrete Cylinders		
	Specimen Name	Number of Specimens	Testing Days	Testing Days	Number of Cylinders per Day	Concrete Mix
Phase I	I-A-20-ABC-I	3	Days 2-28	2,7,14 21 & 28	4	I
	II-A-20-ABC-I	3				
	II-A-40-ABC-I	3				
Phase II	I-C-20-A-II	1	Days 2-28	Not undertaken		
	I-D-20-BC-II	2				
Phase III	II-B-20-ABC-III	3	Days 2-28	2,7,14 21 & 28	4	II
	II-B-40-ABC-III	3				
	III-A-40-ABC-III	3				
	III-A-80-ABC-III	3				

*Specimen name refers to Mould Type-Concrete Mix Type-Electrode Spacing-Specimen Number-Phase of Testing

Phase I consisted of electrical and compression testing on concrete specimens that were cast in the concrete moulds and compression cylinders simultaneously using Concrete Mix I. Slump testing was performed on a sample of each concrete batch before casting and density testing of the cylinders was performed on the same day prior to compression testing. Phase II involved electrical testing on Cement Paste Mix I and Cement Paste Mix II, while the cement paste mixes were not tested for strength and density. Phase III consisted of electrical testing on specimens cast in Concrete Mould II using Concrete Mix II and specimens cast in Concrete Mould III using Concrete Mix I. The compression cylinders in Phase III were cast simultaneously using Concrete Mix II. All of the testing performed in each phase is outlined in the test matrix found in Table 3.8.

In each phase of the experimental program different concrete mixes and moulds were used in different combinations in order to obtain unique results. In order to make it clear which electrical concrete sample is being referenced to later on in the experimental program a labelling methodology was developed. The methodology follows the form of

X-Y-ZZ-N-P, where each letter is representative to a characteristic of the electrical concrete specimen. The characteristics along with each different type can be seen in Table 3.9. Hence, a concrete specimen denoted by II-B-40-C-III indicates that this specimen was cast in Concrete Mould II using Concrete Mix II. The distance between the electrodes was 40 mm. The specimen number is Specimen III and it belongs to Phase III.

Table 3.9: Concrete mould labelling methodology

Term	Symbol Meaning	Designation
1	X- Mould Type	I- Concrete Mould I II- Concrete Mould II III- Concrete Mould III
2	Y- Mix Type	A- Concrete Mix I B- Concrete Mix II C- Cement Paste Mix I D- Cement Paste Mix II
3	ZZ- Electrode Distance	20- 20 mm 40- 40 mm 80- 80 mm
4	N- Specimen Number	A- Specimen I B- Specimen II C- Specimen III ABC- All Specimens in the group AVG- Average of all Specimens
5	P- Phase Number	I- Phase I II- Phase II III- Phase III

*For naming purposes only, Concrete Mix I, Concrete Mix II, Cement Paste Mix I, and Cement Paste Mix II are referred to as Mix types A, B, C, and D respectively.

3.5 Specimens used for Physical Properties of Concrete

3.5.1 Mixing Concrete

The small specimens of concrete cast as trial mixes only required a small scale to measure the individual components and a bowl in which it was mixed. However, the experimental program required larger quantities of concrete to be cast for all of the required physical and electrical testing. The process of casting large quantities began with measuring the precise amount of each of the dry components (cement, sand, and coarse aggregate) using the scale seen in Figure 3.10. The dry ingredients were then mixed together in a wheelbarrow seen in Figure 3.11.
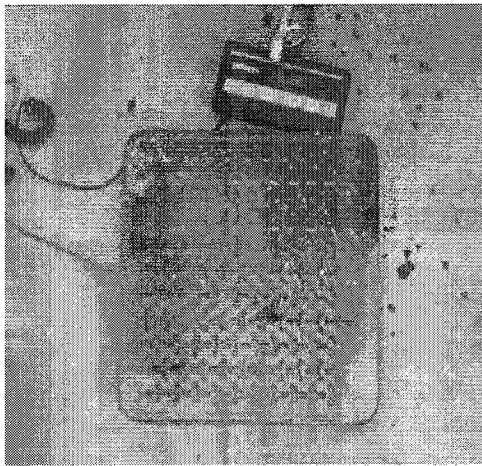
Figure 3.10: Scale used to measure concrete components
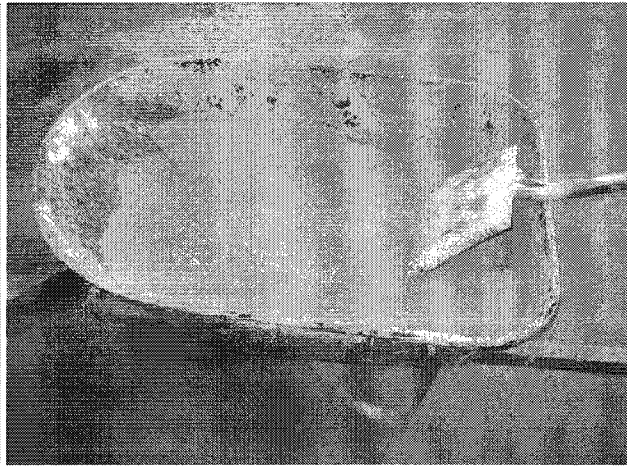
Figure 3.11: Wheel barrow used to mix concrete

After the dry ingredients were mixed, the amount of water needed to achieve the desired W/C ratio was measured and slowly added to create the concrete mixture. The concrete was mixed together with a shovel until all of the ingredients were fully incorporated and a consistent mix was achieved.

3.5.2 Slump Test

After the batch of concrete was mixed slump testing was performed within ten minutes of mixing according to the Canadian Standard specifications (CSA-A23.2, 2009). The following steps were followed as outlined in clause number A23.2.5C.

54

1. A 30 L sample was obtained from the fresh concrete batch.

2. The moist slump cone was placed on the moist slump tray.

3. While standing on the foot lugs throughout the test, the cone was filled to one third by volume and rodded 25 times with a 16 mm diameter x 600 mm long hemispherically tipped steel rod.

4. The cone was then filled to two-thirds of its volume and rodded 25 times as above with the rod just penetrating into the first layer.

5. The cone was finally filled to overflowing and rodded 25 times as above with the rod just penetrating into the second layer.

6. Excess concrete was removed with the rod so that the cone was exactly full. All spilled concrete was removed from around the base.

7. The cone was then lifted vertically with a slow even motion, taking approximately 5 seconds to remove the cone.

8. The rod was laid across the top of the slump cone and the slump was measured to the nearest 10 mm from the bottom of the rod to average top of the slumped concrete.

3.5.3 Concrete Compression Test

The concrete cylinders used to determine the compressive strength were cast in standard plastic non-absorbent cylinder moulds (as seen in Figure 3.12) with an inside diameter of 101.6 mm (4 in) and height of 203.2 mm (8 in). Hence, the cross-sectional area of the concrete specimen was 8107 mm^2. A releasing agent was applied to the moulds before the fresh concrete was added to the moulds in a process very similar to the slump test as outlined in the clauses A23.2.1C, A23.2.3C and A23.2.9C and as follows:

1. The cylinder was filled to approximately one third of the volume and rodded 25 times.

2. The cylinder was then filled to approximately two-thirds of the volume and rodded 25 times.

3. The cylinder was finally filled to overflowing and rodded 25 times, where any excess concrete was removed from the cylinder with a trowel.

4. The cylinder was then capped (Figure 3.13) and placed in a safe place in order to avoid disruption.
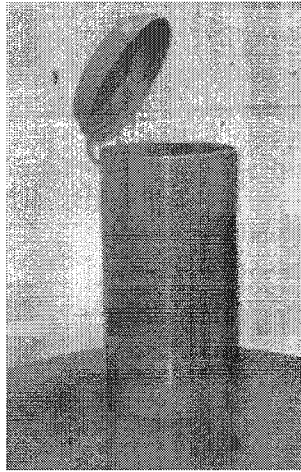
Figure 3.12: Plastic cylinder mould

Figure 3.13: Filled and capped concrete cylinder

The diameter of the cylinders was measured before the cylinders were capped in order to find any variation in size and obtain an accurate measurement of the area for the stress calculation. In order to ensure a flat surface for the concrete compression machine to load the cylinders, a sulphur capping compound was applied to the cylinders before testing. The process began by applying a releasing agent to the capping mould (Figure 3.14). Then the hot liquid sulphur compound was portioned into the mould and the cylinder was slowly placed into the compound and allowed to dry and set hard (Figure 3.15).
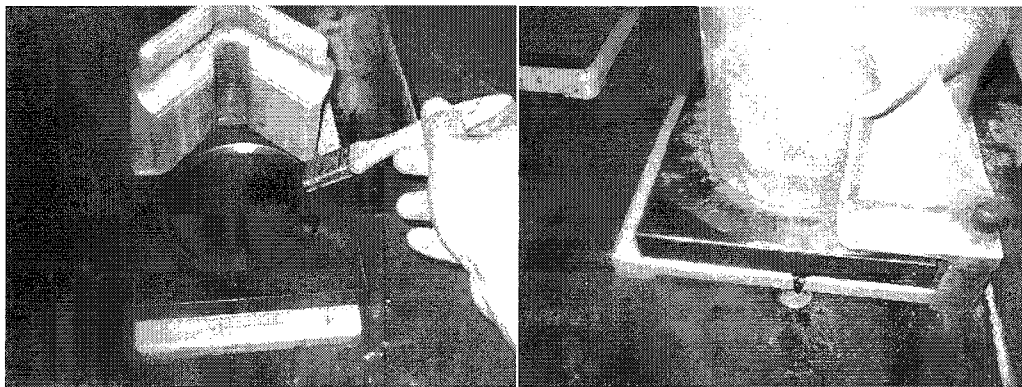
Figure 3.14: Applying the releasing agent   Figure 3.15: Setting the cylinder

The sulphur capping dried after about 20 seconds and the excess capping was removed by hand (Figure 3.16), and the process was repeated for the other surface of the cylinder making the cylinder ready for compression testing (Figure 3.17).
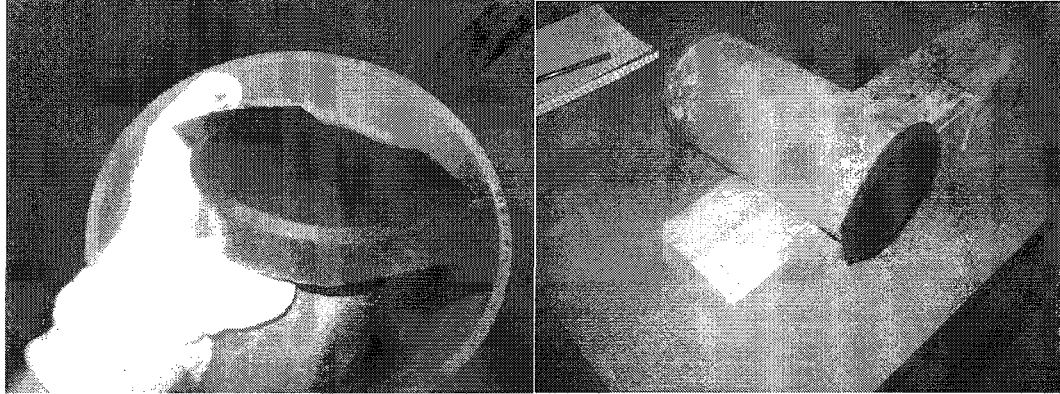
Figure 3.16: Removing excess capping   **Figure 3.17: Completed cylinder**

The compression tests were conducted using a Riehle compression testing machine. The machine has a loading capacity of 1300 kN (300 kips) with a variable loading rate and several load ranges. Each cylinder was centred under the loading head then compressed until failure (Figure 3.18).
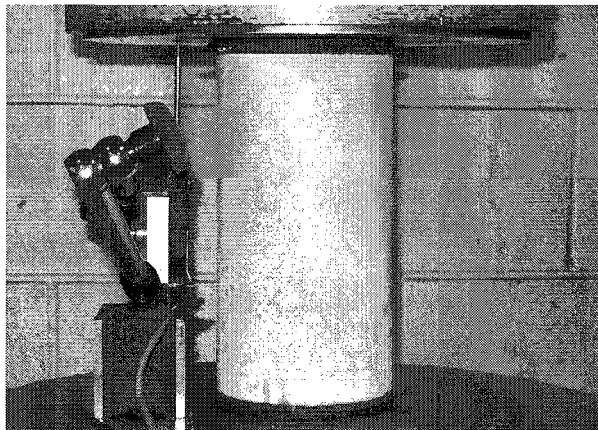
Figure 3.18: Cylinder ready for compression testing

During compression, a Caldaro 13FLP Linear-motion Potentiometer (LP) was used to record the displacement of the cylinder at a specific load. The gauge length (L) of the displacement was taken as 203.2 mm which was the height of the cylinder. The LP was held in place and secured to the concrete compression machine using a NOGA MG61003

magnetic holder. When the specimen reached failure due to crushing, the load was recorded. The LP automatically recorded the displacement for each second of loading and the displacement marker was recorded at specified loadings. The strain (ε) was determined from the displacement using the equation:

$$\varepsilon = \frac{\Delta L}{L} \tag{3.1}$$

The stress (σ) was determined from the load applied (P) and area of the concrete specimen (A) of the cylinder using the equation:

$$\sigma = \frac{P}{A} \tag{3.2}$$

The compressive strength of the concrete was found by calculating the stress at the failure point of the concrete, while an average strength was determined from each set of four cylinders for each day of testing. As seen in the test matrix (Table 3.8) compression tests were conducted at 2, 7, 14, 21, and 28 days and four concrete cylinders were tested for each day.

3.5.4 Concrete Density

The density of concrete (ρ) was measured for each cylinder before it was subjected to compression testing. Prior to being capped the height (H), diameter (D), and mass (M) of each cylinder was measured. The height was measured using a ruler which is accurate to 1 mm (Figure 3.19) and the diameter was measured using a set of callipers accurate to 1 mm and ruler. The mass was measured using a counter balance scale accurate to 1 g (Figure 3.20).

58
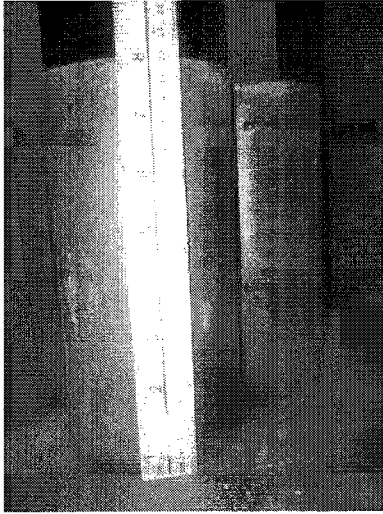
Figure 3.19: Cylinder height   **Figure 3.20: Measuring mass of cylinder**
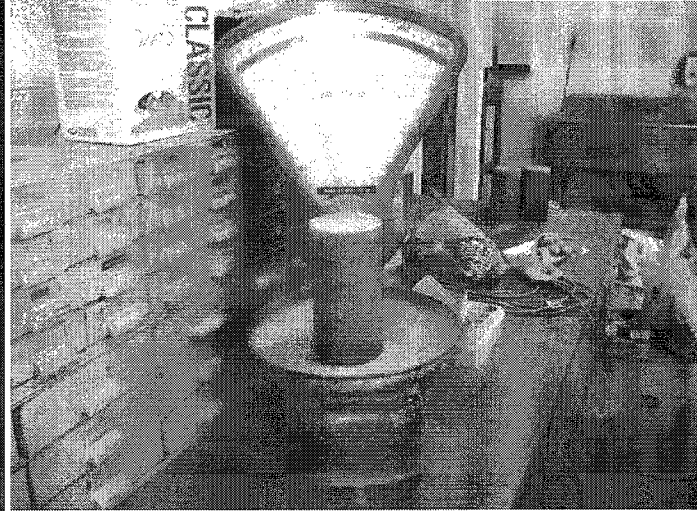
From the measured dimensions and mass, the density of each cylinder was determined using the following equation:

$$\rho = \frac{4M}{\pi D^2 H} \tag{3.3}$$

The average density was determined from the four cylinders tested on each scheduled day for compression testing.

3.6 *Specimens used for Electrical Properties of Concrete*

3.6.1 Casting Concrete for Electrical Measurements

The concrete poured into the moulds was obtained from the same batch of concrete used for the compression strength testing. They were then used to determine any correlation between the physical and electrical properties of concrete. The concrete was cast in the moulds in a manner similar to that of the cylinders, where the first step was to apply a thin coat of releasing agent to the mould in order to ensure the moulds could be reused (Figure 3.21).
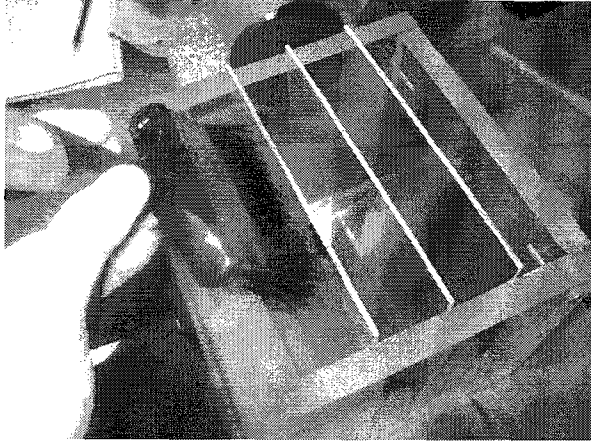
Figure 3.21: Applying releasing agent to the acrylic mould

With the electrodes left in place, the concrete was added with a small spoon to approximately one third of the volume of the first chamber and rodded 25 times. Next the chamber was filled to about two thirds of the volume and again rodded 25 times (Figure 3.22). Finally the chamber was filled to overflow, rodded 25 times and smoothed to the surface of the mould using a large putty knife. This process was followed for each chamber in all of the moulds cast for the experimental program.
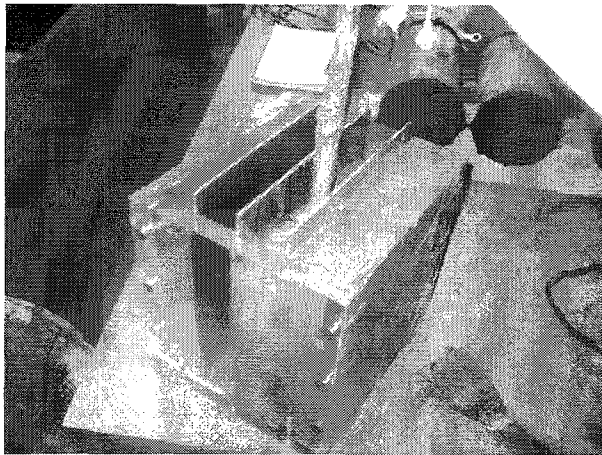
Figure 3.22: Eliminating voids from the concrete mould

3.6.2 Electrical Data Acquisition

The electrical data acquired in the experimental program was obtained using a Keithley 3300 LCZ meter (Figure 3.23) which uses alternating current to measure multiple electrical parameters over a frequency range of 40Hz to 100 kHz. The LCZ stands for inductance (L), capacitance (C), and impedance (Z) which are the primary variables measured by the instrument.
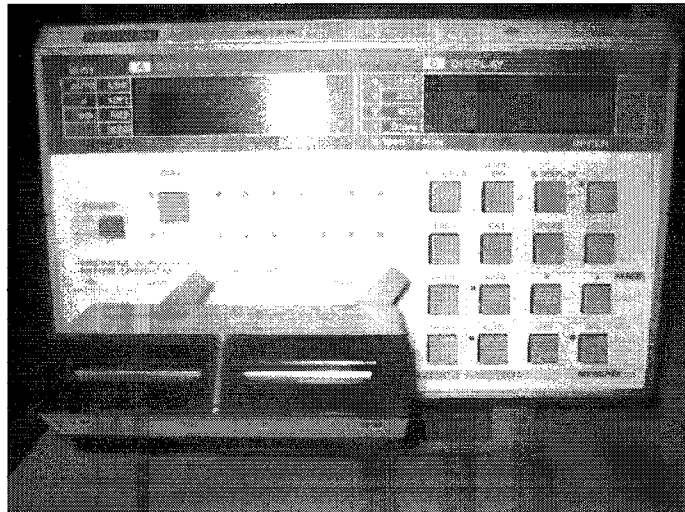
Figure 3.23: Keithley 3330 LCZ meter

For testing purposes a Keithley 3323 test fixture was attached to the input selection on the front of the meter. Insulated wire was inserted into the test fixture and alligator clips were attached to the wire in order to create a stable connection between the LCZ meter and the electrodes of the concrete moulds. The test setup used for all of the electrical data acquisition can be seen in Figure 3.24.
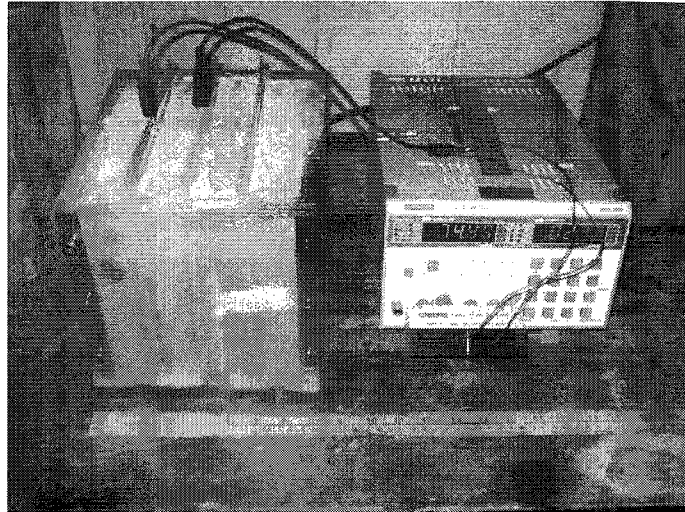
Figure 3.24: Electrical data acquisition test setup

The electrical properties of the concrete were measured everyday beginning from two days after the concrete was cast until twenty-eight days after the concrete was cast. The LCZ meter was used to obtain several electrical parameters of the concrete between the electrodes including capacitance (C), resistance (R), magnitude of impedance (Z), phase angle (θ), and dissipation factor (D). During Phase I, each parameter was measured over a frequency range of 0 to 10 MHz for each day of the 28 day cycle. After completing Phase I, it was apparent that a smaller frequency range for testing would be acceptable, therefore a frequency range of 120 to 100 kHz was used in Phase II. After further investigation it was found that only one frequency (1 kHz) would be most important for the duration of the experimental program, therefore Phase III was completed using a frequency of 1 kHz for each sample over the 28 day cycle.

4   CIRCUIT REPRESENTATION

4.1   *General*

When considering a material as a dielectric it is common practice to assume a model for how current flows through the given material. The most common model used in this representation is an electric circuit for which the electrical properties can be attributed to the different components of the material. As discussed in Chapter 2, it has been widely accepted that concrete for instance has a resistive component and a capacitive component represented by both the aggregate and cement paste that is created during the hydration of cement. If the components of concrete do indeed contribute to different electrical properties, then an electrical circuit model can be devised to explain how concrete behaves as an electrical material.

4.2   *Series Circuit*

The simplest circuit model that can be assumed is a circuit with a resistor (R) in series with a capacitor (C). In this case, it would be assumed that the resistive and capacitive properties of the concrete are provided by the coarse aggregate and the cement paste. A physical representation of this circuit can be seen in the circuit schematic shown in Figure 4.1.

Figure 4.1: Series circuit schematic

When considering the electrical impedance of this circuit, first the individual impedance (Z) of each component must be considered. Therefore, the impedance of the resistor (R) will be represented by Z_1 and the impedance of the capacitor (C) will be represented by Z_2 while the total impedance of the circuit will be represented by the following equation:

$$Z_{total} = Z_1 + Z_2 \tag{4.1}$$

The impedance of the resistor is considered to be the value of resistance supplied by the material leading to the equation:

$$Z_1 = R \tag{4.2}$$

While the impedance of the capacitor or reactance (X) can be expressed by the following equation:

$$Z_2 = X = \frac{1}{j\omega C} \tag{4.3}$$

Where, j = the complex number i (which is used in electrical engineering to avoid confusion with the symbol for current i)

ω = angular frequency in radians per second (represented by the equation $\omega = 2\pi f$, with f denoting frequency in cycles per second)

C = the capacitance of the material in the unit of farads (F)

Therefore the impedance of the series circuit can be separated into both a real quantity (R) and complex quantity (X) and can be represented by the following equation:

$$Z = R + \frac{1}{2\pi f C j} \tag{4.4}$$

The impedance of the series circuit can be represented graphically by plotting the real quantity of impedance along the x-axis and the complex quantity along the y-axis. This graph is referred to as the impedance plot. If a value for both the resistance (R) and the capacitance (C) are assumed over a large frequency range of $1 \leq f \leq 1 \times 10^{10}$ Hz, a plot of the impedance of a series circuit with frequency when only R contributes to the impedance can be seen in Figure 4.2.

Impedance vs. Frequency (R only)
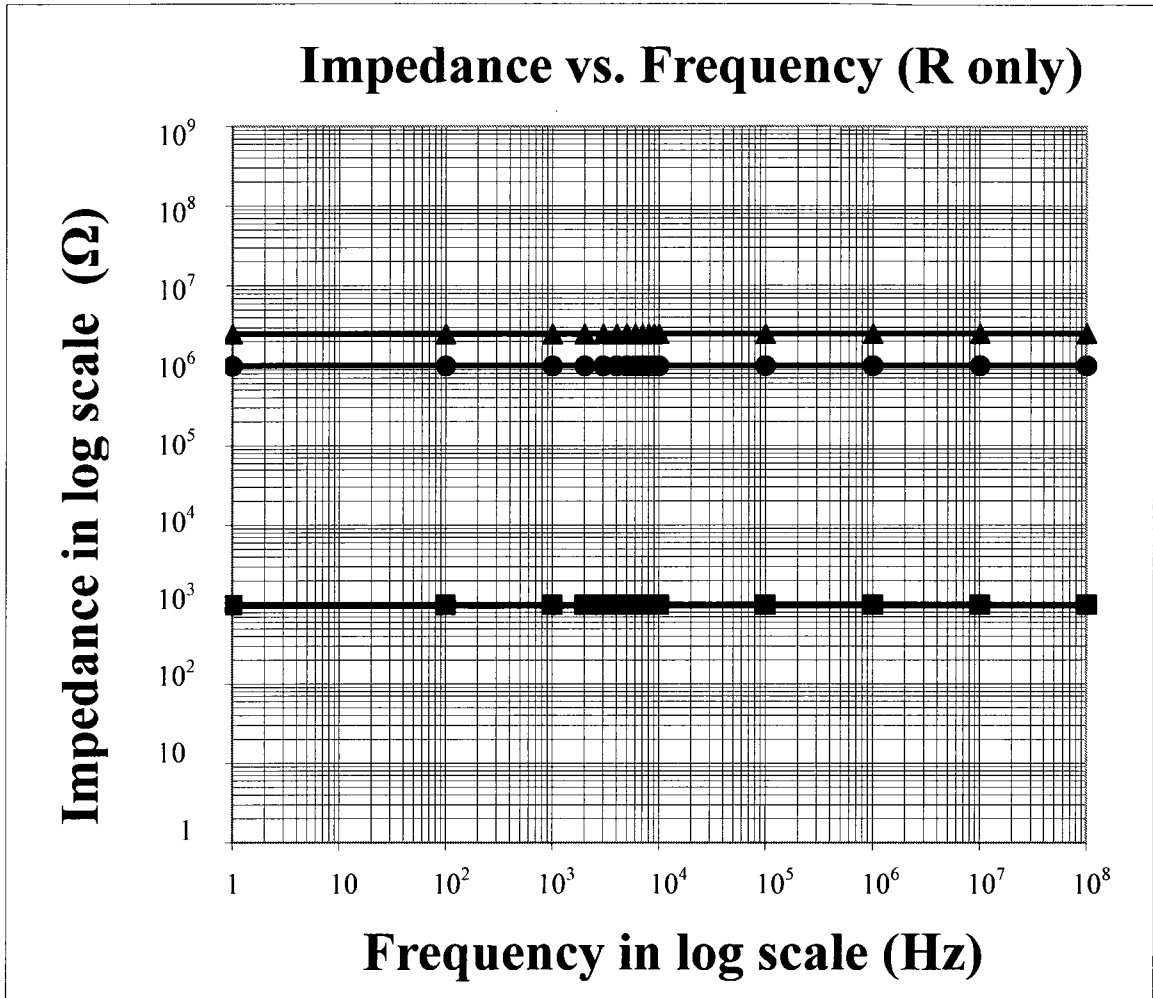
Figure 4.2: Impedance vs. frequency with R only

As seen in Figure 4.2 the impedance of the series circuit (Fig. 4.1) is a horizontal line intercepting the y axis at the value of the resistance R. The same theoretical value of capacitance was used for each plot as the value of the capacitance is assumed to remain constant. A plot of the impedance with frequency, when only the capacitance is considered to contribute to the impedance, can be seen in Figure 4.3.
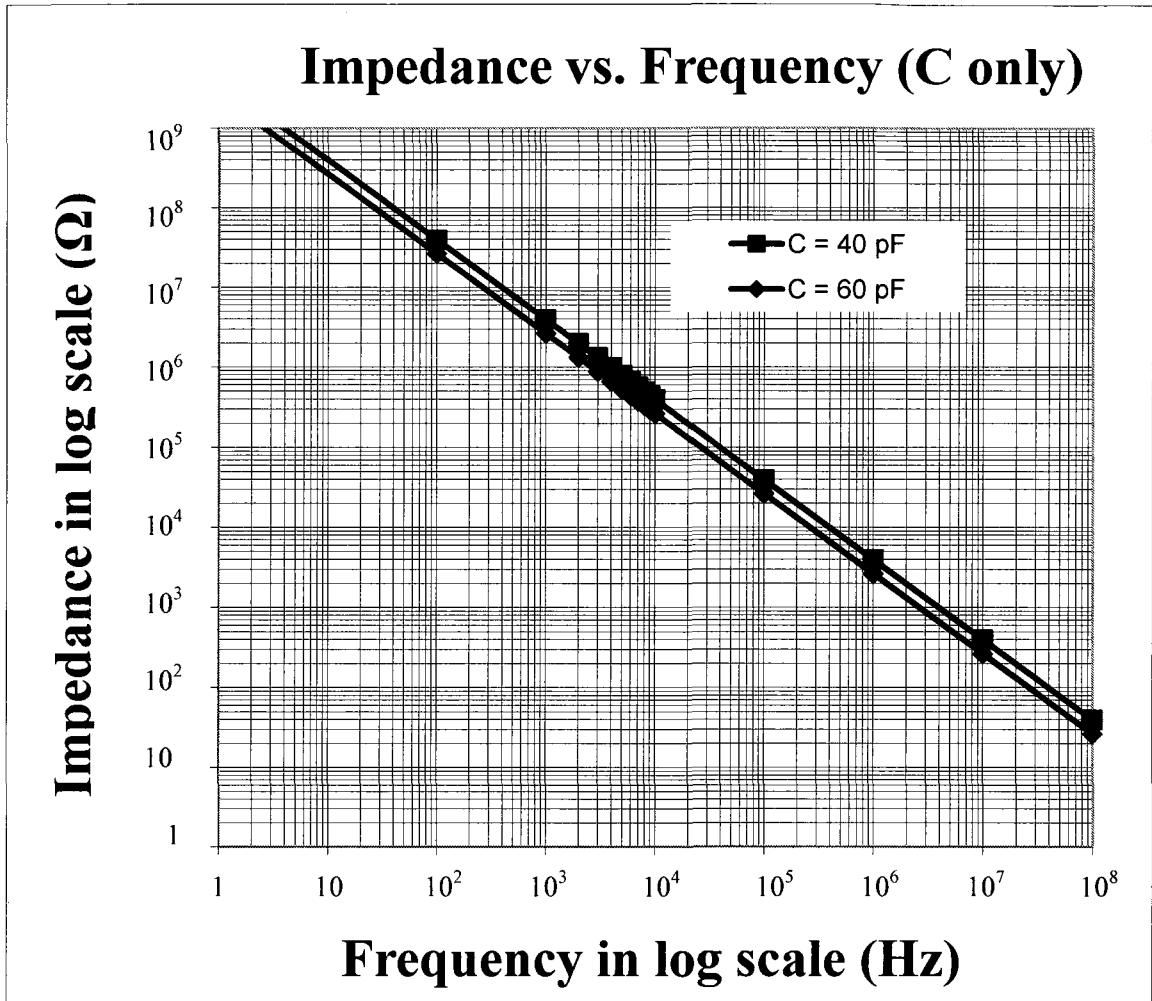
Figure 4.3: Impedance vs. frequency with C only

The plot of impedance with frequency when only C is considered produces a line with a negative slope as seen in Figure 4.3. When only the capacitance is considered to contribute to the impedance, the impedance of the capacitive element seen in Figure 4.3 is given in the following equation.

$$Z_{total} = \frac{1}{j2\pi fC} \tag{4.5}$$

The magnitude of Z, denoted by $|Z|$ is given in the following equation.

$$|Z_{total}| = \left| \frac{1}{j2\pi fC} \right| = \frac{1}{2\pi fC} \; \Omega \tag{4.6}$$

As seen in Figure 4.3 an increase in capacitance will reduce the y intercept of the line. A plot of the impedance when both R and C are considered to contribute to the impedance can be seen in Figure 4.4.
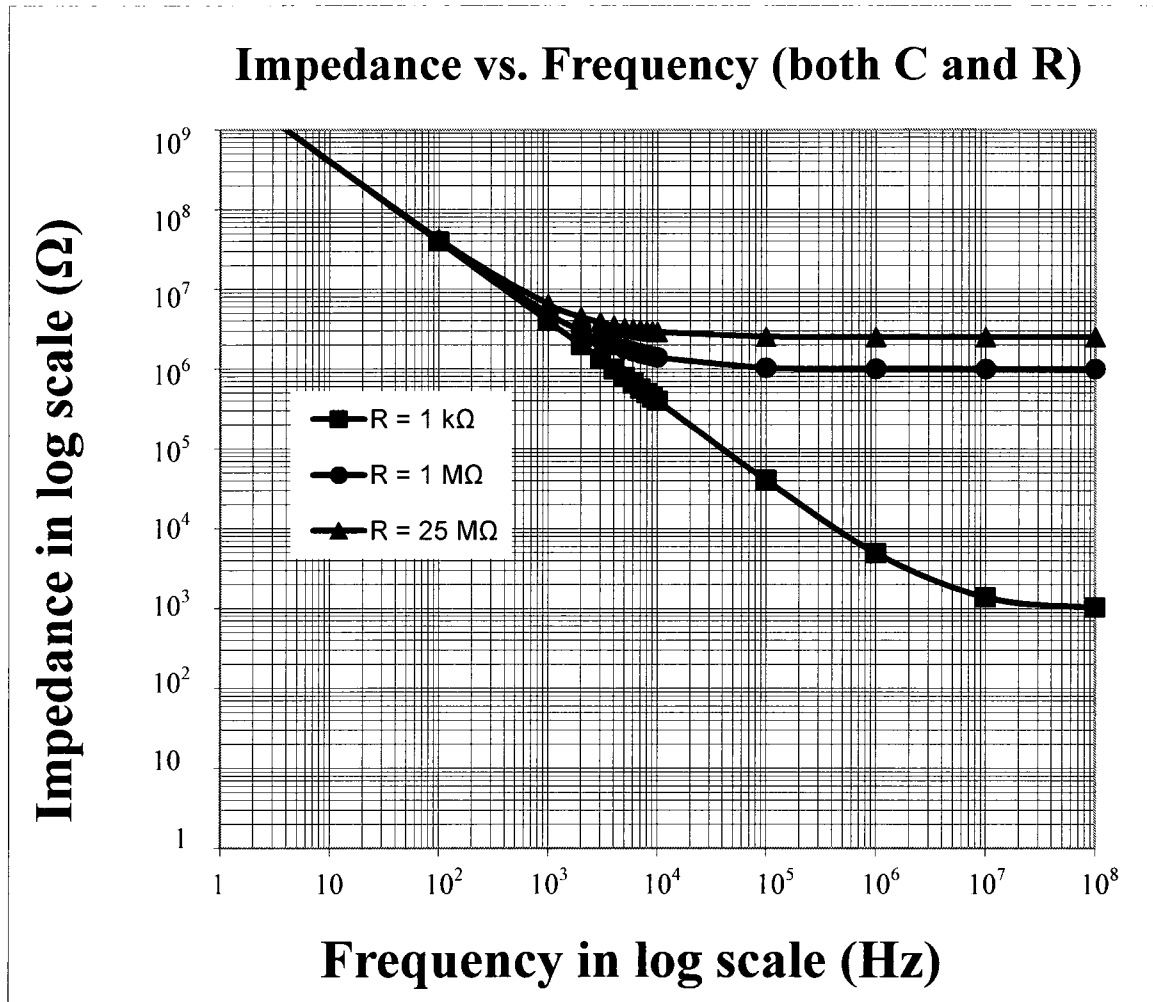
Figure 4.4: Impedance vs. frequency with C and R

In the case where both R and C are considered to contribute to the impedance of the circuit the impedance is denoted in equation 4.4. The magnitude of Z, denoted by $|Z|$ is given in the following equation.

$$|Z_{total}| = \left[R^2 + \left(\frac{1}{2\pi f C} \right)^2 \right]^{1/2} \Omega \qquad (4.7)$$

As it can be seen Figure 4.4 the total impedance of the series circuit when plotted with frequency produces a curve which becomes asymptotic at the value of the resistance found in the circuit, because at higher frequencies the contribution of the capacitive element becomes increasingly smaller and only the resistive element contributes to the impedance.

4.3   *Parallel Circuit*

The next circuit model that can be assumed is a circuit with a resistor in parallel with a capacitor. In this case it is still assumed that the properties of the concrete would be provided by a combination of resistance and capacitance. A physical representation of this circuit can be seen in the circuit schematic shown in Figure 4.5.
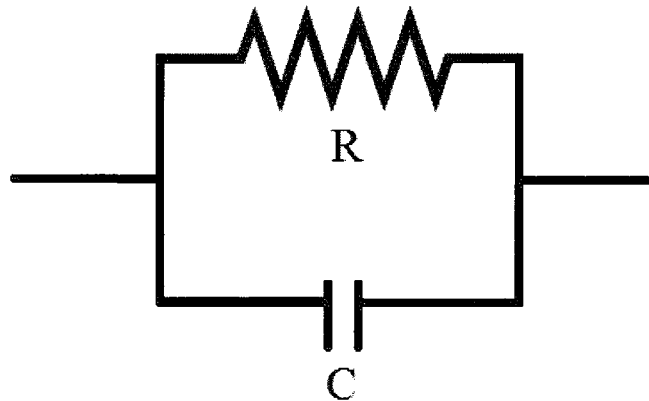
Figure 4.5: Parallel circuit schematic

To calculate the total electrical impedance of the parallel circuit the first step again is to consider the impedance of each component. Once again the impedance of the resistor (R) will be represented by Z_1 and the impedance of the capacitor (C) will be represented by Z_2 while the total impedance (Z_{total}) of the circuit will be represented by the following equation.

$$\frac{1}{Z_{total}} = \frac{1}{Z_1} + \frac{1}{Z_2}$$

(4.8)

Equation 4.4 can be simplified into the following equation.

$$Z_{total} = \frac{Z_1 Z_2}{Z_1 + Z_2}$$

(4.9)

Where, $Z_1 = R$ (4.2)

$$Z_2 = \frac{1}{j\omega C}$$ (4.3)

After substituting equation 4.2 and 4.3 into equation 4.6 the following equation can be obtained as follows.

$$Z_{total} = \frac{R\frac{1}{j\omega C}}{R+\frac{1}{j\omega C}}$$ (4.10)

Equation 4.10 can be simplified by multiplying the numerator and denominator by $j\omega C$ and multiplying the resultant equation by the conjugate of the denominator:

$$Z_{total} = \frac{R}{1+j\omega CR} = \frac{R}{1+j\omega CR}\frac{1-j\omega CR}{1-j\omega CR} = \frac{R(1-j\omega CR)}{1+\omega^2 C^2 R^2}$$ (4.11)

Separating the real quantities from the complex quantities in equation 4.11 will result in the impedance for the parallel circuit:

$$Z_{total} = \frac{R}{1+\omega^2 C^2 R^2} - j\frac{\omega CR^2}{1+\omega^2 C^2 R^2}$$ (4.12)

Solving for the magnitude of Z leads to the following equation.

$$|Z_{total}| = \left[\left(\frac{R}{1+\omega^2 C^2 R^2}\right)^2 + \left(\frac{\omega CR^2}{1+\omega^2 C^2 R^2}\right)^2\right]^{1/2}$$ (4.13)

Using the real quantity and complex quantity calculated using equation 4.12 the impedance plot for the parallel circuit can be constructed. The impedance plot of the parallel circuit can be seen in Figure 4.6.
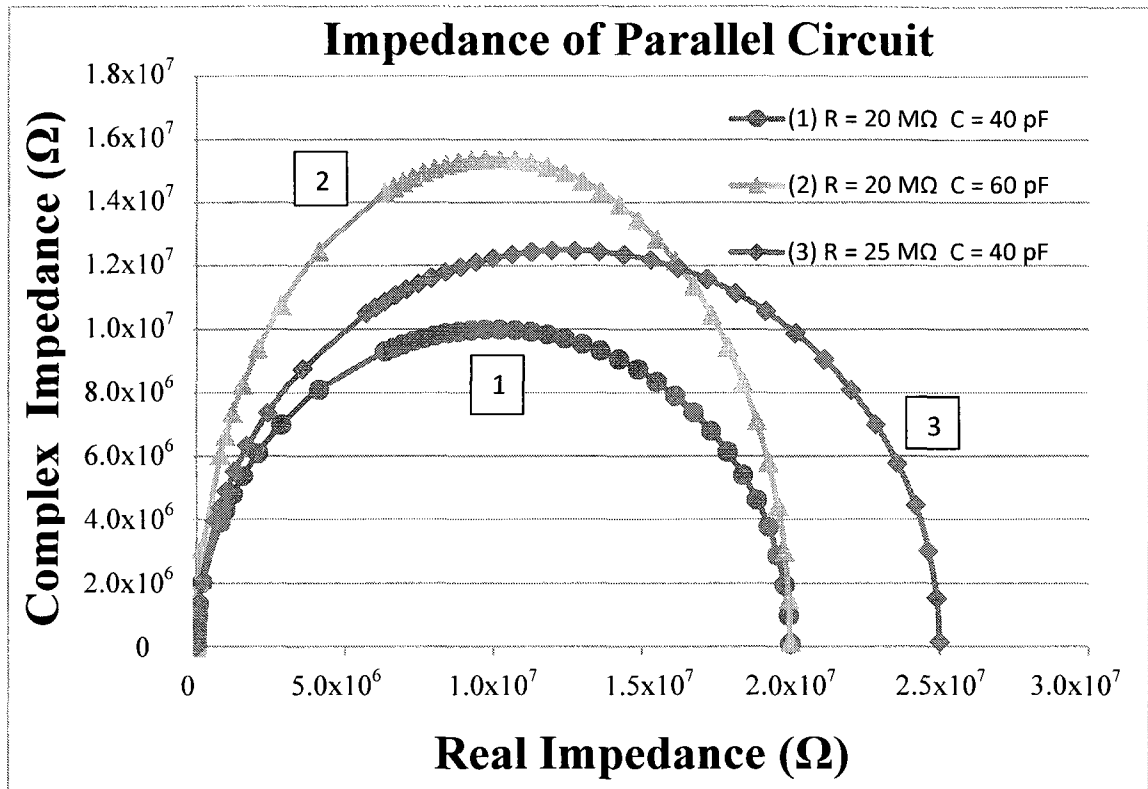
Figure 4.6: Impedance plot for parallel circuit

Each data point in Figure 4.6 corresponds to one frequency and the frequency was varied from 1 Hz to 1^{10} Hz. As can be seen in Figure 4.6, the impedance signature of the parallel circuit possesses a semi-circular shape intercepting the real axis at the origin and at the value of the resistance of the circuit (R). If the plot numbered [1] in Figure 4.6 is considered as the control plot, then it can be seen that the impedance signature will change depending on whether the resistance (R) or capacitance (C) differs from the control plot. For instance plot [2] in Figure 4.6 has the same resistance as plot [1] and therefore, has the same intercepts with the real axis, but the capacitance has increased over that of the control plot resulting in an increase in amplitude for plot [2]. In general it can be assumed that an increase in capacitance will cause an increase in the peak of the curve, while a decrease in capacitance will cause a decrease in the amplitude of the curve. A change in resistance can also affect the behaviour of the impedance signature which is evident from plot [3] in Figure 4.6. Plot [3] was given the same capacitance as the control plot while the resistance has increased causing the right intercept with the real axis to shift to the higher value of R, while the amplitude has increased slightly over that of the

control plot [1]. Therefore, it can be assumed that if the resistance increases, the right intercept with the real axis will shift to the new higher value of R and the amplitude of the curve will slightly increase. Consequently, if the resistance decreases the right intercept with the real axis will shift to the new lower value of R and the amplitude of the curve will slightly decrease.

4.4   *Parallel Circuit in Series with a Resistor*

A more complex circuit that can be assumed to model the electrical behaviour of concrete is the parallel circuit in series with another resistor (R_2). In this case it cannot be assumed one particular material contributes fully to either the capacitive or resistive properties of concrete. Therefore, the assumption will be made that the cement paste will contribute to both the resistance (R_1) and the capacitance (C_1), while the coarse aggregate would contribute to the resistance of the concrete only (R_2). The physical representation of this circuit can be seen in Figure 4.7.
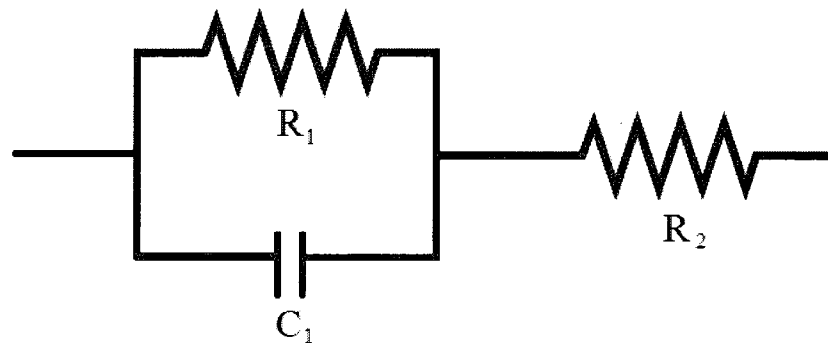
Figure 4.7: Parallel circuit in series with a resistor schematic

To calculate the total electrical impedance of the parallel circuit in series with a resistor, the first step again is to consider the impedance of each component individually. The impedance of the resistor in parallel (R_1) will be represented by Z_1, the impedance of the capacitor (C_1) will be represented by Z_2, and the impedance of the resistor in series (R_2) will be represented by Z_3 while the total impedance of the circuit will be represented by the following equation:

$$Z_{total} = \frac{Z_1 Z_2}{Z_1 + Z_2} + Z_3 \qquad (4.14)$$

71

The impedance is derived in a similar fashion to that of the parallel circuit, therefore, it will not be shown here, the only difference in the final equation is the fact that R_2 is in direct summation with the real quantity in equation 4.12 giving the impedance for this circuit the following form:

$$Z_{total} = \frac{R_1}{1+\omega^2 C_1{}^2 R_1{}^2} + R_2 - j\frac{\omega C_1 R_1{}^2}{1+\omega^2 C_1{}^2 R_1{}^2} \tag{4.15}$$

Using the real and complex quantities derived in equation 4.15 the impedance plot for the parallel circuit in series with a resistor can be constructed as shown in Figure 4.8.
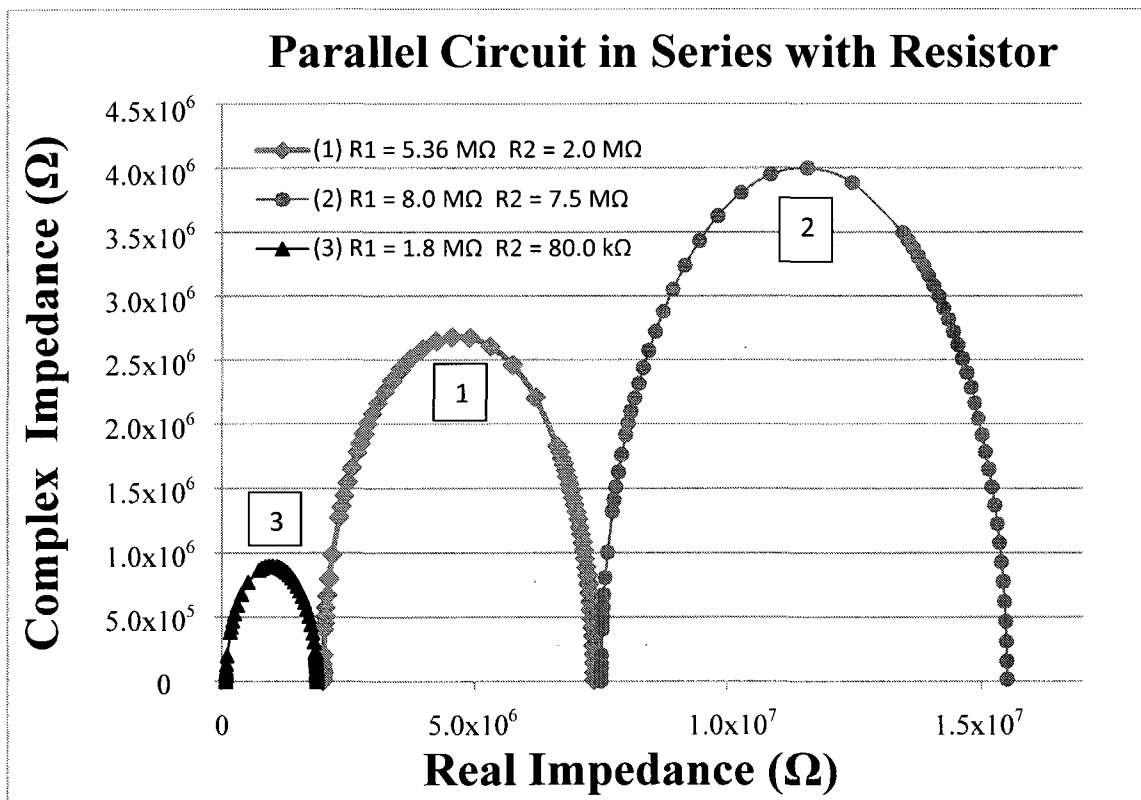
Figure 4.8: Impedance plot for parallel circuit in series with a resistor

As seen in Figure 4.8, the impedance signature of the parallel circuit in series with a resistor possess a parabolic shape where the left intercept with the real axis occurs at the value of the resistance R_1 and the right intercept with the real axis occurs at the value of the real quantity of the impedance found in equation 4.15 at zero frequency. All of the plots found in Figure 4.8 have a capacitance of 40 pF, while having different values of R_1

and R_2. If the plot numbered [1] is considered as the control plot then it can be seen in Figure 4.8 that the impedance signature will shift along the real axis and change in amplitude if the values of R_1 and R_2 change. In contrast a small change in capacitance will have little to no effect on the impedance signature of the parallel circuit in series with a resistor, since only a very small increase in amplitude would occur. As seen in plot [2] of Figure 4.8 an increase in R_1 and R_2, causes an increase in amplitude of the impedance plot while also shifting the impedance plot to the right along the real axis beyond the right intercept of plot [1]. It should be noted that these values are theoretical and were selected to purposefully shift plot [2] beyond the right intercept of plot [1]. When considering plot [3] in Figure 4.8 it can be seen that if the values of R_1 and R_2 decrease then the amplitude of the impedance plot will decrease and the plot will shift to the left along the real axis.

4.5   *Summary*

While only a few different types of circuits were considered in this study of circuit representation it is still concluded that determining the most appropriate circuit model for a material is very important to classifying the material as an electrical substance. A series circuit representation was chosen for the calculations of the electrical parameters in this study. In order to determine the best model representation for concrete, an in depth analysis of the electrical parameters will be required to be performed over a very large frequency range. Since this analysis was not the primary objective of the experimental program the analysis was not completed. However, circuit representation was taken into consideration as it is an important process in classifying concrete as an electrical material. It can be concluded that the best representation of the model circuit can be examined by future research that includes several combinations of R and C elements.

5   EXPERIMENTAL RESULTS

5.1   *Introduction*

The results in this chapter pertain to the cylinder compression testing and electrical testing. The results and their analyses are presented for each phase.

5.2   *Phase I Results*

Phase I used two different moulds; Type I (Fig. 3.7) and Type II (Fig. 3.8) and two different electrode spacings: 20 mm and 40 mm. However only one concrete mix (Concrete Mix I or A) was used, as shown in Tables 3.8 and 3.9.

5.2.1   Slump and Density

The slump test on Concrete Mix I was performed as outlined in section 3.5.2 and it produced a slump of 100 mm, which is considered to be low (or moderate) in terms of workability. The density of each cylinder was calculated prior to capping using equation 3.3 and the values of the densities and the average density obtained at each test day can be found in Table 5.1.

Table 5.1: Density of cylinders in Phase I

Cylinder Number	Cylinder Density (kg/m^3)				
	Day 2	Day 7	Day 14	Day 21	Day 28
1	2204.20	2210.71	2228.84	2195.57	2197.97
2	2236.92	2203.44	2204.37	2196.78	2200.42
3	2262.12	2234.34	2199.81	2233.70	2199.79
4	2245.88	2237.98	2197.36	2187.69	2206.49
Average Density	**2237**	**2222**	**2208**	**2203**	**2201**

*Note: Density was not used in calculation and was reported for reference only.

5.2.2   Compression Strength

The outline of the concrete cylinder testing performed in Phase I can be seen in the test matrix found in Table 3.8. In summary, it can be seen that four concrete cylinders made of Concrete Mix I were tested on days 2, 7, 14, 21, and 28 after the concrete was cast. Each cylinder was loaded to crushing failure and later analyzed for the stress and strain

developed in the cylinder during testing. The stress and strain were calculated from the equations 3.2 and 3.1, respectively, and the average stress-strain curves for each testing day can be seen in Figure 5.1. The average values were obtained from the four cylinder tests completed each day.
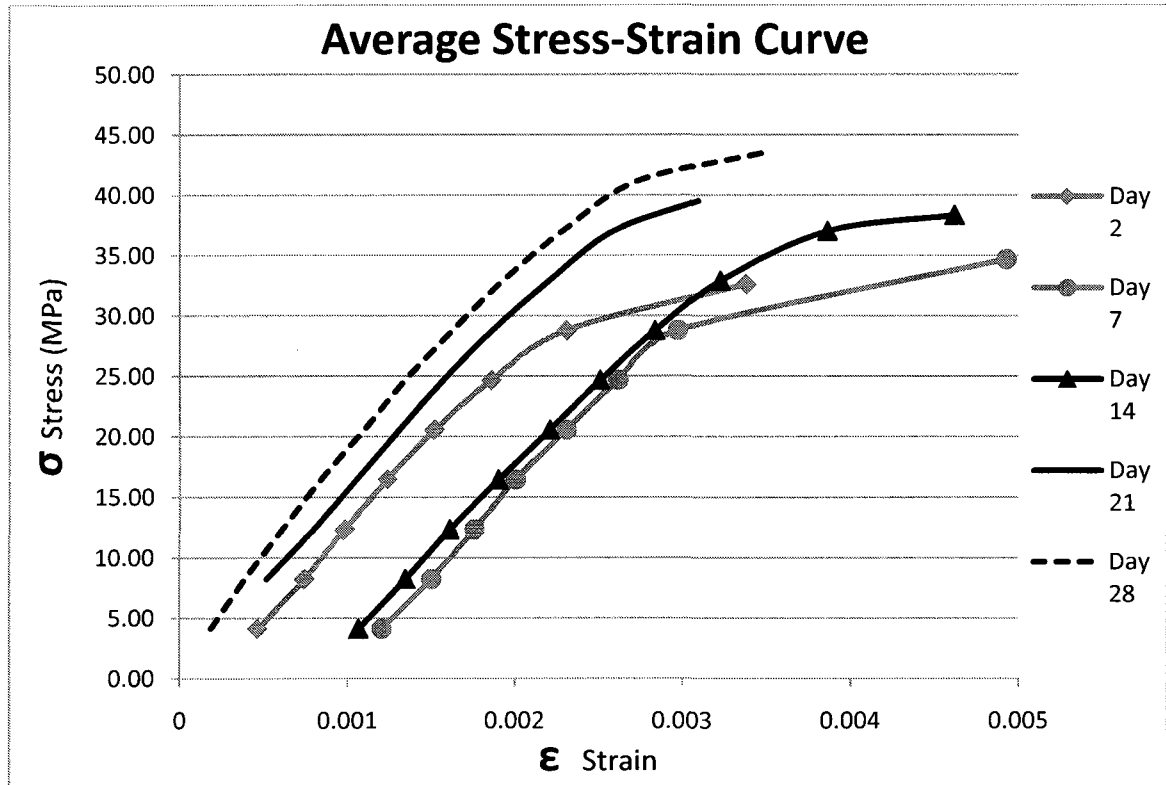
Figure 5.1: Average stress-strain curves for each testing day in Phase I

It can be seen from Figure 5.1 that the ultimate stress (it will be called strength in subsequent discussion) generally increases with time and the initial strain generally decreases with time, with the exception occurring with the curve for Day 2 as the curve does not follow the general trend. While it can be noted that compression testing is rarely executed on concrete at such a premature age due to the fact that concrete at that early stage does not achieve sufficient hydration and testing results can be erratic. However, it can be concluded that the strength of the concrete increases with time. The values of the strength for each testing day along with the average strength calculated for each testing day can be seen in Table 5.2. It should also be noted that due to the non-homogeneous nature of concrete, some of the cylinders tested produced inaccurate results and hence,

these results were discarded (indicated as outlier in Table 5.2). However, the results from a minimum of 3 cylinders were used for each testing day.

Table 5.2: Phase I compression testing strength results

Cylinder Number	Strength (MPa)				
	Day 2	Day 7	Day 14	Day 21	Day 28
1	32.23	34.29	37.17	39.37	43.21
2	32.85	34.57	outlier	39.5	44.3
3	32.29	35.25	38.41	39.92	43.62
4	33.19	outlier	38	39.3	43.21
Average Strength	**32.64**	**34.7**	**38.37**	**39.52**	**43.58**

A plot of the average strength (seen in Table 5.1) with time for the cylinders tested in Phase I can be seen in Figure 5.2.

Time vs. Average Strength

$y = 0.4068x + 31.764$
$R^2 = 0.987$
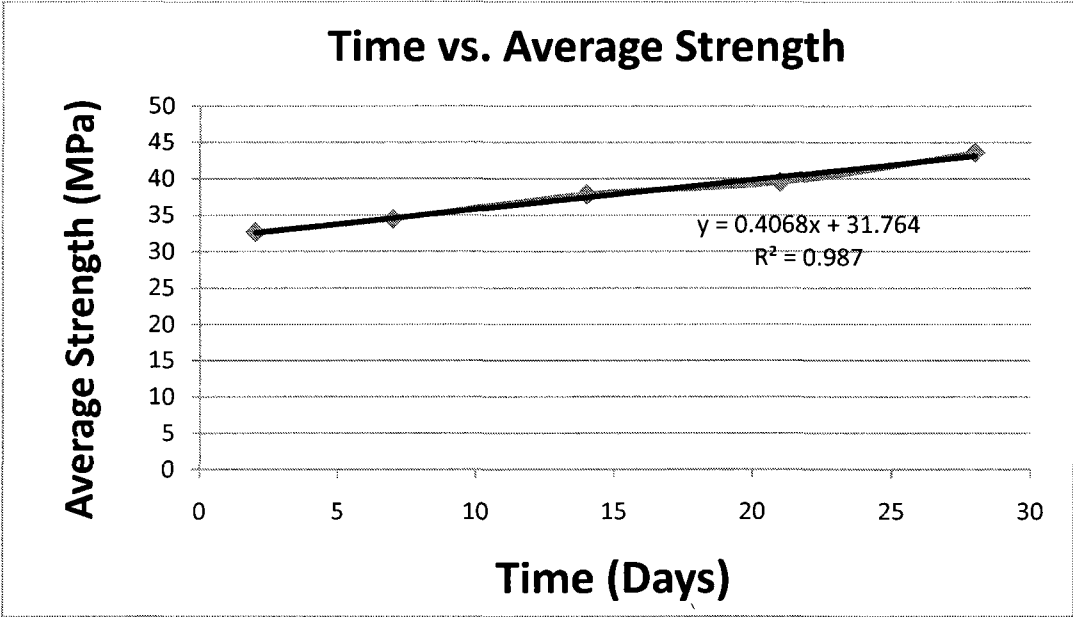
Figure 5.2: Time vs. average strength for cylinders in Phase I

After performing a simple linear regression analysis on the data seen in Figure 5.2 it can be seen that the R^2 value was 0.987 making the linear equation very relevant and reliable

in calculating the strength of Concrete Mix I on the 28th day. The equation for calculating the strength of Concrete Mix I is as follows.

$$f_{c(I)} = 0.4068t + 31.764 \qquad (5.1)$$

Where: f_c = concrete strength at a specific day (MPa)

t = time (days)

Most of the concrete cylinders tested in Phase I exhibited a cone and split type failure (Figure 5.3) while some of the cylinders were found to exhibit a columnar type failure (Figure 5.4). The testing day seemed to have no bearing on the type of failure and the failure type did not cause any major change in the general trend of the values of the strength.
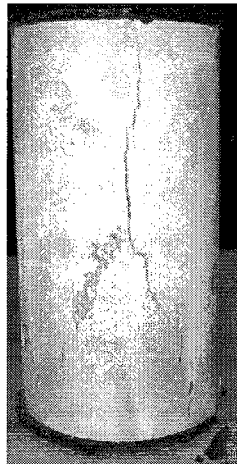
Figure 5.3: Cone and split type failure   **Figure 5.4: Columnar type failure**

5.2.3   Electrical Testing Results

As outlined in section 3.6.2 in chapter 3 the electrical testing was performed over a large frequency range in Phase I. However, after a careful analysis and study of all the test results, it was found that the results at the frequency (f) of 1000 Hz were the most useful in this study. Among the measured parameters including capacitance (C), resistance (R), magnitude of impedance (Z), phase angle (θ), and dissipation factor (D) it was found that the capacitance (C) was the most relevant measured parameter and provided the most interesting result when it was transformed into the imaginary value of impedance called

reactance (X). This was due to the fact that the variance of the other parameters between specimens of the same type was found to be higher than the variance seen in the reactance of the specimens (discussion of the electrical parameter choice can be seen in Appendix B). The reactance was calculated using equation (4.3), assuming that the concrete specimens can be modeled using a series circuit. The use of the frequency (f) of 1000 Hz was determined after plotting the reactance of specimen I-A-20-A-I with time at different frequencies (Figure 5.5).
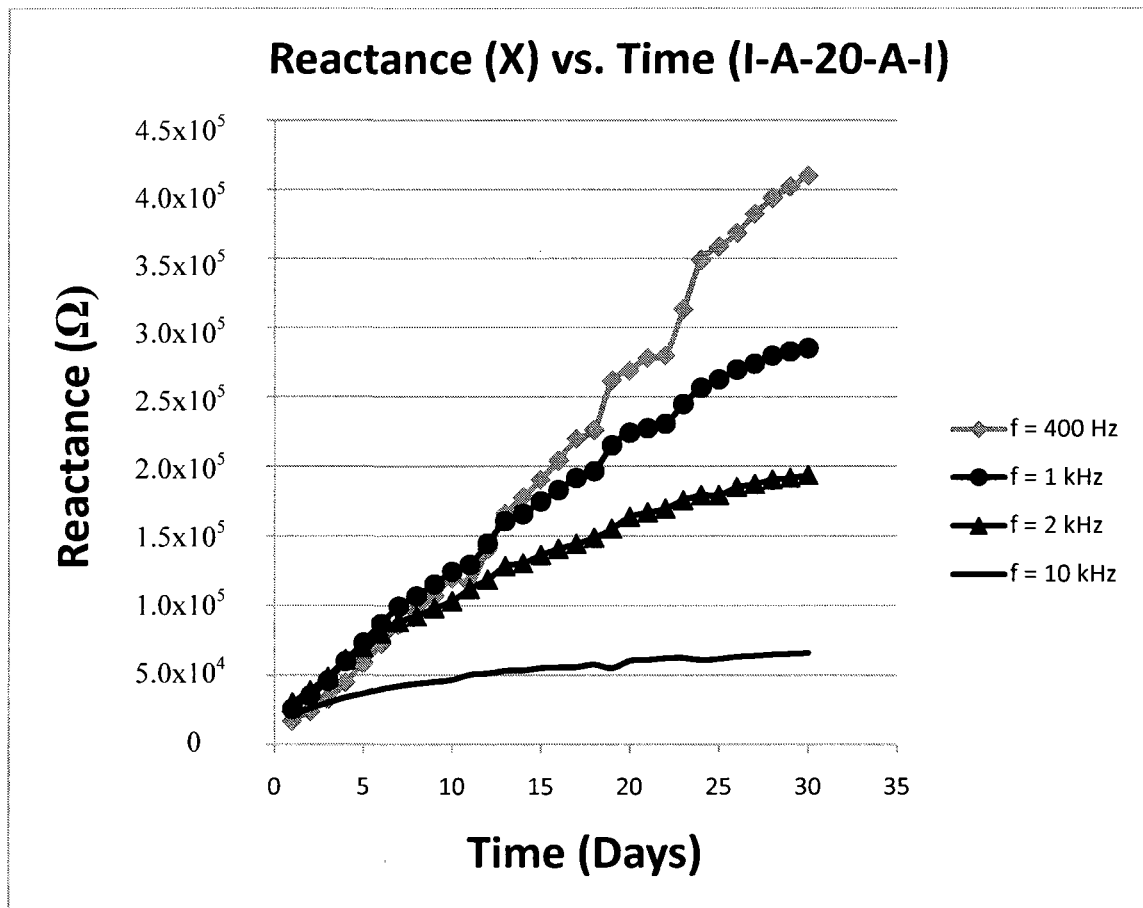
Figure 5.5: Reactance vs. time for specimen I-A-20-A-I at different frequencies

As seen in Figure 5.5 the frequency does not affect the shape of the reactance-time curve, thus it is concluded that a convenient frequency of 1000 Hz could be chosen without changing the results of the study. A frequency of 1000 Hz was chosen due to the fact that it produced reliable results within a larger range of reactance values than other frequencies, while also producing minimal variance in reactance between specimens of the same type. Also, it was observed that the electrical parameters measured at higher

frequencies became erratic when compared to 1000 Hz. Therefore, all of the reactance values reported in this chapter were calculated at the frequency (f) of 1000 Hz. There were three specimens cast for both mould types in Phase I with three different types of specimens used including: I-A-20-ABC-I, II-A-20-ABC-I and II-A-40-ABC-I. This resulted in the testing of mould type I with only one electrode distance of 20 mm and the testing of mould type II with two different electrode distances. After calculating the average (average value of the three specimens) reactance for each specimen type the reactance was plotted over time and can be seen in Figure 5.6. It is worth mentioning here that the cross-sectional area of a concrete specimen of mould type I is one quarter the cross-sectional area of mould type II (Table 3.7).
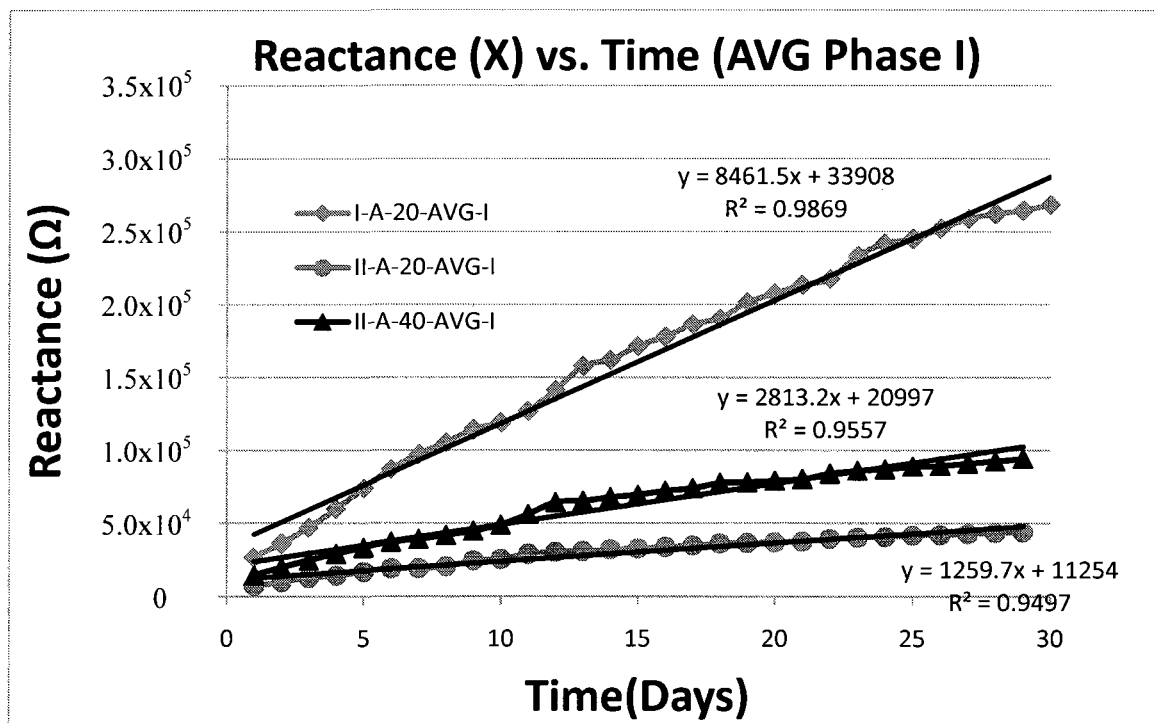
Figure 5.6: Reactance vs. time Phase I

From Figure 5.6 it can be seen that an increase in cross-sectional area (A) of the concrete specimen decreases the reactance of the concrete. This can be seen when comparing specimen I-A-20-AVG-I to specimen II-A-20-AVG-I as the only difference between the two specimens is the fact that the cross-section of I-A-20-AVG-I was 50 mm x 50 mm and the cross-section of II-A-20-AVG-I was 100 mm x 100 mm. It can also be seen that

79

an increase in electrode distance (d) caused an increase in reactance, as specimens II-A-20-AVG-I and II-A-40-AVG-I differ only in electrode distance representing 20 mm and 40 mm, respectively. A linear regression analysis was performed on each specimen resulting in an equation for calculating the reactance (X) if the time (t) is known. Each specimen resulted in R^2 values of 0.9869, 0.9497, and 0.9557 as shown in Figure 5.5. Hence, the linear regression analyses for the test data provide a statistically acceptable fit. The equations for each specimen are as follows.

For I-A-20-AVG-I:

$$X = 8461.5t + 33908 \tag{5.2}$$

For II-A-20-AVG-I:

$$X = 1259.7t + 11254 \tag{5.3}$$

For II-A-40-AVG-I:

$$X = 2813.2t + 20997 \tag{5.4}$$

Where: X = reactance (Ω)

t = time (days)

The results from Phase I can be explained theoretically as the capacitance (C) of a block with cubical shape, having a distance between the measuring electrodes d (m) and cross-sectional area A (m^2) is given by the following formula.

$$C = \varepsilon_0 \varepsilon_r \frac{A}{d} \quad \text{(farads)} \tag{5.5}$$

Where, A = cross-sectional area (m^2)

d = electrode distance (m)

ε_0 = permittivity of free space (F/m)

ε_r = dielectric constant

It can be seen that an increase in d in equation 5.5 causes a decrease in capacitance (C) and therefore, the reactance (X) increases according to equation 4.3. It can also be seen that an increase in A in equation 5.5 causes an increase in capacitance (C) and therefore, the reactance (X) decreases according to equation 4.3. This agrees with the results found experimentally and provides a theoretical background for the results found in this chapter.

5.2.4 Analysis of Phase I Results

Since the equations for the reactance (X) and concrete strength (f_c) both depend on the variable of time linearly, the equations can be arranged to result in a certain reactance representing a corresponding strength. The equations for the strength of concrete (f_c) in terms of reactance (X) for each specimen tested in Phase I are as follows.

For I-A-20-AVG-I:

$$f_c = 4.807 \times 10^{-5}(X) + 30.13 \tag{5.6}$$

For II-A-20-AVG-I:

$$f_c = 3.229 \times 10^{-4}(X) + 28.13 \tag{5.7}$$

For II-A-40-AVG-I:

$$f_c = 1.446 \times 10^{-4}(X) + 28.73 \tag{5.8}$$

Where: X = reactance (Ω)

f_c = concrete strength (MPa)

A plot of equations 5.6 to 5.8 can be seen in Figure 5.7, where the reactance values used are the values obtained experimentally. Each point on the linear plot corresponds to one day in the concrete curing life.
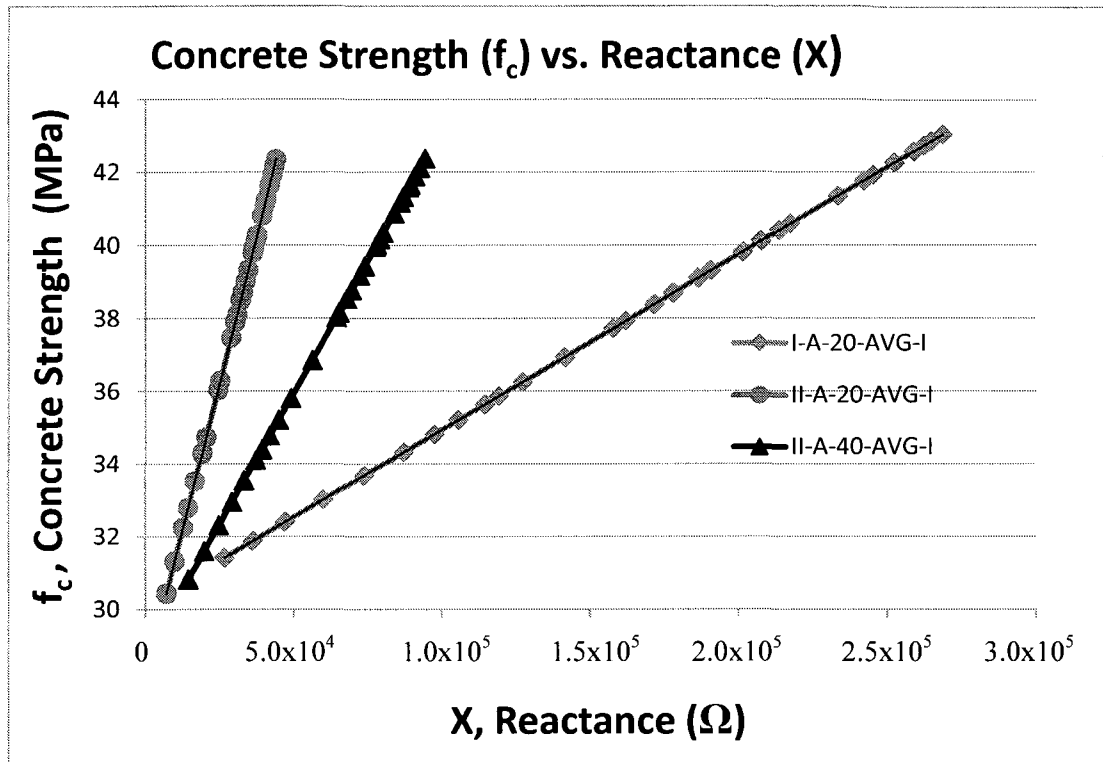
Figure 5.7: Concrete strength vs. reactance in Phase I

As it can be seen in Figure 5.7, each specimen type represents a distinctly different linear plot denoting the concrete strength (f_c) in terms of reactance (X). Specimen I-A-20-AVG-I represents the plot with the lowest slope, while specimen II-A-20-AVG-I represents the plot with the highest slope. Therefore, the slope of the strength-reactance plot increased as the cross-sectional area (A) of the mould increased. It can also be seen in Figure 5.7 that specimen II-A-20-AVG-I has a higher slope than specimen II-A-40-AVG-I. Therefore, the slope of the strength-reactance plot decreased as the electrode distance increased.

Although the relationship between concrete strength and reactance can be made, equations 5.6 to 5.8 are considered valid only for Concrete Mix I as seen in Table 3.4 (Sample mix B4) for a reactance calculated at f = 1000 Hz and for the corresponding dimensions of each mould which can be seen in Table 3.7. A large number of tests would need to be completed in order to develop a generic universal equation relating concrete strength to reactance as there may be a large number of other variables which may affect the reactance of a concrete.

5.3 *Phase II Results*

Phase II used only one mould: Type I (Fig. 3.7); one electrode spacing of 20 mm; and two cement pastes (Cement Paste Mix I and Cement Paste Mix II in Table 3.5). Cement Paste Mix I (C) had a W/C ratio of 0.62, whereas Cement Paste Mix II had a W/C ratio of 0.39. No strength tests were undertaken on these specimens (Table 3.8).

5.3.1 Electrical Testing Results

Phase II consisted of testing the reactance of two different types of cement paste. The mix proportions can be seen in Table 3.7, and it can be seen from Table 3.8 that there was one specimen cast with Cement Paste Mix I (C) and two specimens cast with Cement Paste Mix II (D). Only one mould, Concrete Mould I (A = 50 mm x 50 mm) with electrode distance (d = 20mm) was used in this phase (Table 3.8). The reactance (X) of cement paste specimens I-C-20-A-II and I-D-20-AVG-II can be seen in contrast to the concrete specimen I-A-20-AVG-I of Phase I (same mould with the same electrode distance but with Concrete Mix I or A) in a plot with time in Figure 5.8.
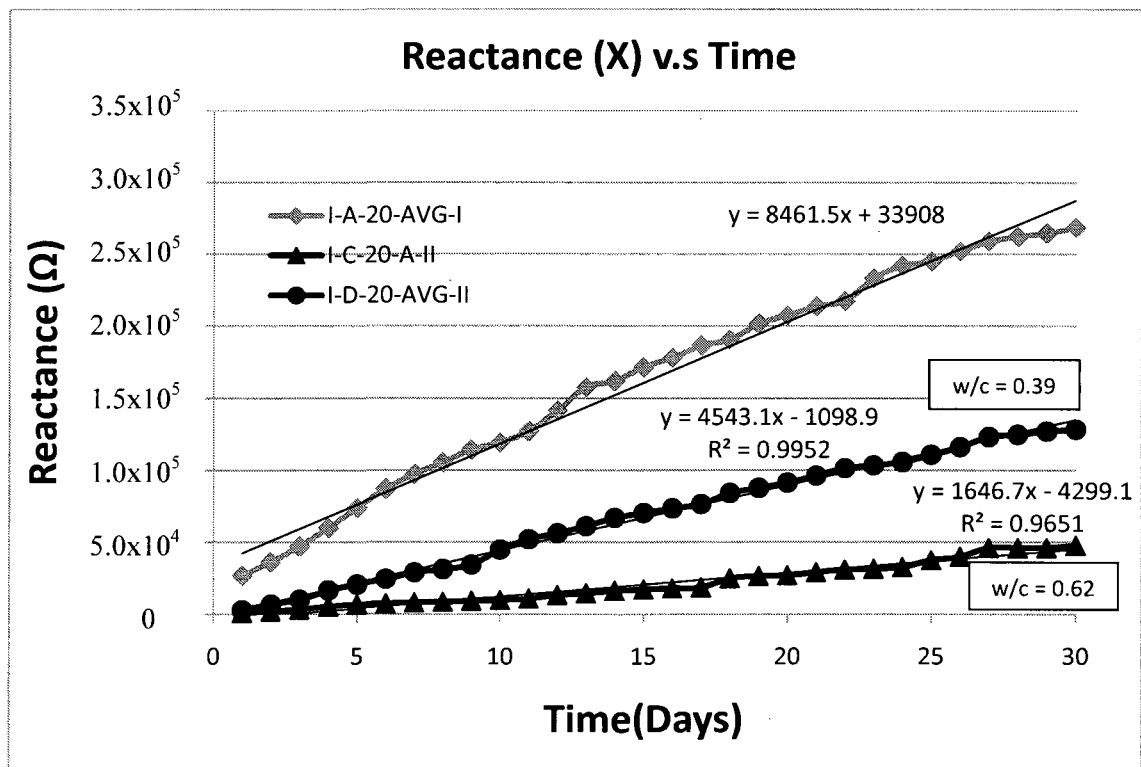
Figure 5.8: Reactance vs. time in Phase II

After plotting the reactance (X) of the two cement paste specimens, it was found that the reactance of a cement paste increased as the W/C ratio decreased. This was expected since the reactance becomes lower as the capacitance of the cement paste increases, and it was expected that as the amount of water increases in the cement paste the capacitance also increases. From Figure 5.8 it can be seen that the reactance of the cement paste was lower than the reactance of the concrete cast in the same mould. This happens because the capacitance of the cement paste was higher than the concrete and this is logical due to the fact that the cement paste contains no aggregate and the current would be able to travel more freely through the cement paste in comparison to the concrete.

There were no cylinders cast in Phase II due to the fact that cement paste cylinders would be very weak and would have very little or no applications in a real world situation. Since there is no direct comparison between the reactance and strength of cement paste, the main conclusion drawn from Phase II is that the cement paste can be seen to greatly affect the reactance of concrete. As seen in Figure 5.8 the reactance of the cement paste lies in the same order of magnitude as that of the concrete specimen cast in the same mould. Thus, it may be reasonable to conclude that the cement paste present in concrete is the main medium in which the current travels.

5.3.2 Analysis of Phase II Results

The relationships between the reactance (X) in terms of time (t) for the cement paste specimens tested in Phase II are as follows.

For I-C-20-A-II:

$$X = 1646.7t - 4299.1 \tag{5.9}$$

For I-D-20-AVG-II:

$$X = 4543.1t - 1098.9 \tag{5.10}$$

When comparing the reactance equations for each of the specimens tested, each specimen type presents a different effect on the coefficients of the reactance equation. If the

coefficient corresponding to the variable t (time) is considered to be β and the coefficient corresponding to the intercept is considered to be α then the equation of the reactance would take the generic form of the following equation.

$$X = \beta t + \alpha \tag{5.11}$$

In comparison to equation 5.2 which consisted of concrete cast in the same mould, the values of the β and α in equations 5.9 and 5.10 are much lower. It can also be seen that the value of α is a negative value for the cement paste specimens. Since concrete and cement paste transform from a liquid state into solid state through the process of hydration in under one day, a definite value of the reactance directly after casting (day 0) does not particularly exist for the specimens in this study as the reactance was only considered for a specific day without considering intermediate values. Therefore, the parameter α is simply a theoretical value used in the reactance equations to estimate the reactance of the specimens used in this study, for the purpose of showing that it is possible to relate the reactance and strength of concrete .

5.4 *Phase III Results*

Phase III used two different moulds: Type II which has an A of 100 mm x 100 mm (Fig. 3.8) and Type III which has an A of 200 mm x 200 mm (Fig. 3.9) as in Table 3.7 and two different concrete mix types: Concrete Mix I and Concrete Mix II (see Tables 3.4 and 3.6). The spacing between electrodes varied between 20 mm and 40 mm for mould Type II, and between 40 mm and 80 mm for mould Type III (Table 3.7). The specimens cast in mould Type III were cast with Concrete Mix I and the specimens cast in mould Type II were cast with Concrete Mix II. It should be noted that Concrete Mix II (Sample C2 in Table 3.6) had a much smaller amount of cement than Concrete Mix I (Sample B4 in Table 3.4).

5.4.1 Slump and Density

The slump test on Concrete Mix II was performed as outlined in section 3.5.2, produced a slump of 250 mm which is considered to be high in terms of workability. The slump of Concrete Mix II was considerably higher than the slump of Concrete Mix I, this was due

to the low cement content and high W/C ratio present in Concrete Mix II. The density of each cylinder was calculated prior to capping using equation 3.3 and the values of the densities and the average density for each testing day can be found in Table 5.3.

Table 5.3: Density of cylinders in Phase III

Cylinder Number	Cylinder Density (kg/m^3)				
	Day 2	Day 7	Day 14	Day 23	Day 28
1	2205.27	2216.98	2257.96	2289.93	2215.62
2	2200.39	2224.83	2210.14	2254.12	2261.72
3	2199.78	2285.47	2212.58	2207.10	2268.00
4	2206.51	2256.66	2260.40	2198.55	2190.60
Average Density	**2203**	**2246**	**2235**	**2237**	**2234**

*Note: Density was not used in calculation and was reported for reference only.

5.4.2 Compression Strength

The details of the concrete cylinders tested in Phase III can be seen in the test matrix found in Table 3.8. In summary, it can be seen that 4 concrete cylinders were cast with Concrete Mix II and they were tested on days 2, 7, 14, 21, and 28 after the concrete was cast. Each cylinder was loaded to failure due to crushing. The load and deformation were then analyzed for the stress and strain that developed on the cylinder during testing. The stress and strain were calculated from the equations 3.2 and 3.1, respectively, and the average stress-strain curves for each testing day can be seen in Figure 5.9.
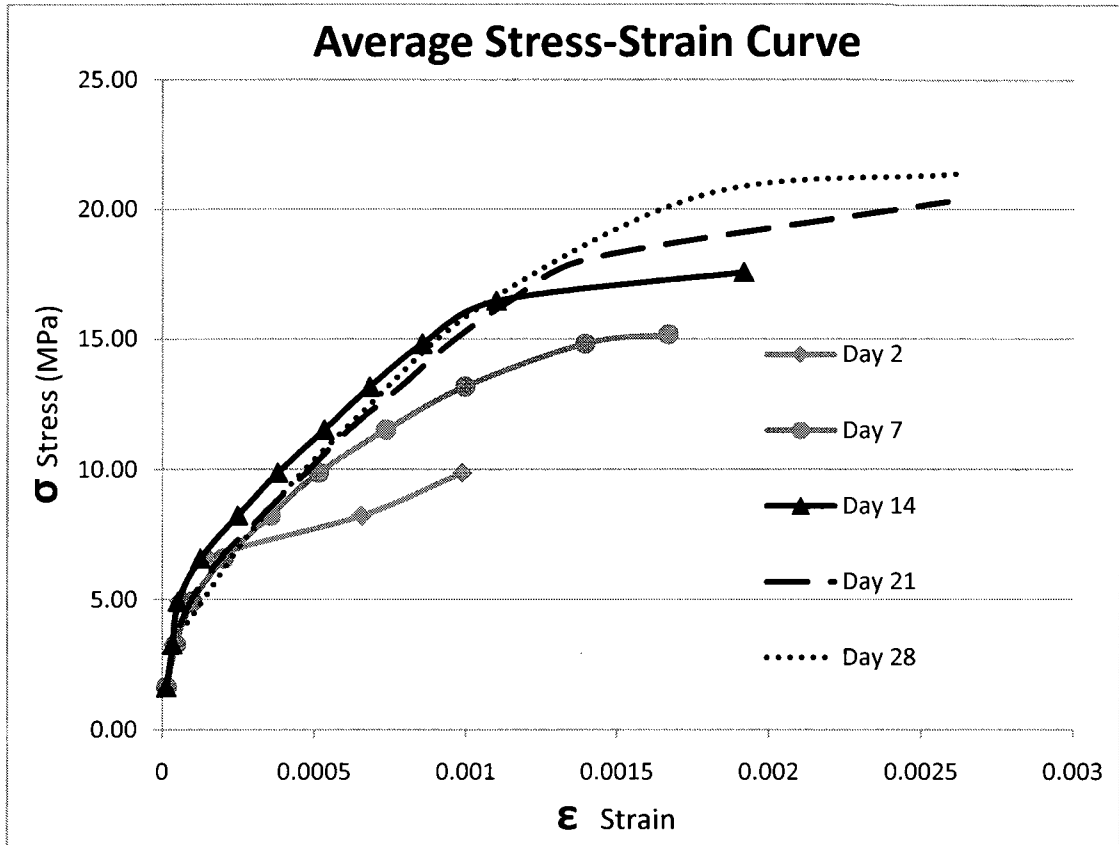
Figure 5.9: Average stress-strain curves for each testing day in Phase III

It can be seen from Figure 5.9 that the strength generally increases with time and the final strain generally increases with time. However, it can be concluded that the strength of the concrete increases with time. The values of the strength for each testing day along with the average strength calculated for each testing day can be seen in Table 5.4. It should also be noted that due to the non-homogeneous nature of concrete, some of the cylinders tested produced inaccurate results and hence, these results were discarded (indicated as outlier in Table 5.4). However, the results from a minimum of 3 cylinders were used for each testing day.

Table 5.4: Phase III compression testing strength results

Cylinder Number	Strength (MPa)				
	Day 2	Day 7	Day 14	Day 21	Day 28
1	14.24	15.20	outlier	21.73	20.99
2	14.05	14.73	17.61	19.64	21.26
3	14.13	15.42	17.50	20.47	22.08
4	13.91	15.31	17.58	19.34	21.12
Average Strength	**14.08**	**15.16**	**17.57**	**20.29**	**21.36**

A plot of the average strength (seen in Table 5.4) with time for the cylinders tested in Phase III can be seen in Figure 5.10.
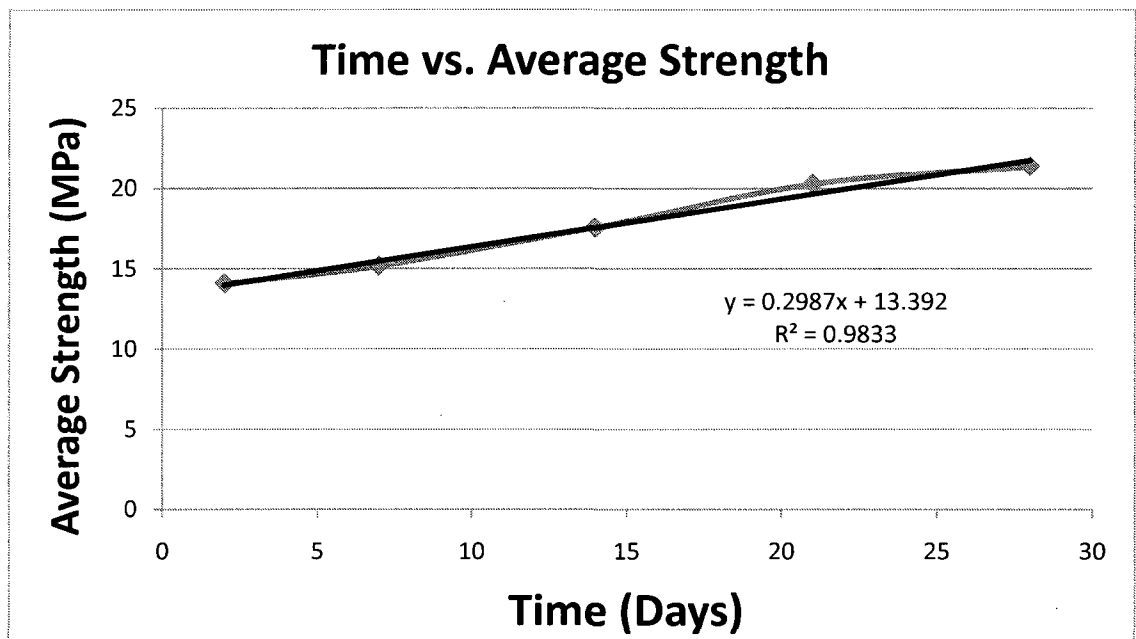
Figure 5.10: Time vs. average strength for cylinders in Phase III

After performing a simple linear regression analysis on the data seen in Figure 5.9 it can be seen that the R^2 value was 0.9833 making the linear equation accurate when calculating the strength of Concrete Mix II on any given day over 28 days. The equation for calculating the strength of Concrete Mix II is as follows:

$$f_{c(II)} = 0.2987t + 13.392 \qquad\qquad (5.12)$$

Where: f_c = concrete strength at a specific day (MPa)

t = time (days)

When comparing the strength of Concrete Mix I to Concrete Mix II it can be seen that Concrete Mix II was considerably weaker in comparison to Concrete Mix I, which was an expected result since Concrete Mix II was created for the sole purpose of making a concrete mix containing the least amount of cement as possible. To see a direct comparison between the strength of each mix on each testing date, the average strength for each mix can be seen in Table 5.5.

Table 5.5: Comparison of strength between Mix I and II

Average Strength (MPa)			
Testing Day	Mix I	Testing Day	Mix II
2	32.64	2	14.08
7	34.70	7	15.16
14	38.37	14	17.57
21	39.52	21	20.29
28	43.58	28	21.36

The failure type of the cylinders in Phase III was found to be the same as the two failure types found in Phase I (Figure 5.3 and Figure 5.4), without an occurrence of any different failure types.

5.4.3 Electrical Testing Results

As outlined in section 3.6.2 in chapter 3 the reactance values recorded in Phase III were executed at a frequency (f) of 1000 Hz.

There were three specimens cast for both mould types in Phase III with four different types of specimens used including: II-B-20-ABC-III, II-B-40-ABC-III, III-A-40-ABC-III and III-A-80-ABC-III. This resulted in the testing of mould type II using Concrete Mix II with two different electrode distances and the testing of mould type III using Concrete Mix I with two different electrode distances. The average reactance of specimens II-B-20-ABC-III and II-B-40-ABC-III can be seen in Figure 5.11.
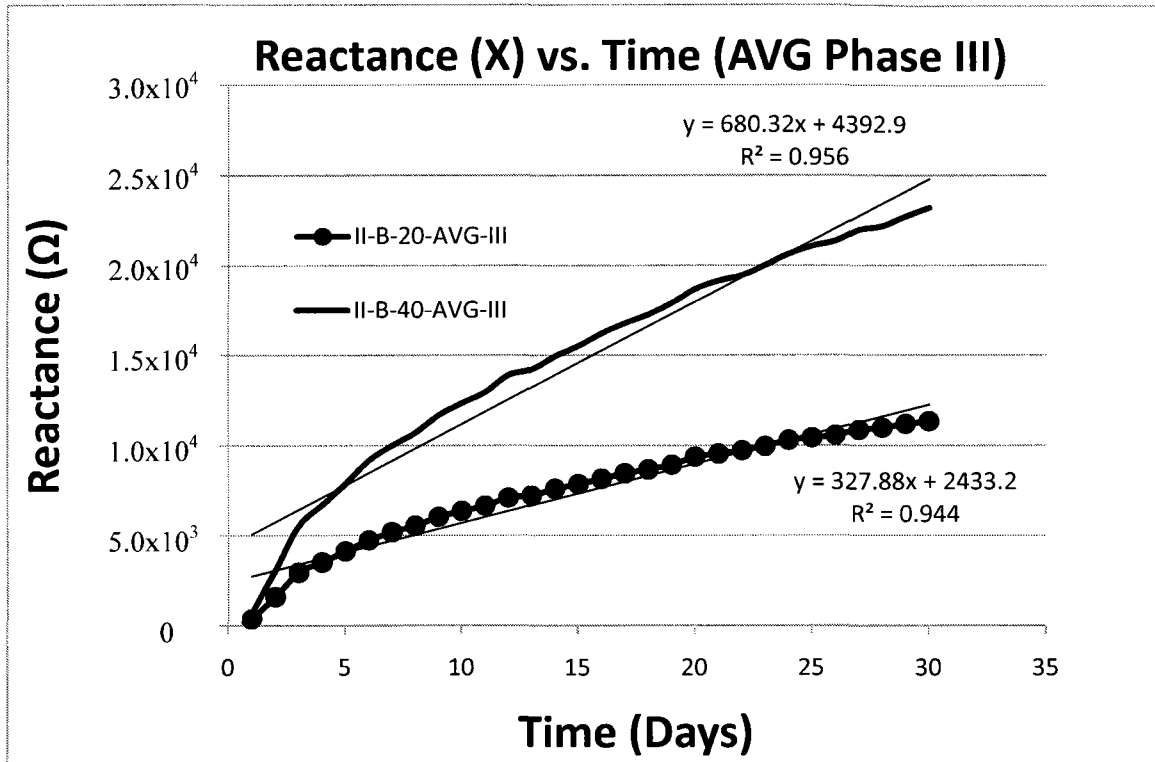
Figure 5.11: Reactance vs. time for specimens II-B-20-AVG-III and II-B-40-AVG-III

From Figure 5.11 it can be seen that the reactance of specimen type II-B-20-AVG-III was lower than the reactance of II-B-20-AVG-III. Since the electrode distance was the only parameter changed for mould type II in Phase III, it can be seen that as electrode distance increased the reactance (X) also increased. A linear regression analysis was performed on the two specimens from Phase III, resulting in an equation for calculating the reactance if the time is known. The analysis resulted in the R^2 values of 0.944 and 0.956 for II-B-20-AVG-III and II-B-40-AVG-III respectively, showing that the resulting equations represent a reliable model fit. The equations for each specimen are as follows.

For II-B-20-AVG-III:

$$X = 327.88t + 2433.2 \tag{5.13}$$

For II-B-40-AVG-III:

$$X = 680.32t + 4392.9 \tag{5.14}$$

The average reactance of specimens III-A-40-ABC-III and III-A-80-ABC-III were also plotted against time and the results can be seen in Figure 5.12.

Reactance (X) vs. Time (AVG Phase III)

y = 317.59x + 5584.1
R^2 = 0.8852

y = 150.12x + 2710.9
R^2 = 0.8797
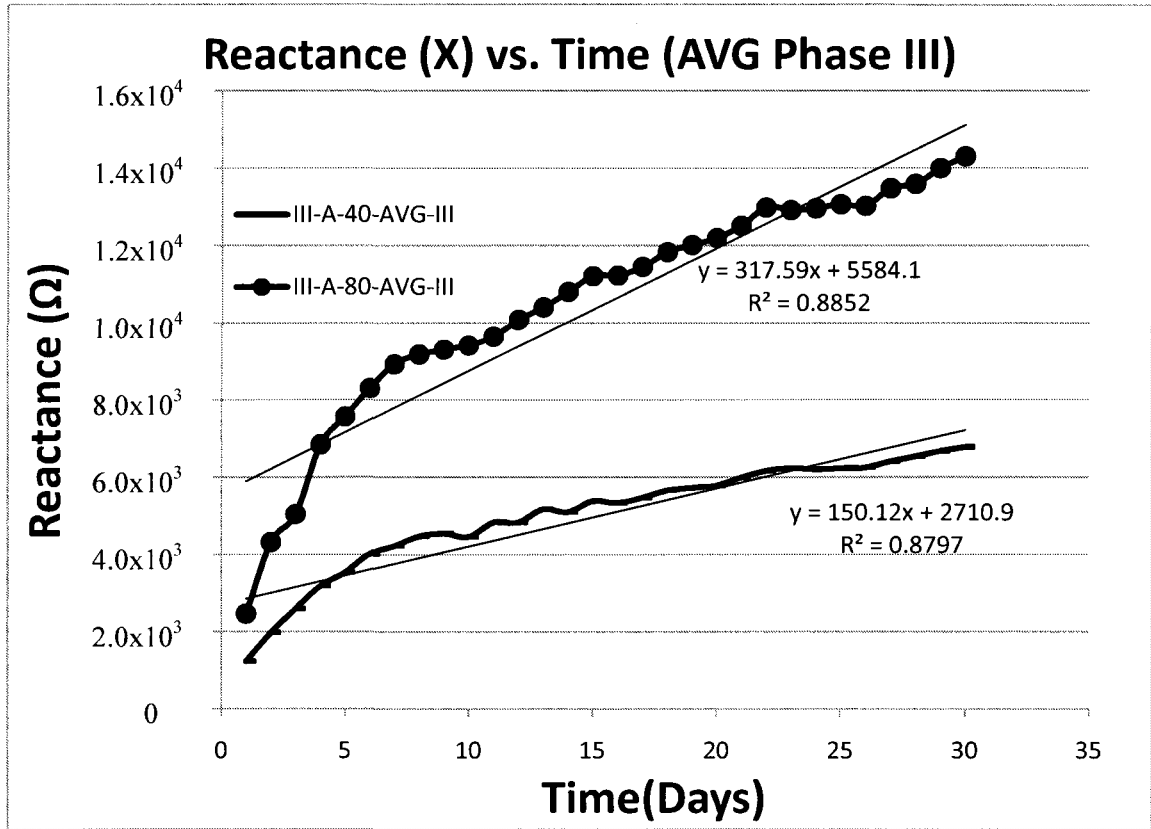
Figure 5.12: Reactance vs. time for specimens III-A-40-AVG-III and III-A-80-AVG-III

From Figure 5.12 it can be seen that the reactance of specimen type III-A-40-AVG-III was lower than the reactance of III-A-80-AVG-III. Since the electrode distance was the only parameter changed for mould type III in Phase III, it can be seen that as electrode distance increases the reactance (X) also increases. A linear regression analysis was performed on the two specimens from Phase III, resulting in an equation for calculating the reactance if the time is known. The analysis resulted in the R^2 values of 0.8797 and 0.8852 for III-A-40-AVG-III and III-A-80-AVG-III respectively, showing that the resulting equations represent a good linear fit. The equations for each specimen are as follows.

For III-A-40-AVG-III:

$$X = 150.12t + 2710.9 \qquad (5.15)$$

For III-A-80-AVG-III:

$$X = 317.59t + 5584.1 \qquad (5.16)$$

5.4.4   Analysis of Phase III Results

Since the equations for the reactance (X) and concrete strength (f_c) both depend on the variable of time linearly, the equations can be arranged to result in a certain reactance representing a corresponding strength. The equations for the strength of concrete (f_c) in terms of reactance (X) for each specimen tested in Phase III are as follows.

For II-B-20-AVG-III:

$$f_c = 9.110 \times 10^{-4}(X) + 11.18 \qquad (5.17)$$

For II-B-40-AVG-III:

$$f_c = 4.391 \times 10^{-5}(X) + 11.46 \qquad (5.18)$$

Where: X = reactance (Ω)

$\quad\quad\quad$ f_c = concrete strength (MPa)

A plot of equations 5.17 and 5.18 can be seen in Figure 5.13, where the reactance values used are the values that were obtained experimentally. Each point on the linear plot denotes 1 day in the concrete life cycle.
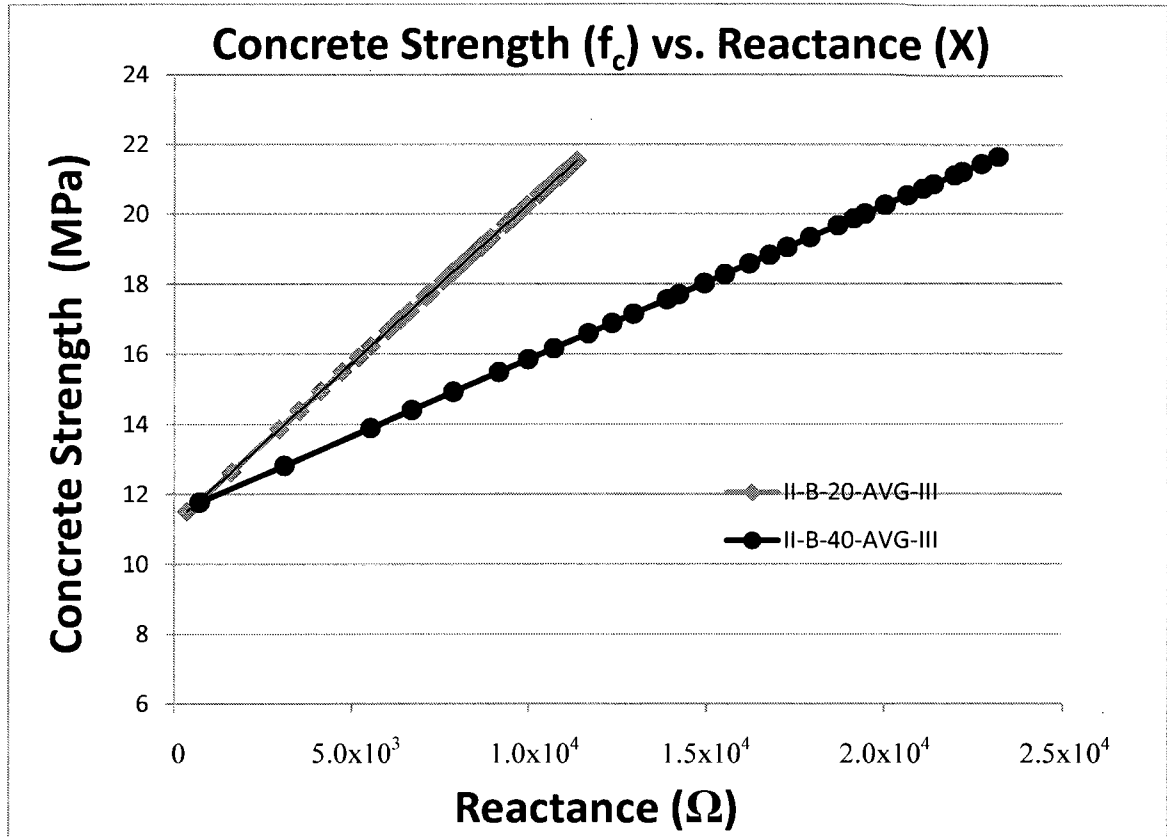
Figure 5.13: Concrete strength vs. reactance in Phase III

As it can be seen in Figure 5.13 each specimen type represents a distinctly different linear plot denoting the concrete strength (f_c) in terms of reactance (X). Specimen II-B-20-AVG-III represents the plot with the highest slope, while specimen II-B-40-AVG-III represents the plot with the lowest slope. Therefore, the slope of the strength-reactance plot decreased as the electrode distance increased.

The two relationships seen in equations 5.17 and 5.18, between concrete strength and reactance are considered valid only for Concrete Mix II as seen in Table 3.6 (Specimen mix C2), for a reactance calculated at f = 1000 Hz, and for the corresponding dimensions of mould Type II which can be seen in Table 3.7.

5.5   *Parametric Study*

In order to determine how the testing parameters of electrode spacing, mould area, and cement content affects the reactance of the concrete tested in the experimental program, a parametric study was undertaken.

5.5.1   Effect of Electrode Spacing

When the specimens II-A-20-AVG-I and II-A-40-AVG-I are considered it is known that the electrode distance of the two specimens is 20 mm and 40 mm, respectively whereas, other parameters such as concrete cross-section and concrete mix type are the same. The value of β (in equation 5.11) for specimen II-A-40-AVG-I is $2.23 = \left(\frac{2813.2}{1259.7}\right)$ times larger than the value of β for the specimen II-A-20-AVG-I, while the value of α for specimen II-A-40-AVG-I is $1.86 = \left(\frac{20997}{11254}\right)$ times larger than the value of α for the specimen II-A-20-AVG-I (see equations 5.3 and 5.4). The average increase between the two parameters is $2.05 = \left(\frac{2.23+1.86}{2}\right)$, showing that for the concrete specimens tested in Phase I the reactance doubled as the electrode distance doubled.

When the specimens III-A-40-AVG-III and III-A-80-AVG-III are considered it is known that the electrode distance between the two specimens is 40 mm and 80 mm, respectively. The value of β for specimen III-A-80-AVG-III is $2.116 = \left(\frac{317.59}{150.12}\right)$ times larger than the value of β for the specimen III-A-40-AVG-III, while the value of α for specimen III-A-80-AVG-III is $2.059 = \left(\frac{5584.1}{2710.9}\right)$ times larger than the value of α for the specimen III-A-40-AVG-III (see equations 5.15 and 5.16). The average increase between the two parameters is $2.0875 = \left(\frac{2.059+2.116}{2}\right)$, showing that the specimens tested in Phase III also exhibited a reactance that doubled as the electrode distance doubled.

When the specimens II-B-20-AVG-III and II-B-40-AVG-III are considered it is known that the electrode distance of the two specimens is 20 mm and 40 mm, respectively. The value of β for specimen II-B-40-AVG-III is $2.07 = \left(\frac{680.32}{327.88}\right)$ times larger than the value of β for the specimen II-B-20-AVG-III, while the value of α for specimen II-B-40-AVG-III

is $1.81 = \left(\frac{4392.9}{2433.2}\right)$ times larger than the value of α for the specimen II-B-20-AVG-III (see equations 5.13 and 5.14). The average increase between the two parameters is $1.94 = \left(\frac{2.07+1.81}{2}\right)$, showing that the other specimens tested in Phase III also exhibited a reactance that doubled as the electrode distance doubled. It is interesting to note that the same relationship between electrode distance and reactance exists in both Phase I and Phase III regardless of the electrode contact area or the concrete mix used. This effect can be seen in Figure 5.14 which shows the reactance plotted with electrode spacing for all of the specimens discussed in this section.
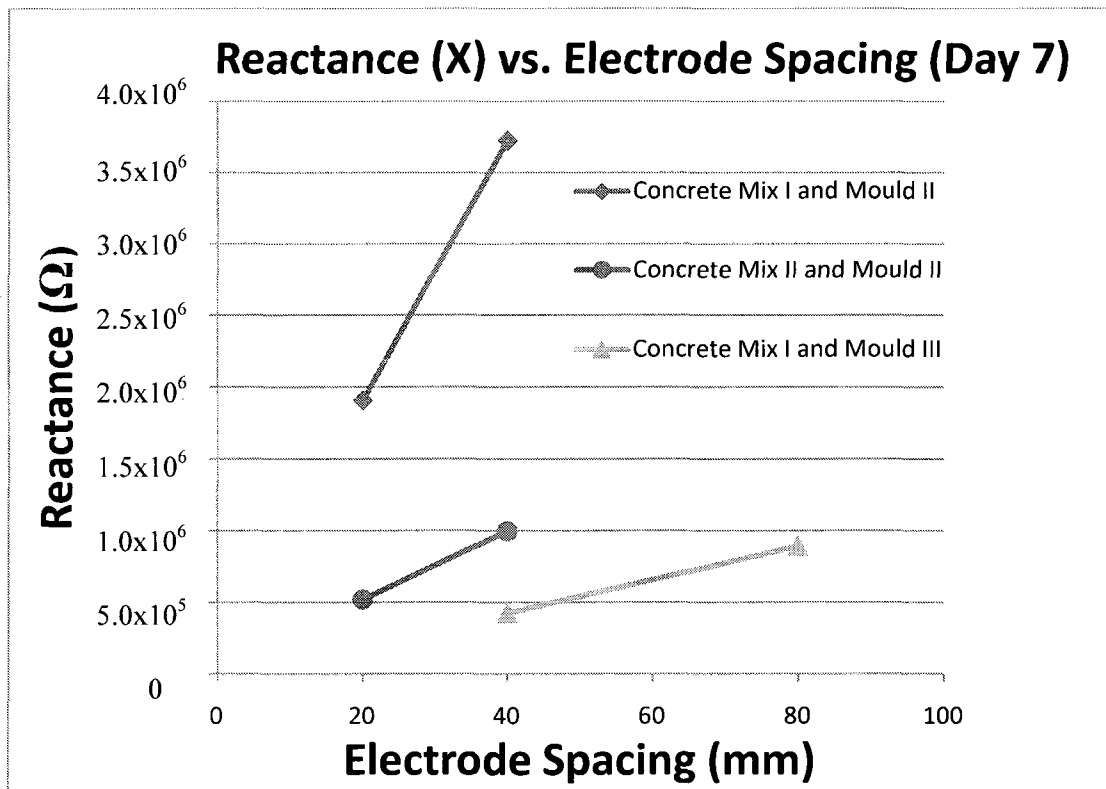
Figure 5.14: Reactance vs. electrode spacing at day 7

However, it is unclear if the same result would occur if the electrodes were spaced at different distances. Therefore, it needs to be tested at a later date to determine the effects of changing the electrode distance at different values.

5.5.2 Effect of Electrode Contact Area

When the specimens I-A-20-AVG-I and II-A-20-AVG-I are considered it is known that the cross-section of each specimen (A) is 50 mm x 50 mm and 100 mm x 100 mm, respectively. The value of β for specimen I-A-20-AVG-I is $6.72 = \left(\frac{8461.5}{1259.7}\right)$ times larger than the value of β for the specimen II-A-20-AVG-I, while the value of α for specimen I-A-20-AVG-I is $3.01 = \left(\frac{33908}{11254}\right)$ times larger than the value of α for the specimen II-A-20-AVG-I (see equations 5.2 and 5.3). Therefore, it seems that an increase of cross-sectional area (A) caused a decrease in reactance and a decrease in the parameters β and α in Phase I.

When the specimens II-A-40-AVG-I and III-A-40-AVG-III are considered it is known that the cross-section of each specimen is 100 mm x 100 mm and 200 mm x 200 mm, respectively. The value of β for specimen II-A-40-AVG-I is $18.74 = \left(\frac{2813.2}{150.12}\right)$ times larger than the value of β for the specimen III-A-40-AVG-III, while the value of α for specimen II-A-40-AVG-I is $7.75 = \left(\frac{20997}{2710.9}\right)$ times larger than the value of α for the specimen III-A-40-AVG-III (see equations 5.4 and 5.15). Therefore, in Phase III it still seems that an increase in electrode contact area (A) caused a decrease in reactance and a decrease in the parameters β and α in Phase III. The general trend that relates the electrode contact area to the parameter β can be seen in Figure 5.15.
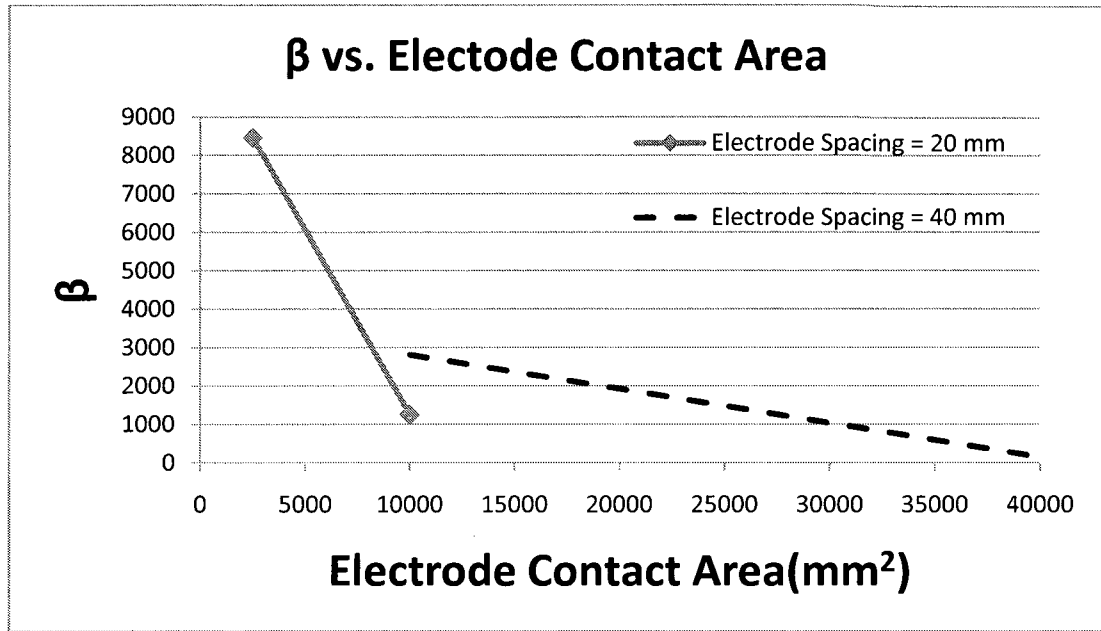
Figure 5.15: Variation of β with electrode contact area

As seen in Figure 5.15, β decreases as the electrode contact area increases. This general trend cannot be further explored in this study since only limited data is available. Thus, in the future, a larger number of contact areas need to be tested in order to determine the exact effect of electrode contact area (A) on the parameter β. The general trend that relates the electrode contact area to the parameter α can be seen in Figure 5.16.
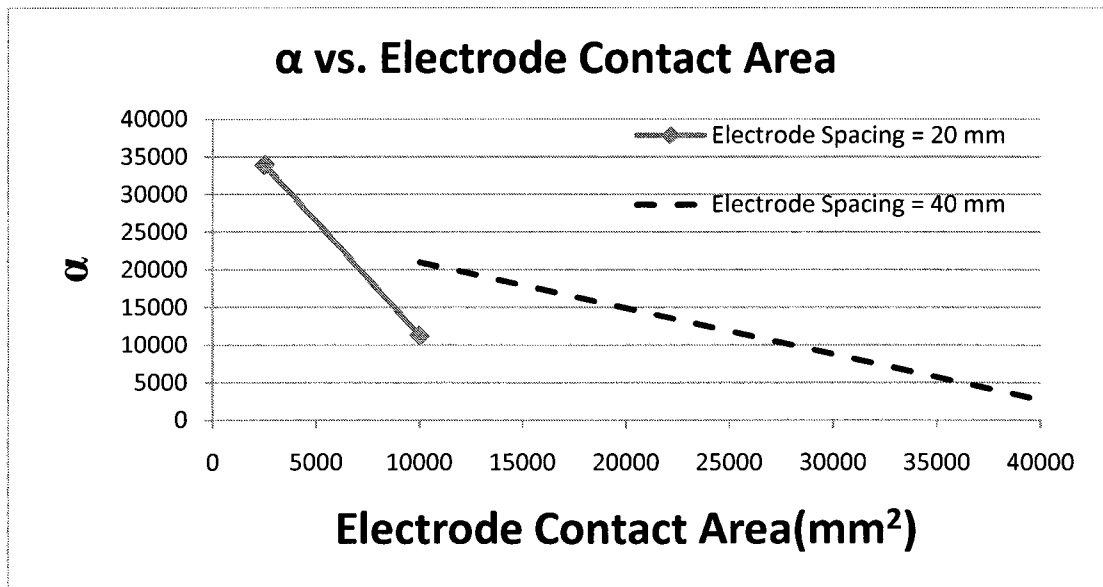
Figure 5.16: Variation of α with electrode contact area

97

As seen in Figure 5.16, α also decreases as the electrode contact area increases. This general trend needs to be further explored with more specimens with different contact areas in order to determine the exact effect of electrode contact area on the parameter α. The main conclusion that can be drawn from the effect of electrode contact area on the reactance of concrete is that, the reactance decreases as the electrode contact area increases. This relationship can be seen in the plots of reactance with time for the specimens discussed in this section (Figure 5.17).

Figure 5.17: Reactance vs. time for specimens with varying electrode contact area

5.5.3 Effect of Cement Content

When the specimens II-A-20-AVG-I and II-B-20-AVG-III are considered it is known that the specimens differ in concrete mix only. Specimen II-A-20-AVG-I used Concrete Mix I and specimen II-B-20-AVG-III used Concrete Mix II, respectively, Concrete Mix II (B) used a much smaller proportion of cement than Concrete Mix I (A). The value of β for

specimen II-A-20-AVG-I is $3.84 = \left(\frac{1259.7}{327.88}\right)$ times larger than the value of β for the specimen II-B-20-AVG-III, while the value of α for specimen II-A-20-AVG-I is $4.63 = \left(\frac{11254}{2433.2}\right)$ times larger than the value of α for the specimen II-B-20-AVG-III. While there is no direct correlation that can be made, it can be seen that reducing the amount of cement in the concrete caused a reduction in the reactance of the specimens tested.

When the specimens II-A-40-AVG-I and II-B-40-AVG-III are considered it is known that the specimens differ by concrete mix type only. These two specimens used Concrete Mix I and Concrete Mix II, respectively. The value of β for specimen II-A-40-AVG-I is $4.14 = \left(\frac{2813.2}{680.32}\right)$ times larger than the value of β for the specimen II-B-40-AVG-III, while the value of α for specimen II-A-40-AVG-I is $4.78 = \left(\frac{20997}{4392.9}\right)$ times larger than the value of α for the specimen II-B-40-AVG-III. There still does not seem to be a direct relationship between the amount of cement content and reactance but it is interesting that the parameters β and α seem to increase by roughly the same amount regardless of the electrode distance. It is concluded that in general a decrease in cement content will cause a decrease in reactance, which can be seen in the plots of reactance with time for the specimens discussed in this section (Figure 5.18).

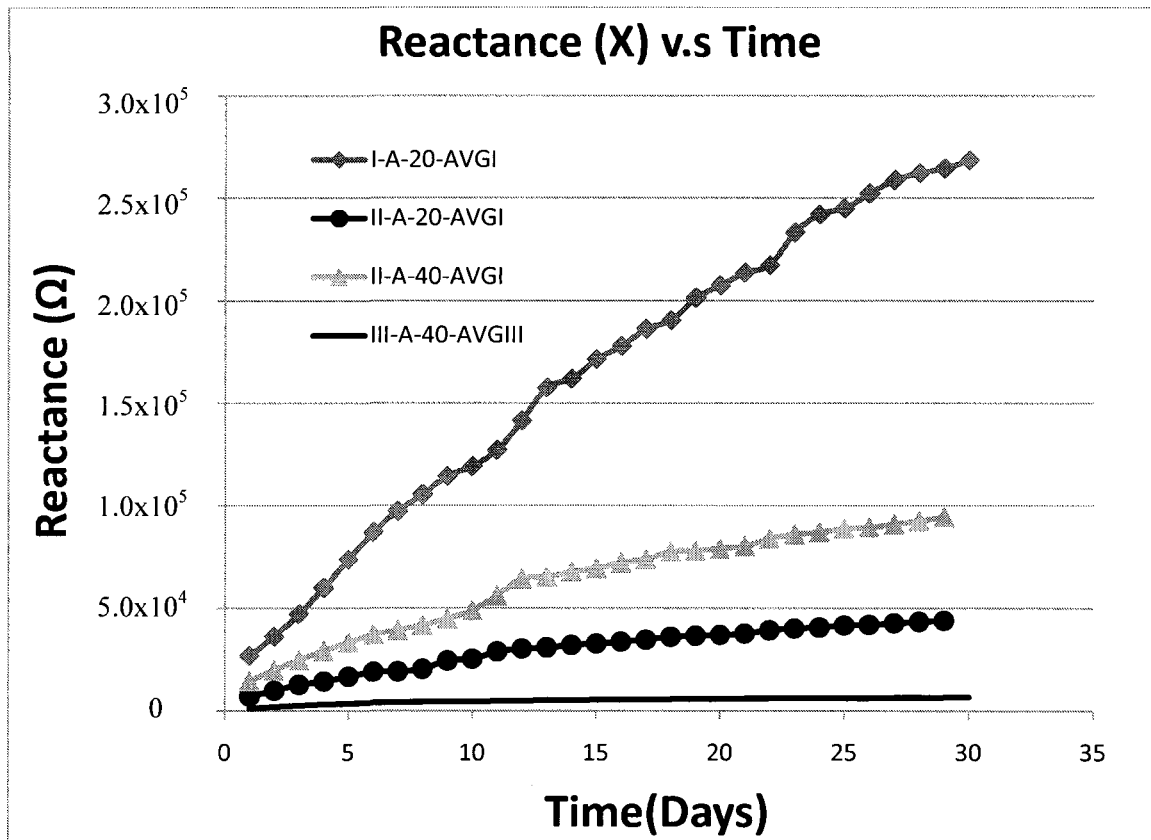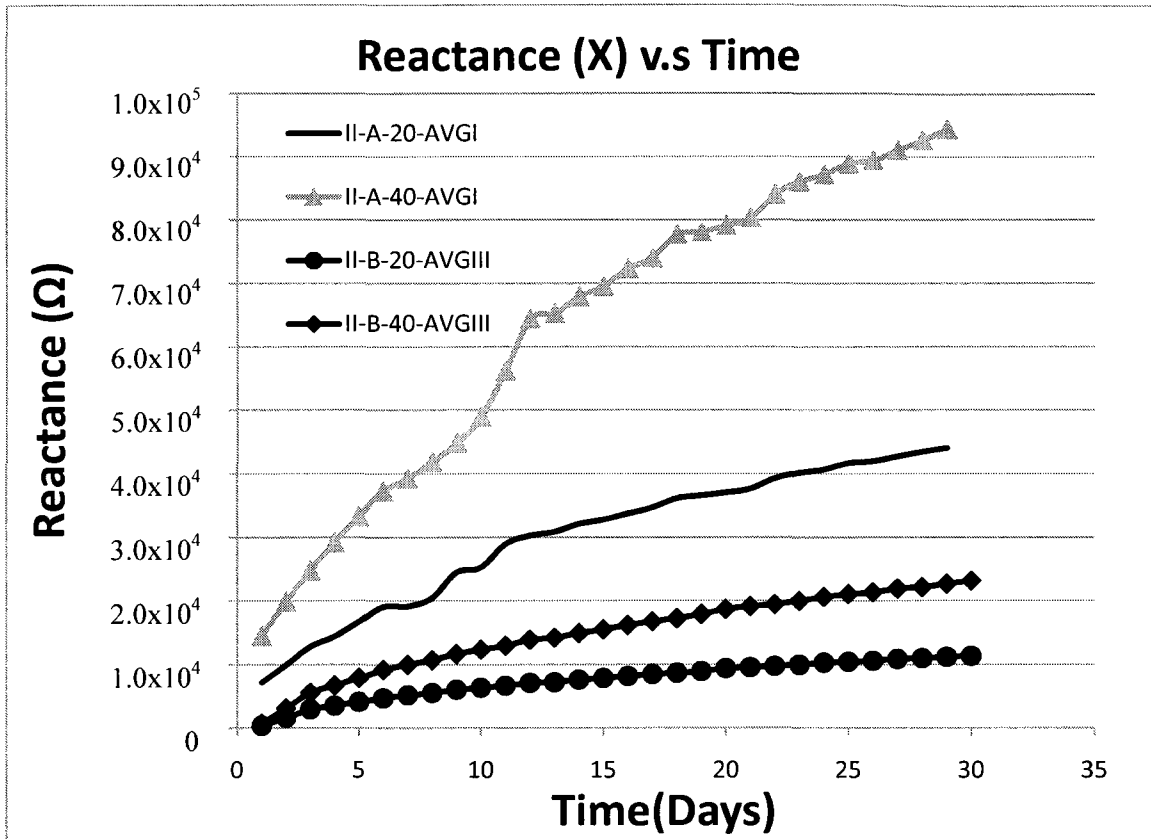**Figure 5.18: Reactance vs. time for specimens with varying cement content**

However, a distinct relationship between the reactance and cement content cannot be determined using the data in this study. A number of specimens with different cement contents need to be tested in the future in order for it to become more apparent as to what distinct effect that changing the cement content of the specimen has on the reactance of concrete besides simply lowering it.

5.6   *Summary*

This chapter presented and discussed the results of the experimental program followed in this study. The results of each phase were presented including both the compression strength results and the electrical testing results. It was concluded that the reactance of concrete is not greatly affected by frequency as the shape of the reactance-time curve does not change with frequency. After analyzing the data it was apparent that a linear relationship existed between the reactance and compressive strength of concrete. It was also discussed how the parameters of the concrete specimens effected the reactance of the

concrete tested in this study. It was found that an increase in electrode distance caused an increase in reactance, an increase in electrode contact area caused a decrease in reactance and a decrease in cement content caused a decrease in reactance. These general relationships were discovered in the experimental program of this study, whereas a definite relationship between these parameters and the reactance of concrete cannot be developed without further research.

6 SUMMARY, CONCLUSIONS AND RECOMMENDATIONS

6.1 *Summary*

The objectives of this study were to determine if a relationship exists between the electrical properties and strength of concrete and investigate the effect of electrode distance, electrode contact area, and cement content on the electrical properties of concrete. The study was carried out in three distinct phases in order to organize the results in an appropriate manner.

Phase I used two different moulds: Type I (Fig. 3.7) and Type II (Fig. 3.8) and two different electrode spacings: 20 mm and 40 mm. However only one concrete mix (Concrete Mix I or A) was used, as shown in Tables 3.8 and 3.9. The reactance of the concrete specimens was linearly correlated to the strength of the concrete and the results are given in equations 5.6, 5.7, and 5.8. The physical parameters tested in Phase I include the electrode spacing and electrode contact area. It was found that doubling electrode distance doubled the reactance, and in general an increase in electrode contact area caused a reduction in reactance.

Phase II used only one mould: Type I (Fig. 3.7): one electrode spacing of 20 mm; and two cement pastes (Cement Paste Mix I and Cement Paste Mix II). Cement Paste Mix I (C) had a W/C ratio of 0.62, whereas Cement Paste Mix II (D) had a W/C ratio of 0.39. No strength tests were undertaken on these specimens (Table 3.8). Although there was no strength data to correlate the reactance with for the cement paste, it was found that the reactance of the cement paste increased as the W/C ratio decreased. This result was expected as Cement Paste Mix II (D) had a higher amount of water than Cement Paste Mix I (C) and it was assumed that the capacitance would increase as the amount of water present increased. It was also found that the reactance of the cement paste was in the same order of magnitude of the concrete tested in the same mould. Therefore, it may be concluded that the cement paste is the main medium in which the current travels in concrete.

Phase III used two different moulds: Type II (Fig. 3.8) and Type III (Fig. 3.9) as in Table 3.7 and two different concrete mix types: Concrete Mix I (A) and Concrete Mix II (B).

The spacing between electrodes varied between 20 mm and 40 mm for mould Type II, and between 40 mm and 80 mm for mould Type III (Table 3.7). The specimens cast in mould Type III were cast with Concrete Mix I and the specimens cast in mould Type II were cast with Concrete Mix II. The reactance of the concrete specimens cast with Concrete Mix II were found to correlate linearly with the strength of the concrete tested and the results can be seen in equations 5.17 and 5.18. The physical parameters tested in Phase III include the electrode spacing, electrode contact area, and cement content. It was found when comparing the results from Phase I and Phase III that once again doubling the electrode distance doubled the reactance, although it was seen in three different cases it cannot be assumed that the reactance will double in every case that the electrode distance doubles. It was found once again that in general an increase in electrode contact area caused a reduction in reactance, this general statement is the only definite evidence found for how the electrode contact area affects the reactance. It was also found that a reduction of cement content from Concrete Mix I to Concrete Mix II caused a reduction of the reactance as well.

6.2   *Conclusions*

Based on the results obtained in this study the following conclusions were made. It must be noted that the conclusions made here only pertain to the concrete mixes and mould sizes used in this study.

- The strength of concrete can definitely be related to the reactance of concrete, since both of the variables vary linearly with time.
- The reactance of the concrete increases if the electrode distance in the concrete mould increases.
- The reactance of the concrete decreases if the electrode contact area in the concrete mould increases.
- The reactance of the concrete decreases if the cement content of the concrete decreases.
- The reactance of concrete is not greatly affected by frequency as the shape of the reactance-time curve does not change with frequency.

6.3   *Recommendations*

In order to further establish the relationship between the reactance and strength of concrete, further testing is required with other parameters not discussed in this study. An increased number of electrode distances should be studied with varying factors of increase, including triple the electrode distance and quadruple the electrode distance. An increased electrode contact area with the same electrode distance should also be studied, in order to establish a more definite trend between the electrode contact area and the reactance. Also, the effect of increased aggregate size should be studied to further investigate the relationship between the reactance and strength of concrete. Further research should also be completed in order to establish the proper circuit representation for concrete as an electrical material.

APPENDIX A – REACTANCE DATA

Table A.0.1: Average reactance of specimens tested in Phase I

Day	I-A-20-AVG-I X Reactance (Ω)	II-A-20-AVG-I X Reactance (Ω)	II-A-40-AVG-I X Reactance (Ω)
1	2.6761E+04	N/A	N/A
2	3.6265E+04	7.1313E+03	1.4502E+04
3	4.7161E+04	9.8779E+03	1.9889E+04
4	6.0052E+04	1.2761E+04	2.4806E+04
5	7.3842E+04	1.4417E+04	2.9246E+04
6	8.7172E+04	1.6712E+04	3.3332E+04
7	9.7416E+04	1.9056E+04	3.7255E+04
8	1.0557E+05	1.9160E+04	3.9218E+04
9	1.1446E+05	2.0448E+04	4.1845E+04
10	1.1923E+05	2.4489E+04	4.4837E+04
11	1.2720E+05	2.5284E+04	4.8972E+04
12	1.4154E+05	2.8927E+04	5.6193E+04
13	1.5782E+05	3.0286E+04	6.4392E+04
14	1.6205E+05	3.0875E+04	6.5284E+04
15	1.7164E+05	3.2124E+04	6.7887E+04
16	1.7809E+05	3.2788E+04	6.9545E+04
17	1.8646E+05	3.3725E+04	7.2326E+04
18	1.9076E+05	3.4697E+04	7.4033E+04
19	2.0157E+05	3.6138E+04	7.7711E+04
20	2.0768E+05	3.6608E+04	7.8124E+04
21	2.1379E+05	3.7056E+04	7.9151E+04
22	2.1758E+05	3.7626E+04	8.0337E+04
23	2.3347E+05	3.9275E+04	8.4041E+04
24	2.4214E+05	4.0172E+04	8.6093E+04
25	2.4516E+05	4.0686E+04	8.7159E+04
26	2.5237E+05	4.1703E+04	8.8944E+04
27	2.5891E+05	4.1990E+04	8.9423E+04
28	2.6234E+05	4.2774E+04	9.1048E+04
29	2.6465E+05	4.3490E+04	9.2662E+04
30	2.6867E+05	4.4072E+04	9.4412E+04

Table A.0.2: Average reactance of specimens tested in Phase II

Day	I-C-20-A-II X Reactance (Ω)	I-D-40-AVG-II X Reactance (Ω)
1	9.6736E+02	2.8180E+03
2	1.8787E+03	6.7758E+03
3	3.3112E+03	1.0148E+04
4	5.2454E+03	1.6549E+04
5	6.6501E+03	2.0720E+04
6	7.2244E+03	2.4360E+04
7	8.0271E+03	2.8903E+04
8	8.5450E+03	3.1237E+04
9	9.2405E+03	3.4445E+04
10	9.8719E+03	4.4867E+04
11	1.0961E+04	5.2081E+04
12	1.3356E+04	5.6279E+04
13	1.4581E+04	6.1258E+04
14	1.6385E+04	6.7007E+04
15	1.7276E+04	7.0316E+04
16	1.7858E+04	7.3534E+04
17	1.8481E+04	7.6563E+04
18	2.4834E+04	8.4229E+04
19	2.6490E+04	8.7801E+04
20	2.7076E+04	9.1494E+04
21	2.9163E+04	9.6336E+04
22	3.0982E+04	1.0156E+05
23	3.1598E+04	1.0352E+05
24	3.2838E+04	1.0591E+05
25	3.7574E+04	1.1086E+05
26	4.0035E+04	1.1626E+05
27	4.6069E+04	1.2323E+05
28	4.6136E+04	1.2479E+05
29	4.6203E+04	1.2719E+05
30	4.7873E+04	1.2857E+05

Table A.0.3: Average reactance of specimens tested in Phase III

Day	II-B-20-AVG-III X Reactance (Ω)	II-B-40-AVG-III X Reactance (Ω)	III-A-40-AVG-III X Reactance (Ω)	III-A-80-AVG-III X Reactance (Ω)
1	3.7113E+02	7.1390E+02	1.2398E+03	2.4710E+03
2	1.6088E+03	3.1014E+03	1.9846E+03	4.3224E+03
3	2.9559E+03	5.5347E+03	2.6006E+03	5.0494E+03
4	3.5267E+03	6.7065E+03	3.1929E+03	6.8487E+03
5	4.1334E+03	7.8793E+03	3.5447E+03	7.5703E+03
6	4.7397E+03	9.1657E+03	4.0194E+03	8.3120E+03
7	5.1937E+03	9.9900E+03	4.2284E+03	8.9318E+03
8	5.5490E+03	1.0709E+04	4.4766E+03	9.1841E+03
9	6.0396E+03	1.1680E+04	4.5480E+03	9.3106E+03
10	6.3640E+03	1.2347E+04	4.4652E+03	9.4218E+03
11	6.6541E+03	1.2950E+04	4.8365E+03	9.6476E+03
12	7.0985E+03	1.3892E+04	4.8377E+03	1.0086E+04
13	7.2171E+03	1.4220E+04	5.1792E+03	1.0409E+04
14	7.6094E+03	1.4943E+04	5.1058E+03	1.0809E+04
15	7.8603E+03	1.5527E+04	5.3881E+03	1.1218E+04
16	8.1571E+03	1.6220E+04	5.3418E+03	1.1233E+04
17	8.4577E+03	1.6789E+04	5.4769E+03	1.1456E+04
18	8.6721E+03	1.7279E+04	5.6650E+03	1.1839E+04
19	8.9344E+03	1.7926E+04	5.7308E+03	1.2019E+04
20	9.3715E+03	1.8705E+04	5.7873E+03	1.2200E+04
21	9.5408E+03	1.9157E+04	5.9893E+03	1.2515E+04
22	9.7224E+03	1.9463E+04	6.1680E+03	1.2988E+04
23	9.9609E+03	2.0031E+04	6.2350E+03	1.2924E+04
24	1.0302E+04	2.0653E+04	6.2039E+03	1.2966E+04
25	1.0438E+04	2.1096E+04	6.2332E+03	1.3073E+04
26	1.0578E+04	2.1380E+04	6.2517E+03	1.3030E+04
27	1.0861E+04	2.1972E+04	6.4105E+03	1.3481E+04
28	1.0992E+04	2.2185E+04	6.5384E+03	1.3590E+04
29	1.1205E+04	2.2726E+04	6.6767E+03	1.3998E+04
30	1.1345E+04	2.3192E+04	6.7803E+03	1.4300E+04

APPENDIX B – ELECTRICAL PARAMETER PLOTS

As discussed in the body of this thesis, the reactance was found to be the most important electrical parameter in this study. However, other electrical parameters were tested to investigate which parameter would be best suited for this study. The resistance (R), impedance (Z), phase angle (θ), and dissipation factor (D) were also acquired in each phase. It was found that like reactance (X), the resistance (R) and impedance (Z) also exhibited a linear relationship with time. However, the variance between specimens of the same type was found to be higher than the variance seen in the reactance of the specimens. Therefore, these parameters were not used in the analysis of the test results. Also, it was found that the phase angle (θ) and dissipation factor (D) did not produce a linear relationship with time and were therefore, disregarded as well. Following are plots of the parameters described above plotted with time, for specimens I-A-20-A-I and I-A-20-B-I at a frequency (f) of 1000 Hz.
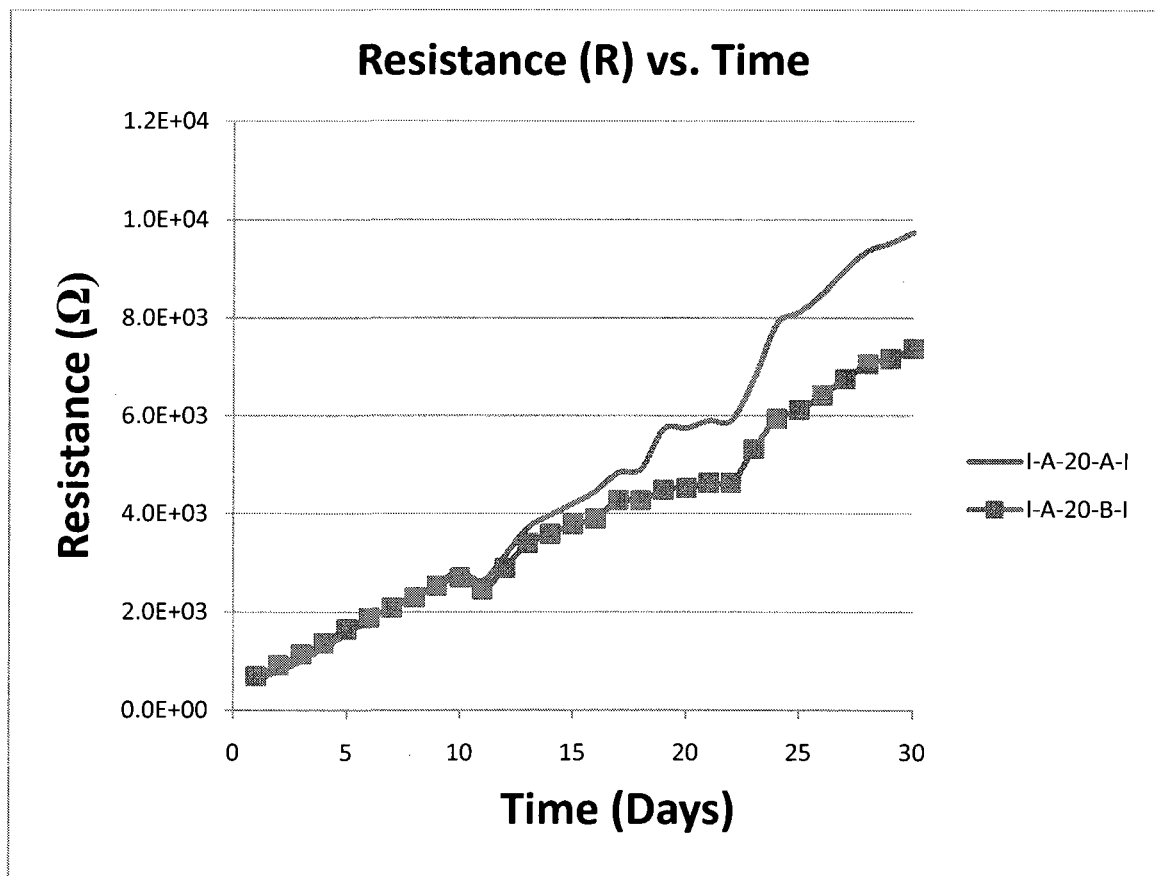

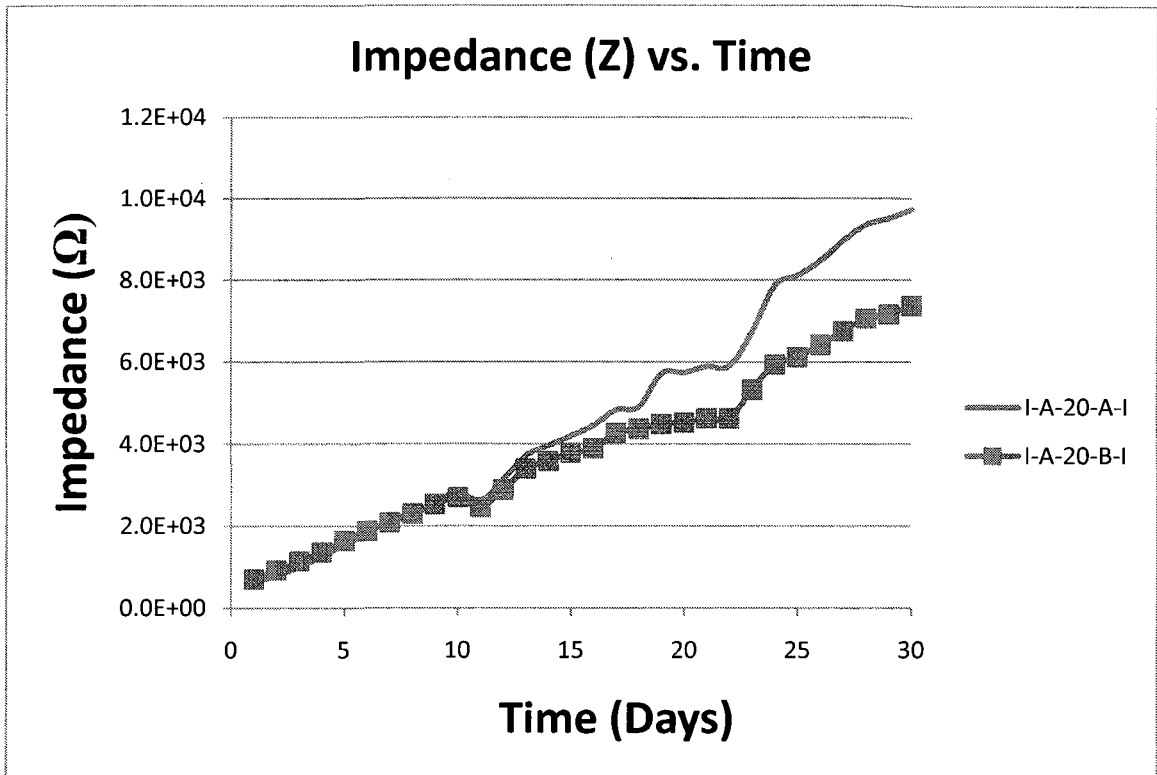**Figure B.0.1: Resistance vs. time for specimens I-A-20-A-I and I-A-20-B-I**

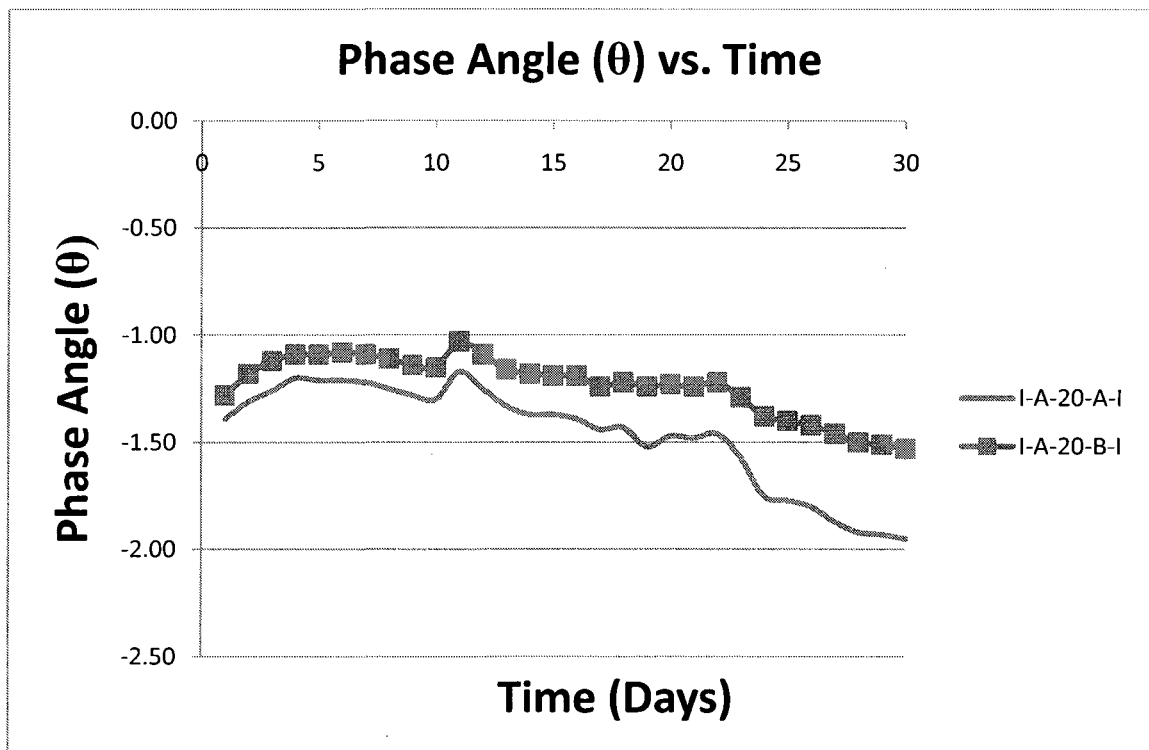Figure B.0.2: Impedance vs. time for specimens I-A-20-A-I and I-A-20-B-I

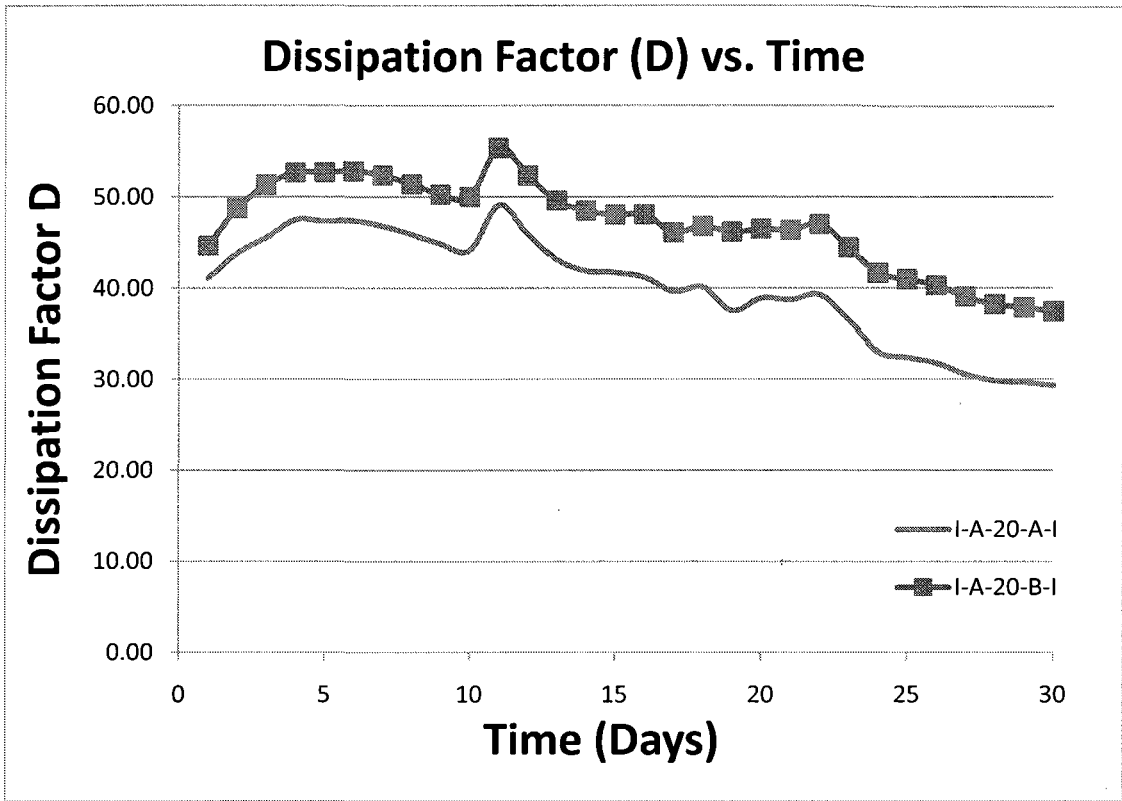Figure B.0.3: Phase angle vs. time for specimens I-A-20-A-I and I-A-20-B-I

Figure B.0.4: Dissipation factor vs. time for specimens I-A-20-A-I and I-A-20-B-I

APPENDIX C – STRESS-STRAIN PLOTS

The average stress-strain curves were given for each testing day in the Phase I compressive strength testing section (5.2.2) in Figure 5.1. However, each compression cylinder tested developed a unique stress-strain curve, and therefore, the stress-strain curve for each cylinder tested in Phase I can be seen in the following figures.
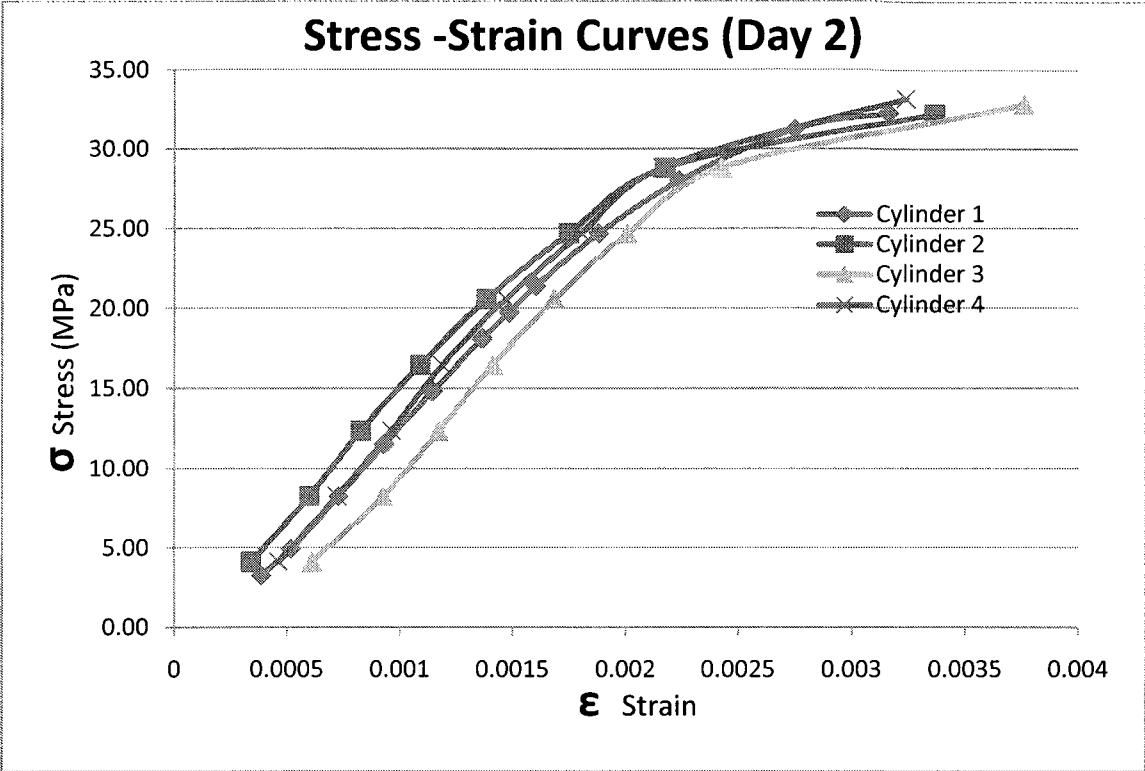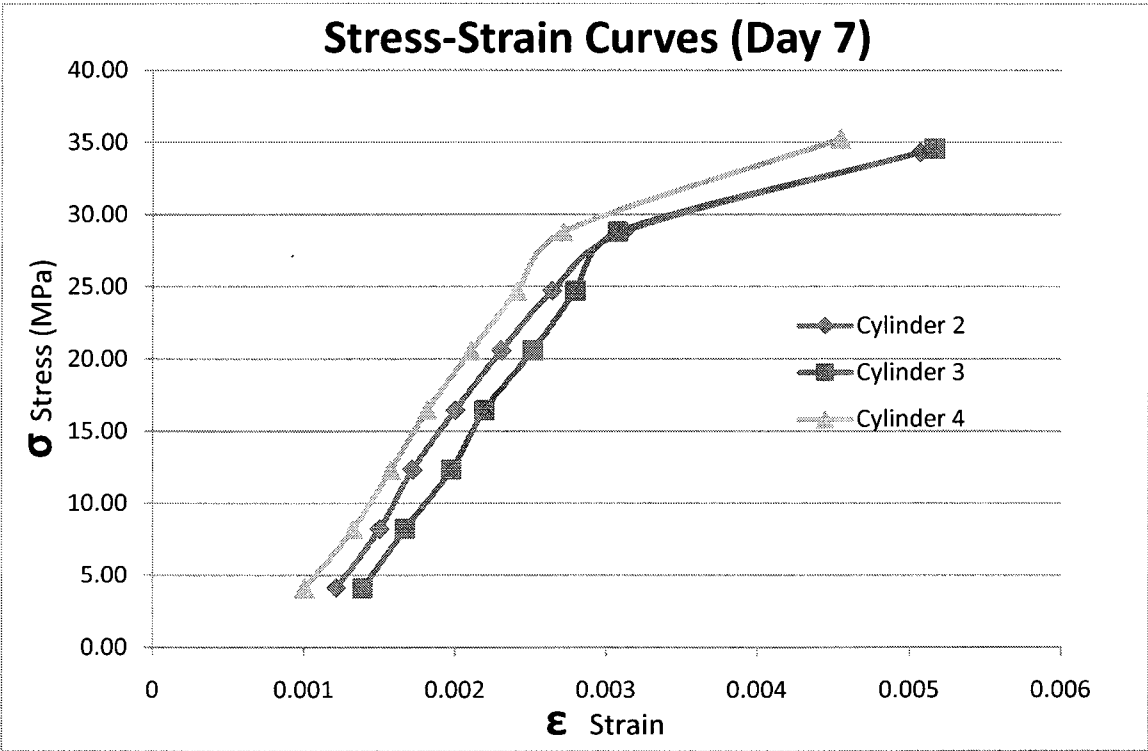
Figure C.0.1: Day 2 stress-strain curves

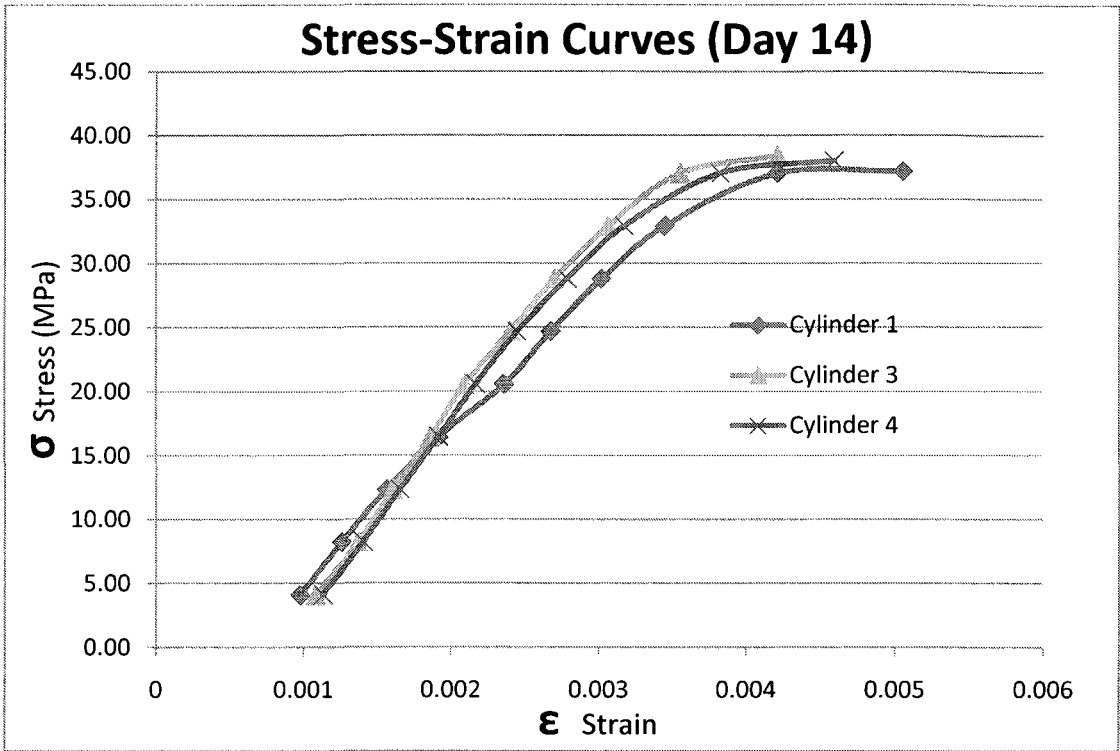**Figure C.0.2: Day 7 stress-strain curves**

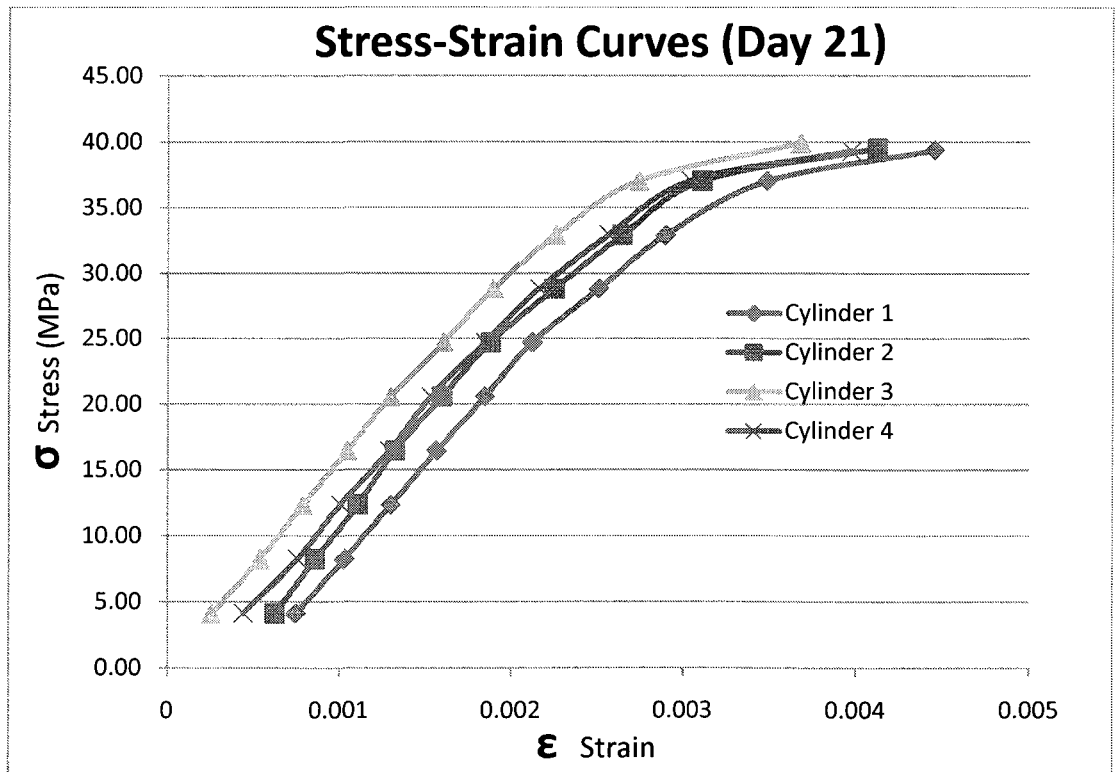**Figure C.0.3: Day 14 stress-strain curves**
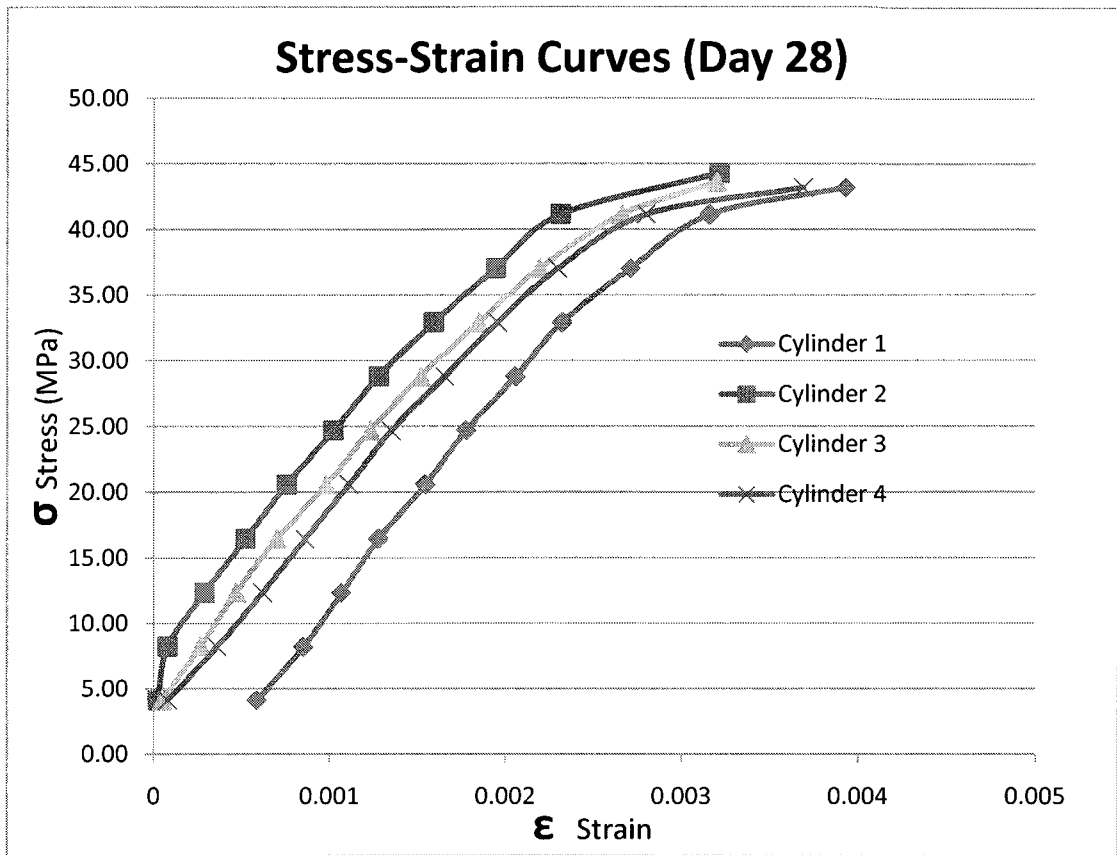

Figure C.0.4: Day 21 stress-strain curves

Figure C.0.5: Day 28 stress-strain curves

APPENDIX D – INTRODUCTION OF DEFECT INTO CONCRETE

The effect of introducing a defect into a concrete specimen at specific days in the concrete curing life cycle was also completed in this study. Six concrete specimens were cast in Concrete Mould II (Figure D.0.1) with an electrode spacing of 40 mm only, using Concrete Mix I (A).
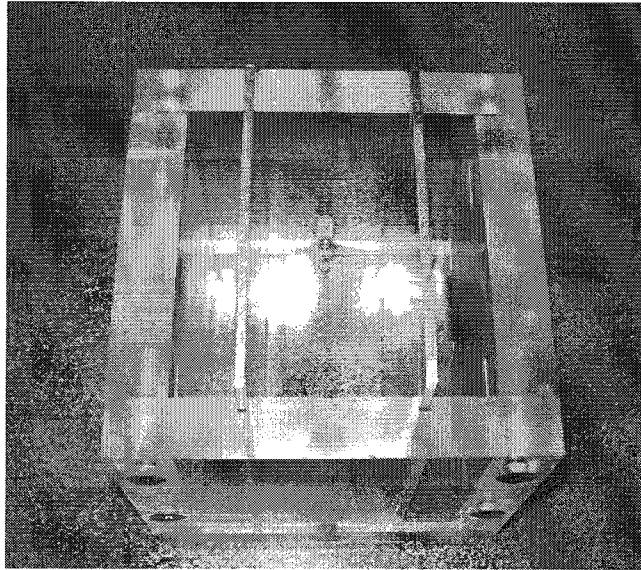

Figure D.0.1: Concrete Mould II with electrodes spaced 40 mm

One specimen was considered the control specimen and no defect was introduced into the specimen, while the other specimens had a 10 mm hole drilled into the centre of the concrete on the days 2, 7, 14, 21, and 28 (Figure D.0.2).
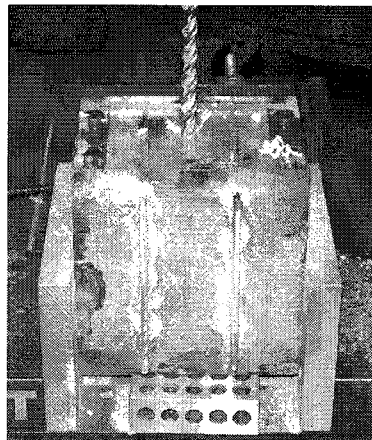

Figure D.0.2: Hole being drilled in concrete mould

Cylinders were also cast using Concrete Mix I (A), and were tested for strength on days 2, 7, 14, 21, and 28. A 10 mm hole was also drilled in the centre of the cylinders on the day of testing and it can be seen in Figure D.0.3.
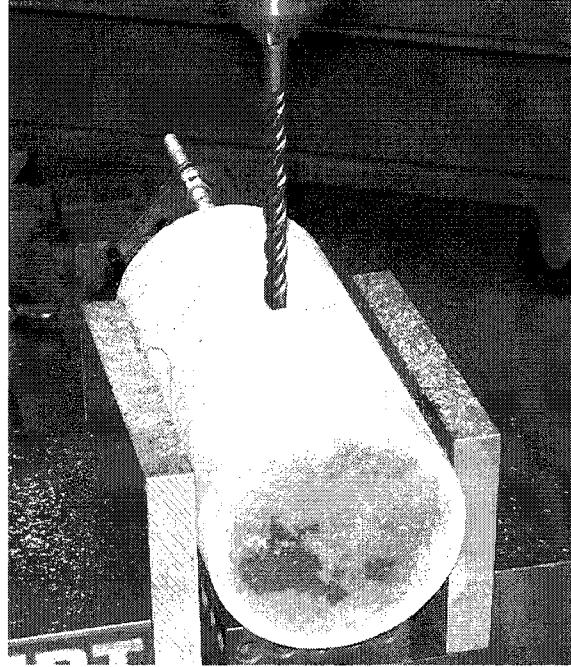

Figure D.0.3: Hole being drilled in concrete cylinder

The results of the compression testing can be seen in Table D.0.1 where the strength of each cylinder and the average strength for each testing day is given.

Table D.0.1: Compression testing strength results for defected cylinders

Cylinder Number	Strength (MPa)				
	Day 2	Day 7	Day 14	Day 21	Day 28
1	22.08	33.47	34.98	38.13	38.27
2	20.85	32.37	35.39	outlier	38.41
3	23.18	32.47	34.70	37.58	39.23
4	21.54	36.21	35.18	37.72	39.09
Average Strength	**21.91**	**33.88**	**35.09**	**37.81**	**38.75**

Each concrete specimen used for measuring electrical parameters was measured from days 2 to 28 and on the day of defect introduction the reactance was measured before the

115

hole was drilled and directly after the hole was drilled to determine the effect of introducing a defect on the reactance of concrete. A plot of the reactance with time for the samples tested can be seen in Figure D.0.4. It should be noted that only the plots for the control and days 2 and 14 were included as it was found that the moulds used for the other testing days were of poor quality and provided inconsistent results.
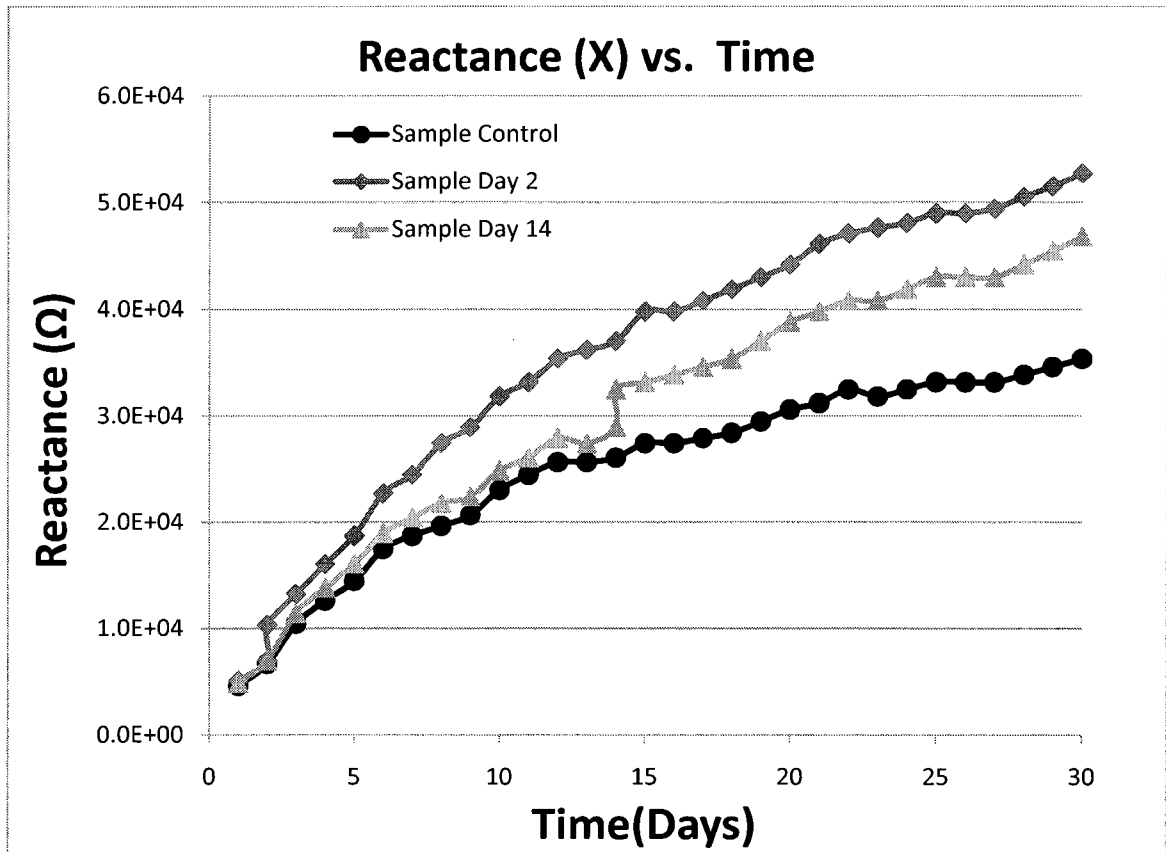

Figure D.0.4: Reactance vs. time for defected concrete specimens

In Figure D.0.4 it can seen that the reactance increased directly after the defect was introduced, and that the reactance of the other specimens followed the reactance of the control specimen closely until the defect was introduced. From this result it can be concluded that the existence of a defect in concrete can be determined using the reactance as an indication, since the reactance increases directly after a defect is introduced into the concrete.

LIST OF REFERENCES

Abd El Wahed, and M.G., Hekal, E.E., 1989, "Electrical conductivity of cement pastes in different curing media." Journal of Materials Science Letters, Chapman and Hall Ltd., vol.8, no. 8, pp 875-878.

Berg, A., Niklasson, G.A., Brantervik, K., Hedberg. B, and Nilsson, L.O., 1992, "Dielectric properties of cement mortar as a function of water content." Journal of Applied Physics, American Physics Institute, vol. 71, no. 12, pp 5897-5903.

CSA, 2009. "A23.1: Concrete materials and methods of concrete construction." Canadian Standard Association, Mississauga, Ontario Canada.

CSA, 2009. "A23.2: Test methods and standard practices for concrete." Canadian Standard Association, Mississauga, Ontario Canada.

Manchiryal, R.K., and Neithalath, N., 2008, "Electrical property-based sensing of concrete: influence of material parameters on dielectric response." American Concrete Institute, ACI Special Publication, no. 252, pp 23-40.

McCarter, W.J., Garvin, S., and Bouzid,N. , 1988, "Impedance measurements on cement paste." Journal of Materials Science Letters, Springer US, vol. 7, no. 10, pp 1056-1057.

McCarter,W.J., 1996, "The a.c. impedance response of concrete during early hydration." Journal of Materials Science, Springer US, vol. 31, no. 23, pp 6285-6292.

Tashiro, C., Ishida, H., and Shimamura, S., 1987, "Dependence of the electrical resistivity on evaporable water content in hardened cement pastes." Journal of Materials Science Letters, Springer US , vol. 6, no. 12, pp 1379-1381.

Taylor, M.A., and Arulanandan, K., 1974, "Relationships between electrical and physical properties of cement pastes." Cement and Concrete Research, Elsevier, vol.4, pp 881-897.

Whittington, H.W., and Wilson, J.G., 1986, "Low-frequency electrical characteristics of fresh concrete." IEE Proceedings A (Physical Science, Measurements, Instrumentation, Management & Education, Reviews), Institution of Electrical Engineers, Lancaster, UK, vol. 133, no. 5, pp 265-271.

Whittington, H.W., McCarter, W.J, and Forde, M.C., 1981, "The conduction of electricity through concrete." Magazine of Concrete Research, Institute of Civil Engineers, vol. 33, no. 114, pp 48-60.

Wilson, J.G., and Khalaf, F.M., 1999, "Electrical properties of freshly mixed concrete." Journal of Materials in Civil Engineering, American Society of Civil Engineers, vol. 11, no. 3, pp 242-248.

Wilson, J.G., Whittington, H.W., and Forde, M.C., 1984, "Dielectric properties of concrete at different frequencies." Fourth International Conference on Dielectric Materials, Measurements & Applications, Institution of Electrical Engineers, Lancaster, UK, pp 157-160.

Wilson, J.G., and Whittington, H.W., 1990, "Variations in the electrical properties of concrete with change in frequency." IEE Proceedings A (Physical Science, Measurements, Instrumentation, Management & Education, Reviews), Institution of Electrical Engineers, Lancaster, UK, vol. 137, no. 5, pp 246-254.

VITA AUCTORIS

NAME:	William Clements
PLACE OF BIRTH:	Chatham, Ontario
YEAR OF BIRTH:	1986
EDUCATION:	Blenheim District High School, Blenheim, Ontario
	2000-2004
	University of Windsor, Windsor, Ontario
	2004-2008 B.A.Sc
	University of Windsor, Windsor, Ontario
	2008-2010 M.A.Sc